Tight Bounds on 3-Neighbor Bootstrap Percolation

by

Abel Emanuel Romer
B.A.Sc., Quest University Canada, 2017

A Thesis Submitted in Partial Fulfillment of the
Requirements for the Degree of

MASTER OF SCIENCE

in the Department of Mathematics and Statistics

We acknowledge with respect the Lekwungen peoples on whose traditional territory the university stands, and the Songhees, Esquimalt, and W̱SÁNEĆ peoples whose historical relationships with the land continue to this day.

Tight Bounds on 3-Neighbor Bootstrap Percolation

by

Abel Emanuel Romer
B.A.Sc., Quest University Canada, 2017

Supervisory Committee

Dr. Peter Dukes, Co-Supervisor
(Department of Mathematics and Statistics)

Dr. Jonathan Noel, Co-Supervisor
(Department of Mathematics and Statistics)

ABSTRACT

Consider infecting a subset $A_0 \subseteq V(G)$ of the vertices of a graph G. Let an uninfected vertex $v \in V(G)$ become infected if $|N_G(v) \cap A_0| \geq r$, for some integer r. Define $A_t = A_{t-1} \cup \{v \in V(G) : |N_G(v) \cap A_{t-1}| \geq r\}$, and say that the set A_0 is *lethal* under r-neighbor percolation if there exists a t such that $A_t = V(G)$. For a graph G, let $m(G, r)$ be the size of the smallest lethal set in G under r-neighbor percolation.

The problem of determining $m(G, r)$ has been extensively studied for grids G of various dimensions. We define

$$m(a_1, \ldots, a_d, r) = m\left(\prod_{i=1}^{d}[a_i], r\right)$$

for ease of notation. Famously, a lower bound of $m(a_1, \ldots, a_d, d) \geq \frac{\sum_{j=1}^{d}\prod_{i \neq j} a_i}{d}$ is given by a beautiful argument regarding the high-dimensional "surface area" of $G = [a_1] \times \cdots \times [a_d]$. While exact values of $m(G, r)$ are known in some specific cases, general results are difficult to come by.

In this thesis, we introduce a novel technique for viewing 3-neighbor lethal sets on three-dimensional grids in terms of lethal sets in two dimensions. We also provide a strategy for recursively building up large lethal sets from existing small constructions. Using these techniques, we determine the exact size of all lethal sets under 3-neighbor percolation in three-dimensional grids $[a_1] \times [a_2] \times [a_3]$, for $a_1, a_2, a_3 \geq 11$.

The problem of determining $m(n, n, 3)$ is discussed by Benevides, Bermond, Lesfari and Nisse in [7]. The authors determine the exact value of $m(n, n, 3)$ for even n, and show that, for odd n,

$$\left\lceil \frac{n^2 + 2n}{3} \right\rceil \leq m(n, n, 3) \leq \left\lceil \frac{n^2 + 2n}{3} \right\rceil + 1.$$

We prove that $m(n, n, 3) = \left\lceil \frac{n^2+2n}{3} \right\rceil$ if and only if $n = 2^k - 1$, for some $k > 0$.

Finally, we provide a construction to prove that for $a_1, a_2, a_3 \geq 12$, bounds on the minimum lethal set on the the torus $G = C_{a_1} \square C_{a_2} \square C_{a_3}$ are given by

$$2 \leq m(G, 3) - \frac{a_1a_2 + a_2a_3 + a_3a_1 - 2(a_1 + a_2 + a_3)}{3} \leq 3.$$

Table of Contents

List of Tables

List of Figures

ACKNOWLEDGEMENTS

I would like to thank Dr. Peter Dukes and Dr. Jonathan Noel for their help and support with, and ongoing interest in, the research that has gone into producing this thesis. It has been both fun and exciting to explore the intricacies of this problem, and toy around with different methods for communicating our results. Furthermore, I would like to acknowledge your flexibility regarding the difficulties brought on by COVID-19, and my frequent departures from Victoria throughout the duration of my master's.

Of course, I would like to thank my parents, Sallie and Chip, for their ongoing encouragement and support, even when it means entertaining some arcane question about a particular configuration of dots on a grid. (Dots-and-boxes in undergrad, bootstrap percolation in grad school; it always comes back to dots, huh? Weird.)

I'd like to thank my partner, Athena, for tolerating my frequent departures to Victoria, joining me on some pretty sweet road trips, and making me dinner when I'm desperately cramming to meet a deadline.

I'd like to thank my van, for achieving 90% of the things a normal car can, and 60% of what a house can. (And, I'd like to thank the David Turpin Building for filling in where the van missed.)

Finally, I'd like to thank my friends for their generosity, their kindness, and for being fun.

Chapter 1
Introduction

Consider the lattice depicted in the leftmost diagram of Figure 1.1. We refer to the elements of this lattice as *cells*. Suppose we have the capacity to infect some cells (colored red) with a disease, and that this disease will, over a period of time, propagate through uninfected cells of the lattice. We define that uninfected cells become infected if they are exposed to at least two infected neighboring cells in the vertical and/or horizontal directions. We say that the initial infection is *lethal* if the entire lattice ultimately becomes infected. Here is a puzzle:

Question. *What is the fewest number of infected cells necessary to spawn a lethal infection?*

Before we present the solution, let us take a moment to examine properties of sets of infected cells and attempt to identify some attributes which may correspond to lethality. It should not take too long to observe that if an initial infection is in some way "spread too thinly," then it will be unable to "jump" between infected areas, leading to gaps in infection or *immune regions*. For example, an infection cannot cross any two consecutive uninfected columns or rows. In particular, the final image of Figure 1.1 contains an infected region in the upper right that cannot expand further due to being surrounded by too many uninfected cells. The perimeter of the lattice is particularly difficult to reach, as vertices there have fewer neighbors from which they might be exposed. Heuristically, then, a lethal set should have the ability to effectively span the entire lattice, and should be particularly virulent along the perimeter.

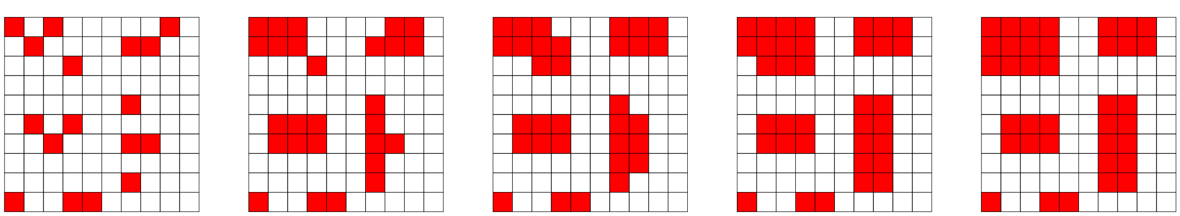

Figure 1.1: An arbitrary set of initially infected cells in the 10×10 lattice, and the stages of infection.

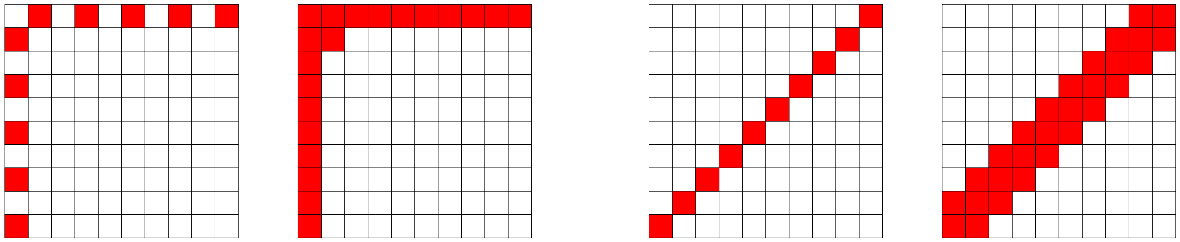

(a) Perimeter construction.　　　(b) Diagonal construction.

Figure 1.2: Two lethal sets and their resulting infections after one time-step.

With this criteria in mind, we are able to make educated guesses regarding the specific structure of sets that are likely to be lethal. In particular, we would like to consider the two starting infections illustrated in Figure 1.2. Notice that while Figure 1.2 (b) has far fewer perimeter infections, both (a) and (b) manage to form "continuous bands" of infected cells that appear to span the entire lattice from the bottom left to top right after one step. Indeed, this fits with our notion of immune regions (or lack thereof), and we see that both infections propagate outwards from these bands until all cells become infected. However, we caution that no specific paradigm for the infection process should be taken as gospel; while heuristics are valuable, it is often easy to find lethal sets that violate them.

It is clear from Figure 1.2 that we may obtain lethal sets on the $n \times n$ lattice of size n by simply infecting the diagonal. What is less obvious is whether it is possible to improve upon this result. Perhaps a most natural first attempt at improvement is to remove an infection from one of the cells along the diagonal. However, this seems to form an immune region containing the removed cell. After some experimentation, one begins to believe it impossible to simultaneously satisfy the heuristic that a starting infection must span the lattice, while also using fewer than n initial infections. The question therefore becomes: how do we prove it?

1.0.1 An early result

We shall consider the cumulative perimeter of infected cells. For a given infectious set A, let $P(A)$ be the total perimeter of the infected cells of A. More precisely, we define $P(A)$ to be the number of sides of infected cells that *do not* border other infected cells. Let A_0 be an initial infection, and observe that $P(A_0) \leq 4|A_0|$. (This bound is only tight if no two infected cells are adjacent. Otherwise, the edge between such cells lies within the infected region, and cannot contribute to the infection's perimeter.) Observe that for any uninfected cell to become infected, it must abut at least two infected cells. Upon infection, the edges adjacent to these cells no longer lie on the infection's perimeter; additionally, the remaining edges of this newly infected cell contribute at most 2 to this perimeter. All told, after infection, $P(A_1) \leq P(A_0)$, where A_1 is the set of cells infected after one time step.

If we suppose that A_0 is a lethal set, then at some point in time the entire grid will become infected. This infection will have perimeter $4n$. Since this perimeter cannot have increased, A_0 must have originally had a perimeter of at least $4n$. Since each cell in A_0 can contribute at most 4 to this perimeter, it must be the case that $|A_0| \geq n$. Our diagonal construction shows that an optimal set A_0 satisfies $|A_0| \leq n$, and so we are able to conclude that n is indeed best possible.

This proof is an instance of the famous *perimeter argument*, which has belonged to bootstrap percolation folklore since at least the work of Pete [19]. It also appears in the wonderful book *The Art of Mathematics: Coffee Time in Memphis* by Béla Bollobás as Problem 34, along with similar questions in Problems 35, 65 and 66 [11]. In the following section, we present additional well-known generalizations of this problem to higher dimensional rectangular grids.

1.1 Bootstrap Percolation

The study of such cellular infection spread in grids (and, more generally, in graphs) is known in the literature as *bootstrap percolation*, and was introduced in the 1970s by Chalupa, Leath and Reich as a simplified model for the behavior of ferromagnetic fields [12]. In their original 1979 paper, the authors research the stable structure of probabilistically selected initial infections. While this differs from the problem posed in Question 1, the rules for the spread of infection and its broad behavior remain the same. It is worth noting that a large portion of contemporary research on bootstrap problems is focused on questions of probabilistic nature; while these problems are certainly interesting and of merit, they do not fall within the scope of this thesis. Rather, we shall focus on those problems where we have specific control over the structure of the initial infections; in particular, we aim to determine the smallest lethal set on the Cartesian product of paths and cycles.

Let us now define the problem in concrete terms. Let G be a graph, let $r \geq 0$ and let $A_0 \subseteq V(G)$ be a set of initially infected vertices. Iteratively, infect those vertices of G with at least r infected neighbors. For all $t > 0$, let A_t be the set of infected vertices at time step t. We then have

$$A_t = A_{t-1} \cup \{v \in V(G) : |N_G(v) \cap A_{t-1}| \geq r\},$$

where $N_G(v)$ is the set of vertices adjacent to v in G. We define the *closure* of A_0 under r-neighbor bootstrap percolation to be $[A_0] = \bigcup_{t=0}^{\infty} A_t$. We say that A_0 *percolates* or is *lethal* if $[A_0] = V(G)$. We define the size of the smallest lethal set in a graph G under r-neighbor bootstrap percolation by the quantity $m(G, r)$. We note that under these rules, it is not possible for vertices to become uninfected.

r	Grids								
	$[a_1]$	$[a_1] \times [a_2]$	$[n]^2$	$[a_1] \times [a_2] \times [a_3]$	$[n]^3$	$\cdots$	$\prod_{i=1}^{d}[a_i]$	$[n]^d$	$[2]^d$
$r = 0$	0	0	0	0	0		0	0	0
$r = 1$	1	1	1	1	1		1	1	1
$r = 2$	$\lceil \frac{a_1-1}{2} \rceil + 1$	$\lceil \frac{a_1+a_2-2}{2} \rceil + 1$	n	$\lceil \frac{a_1+a_2+a_3-3}{2} \rceil + 1$	$\left\lceil \frac{3(n-1)}{2} \right\rceil + 1$		$\left\lceil \frac{\sum_{i=1}^{d}(a_i-1)}{2} \right\rceil + 1$	$\left\lceil \frac{d(n-1)}{2} \right\rceil + 1$	$\lceil \frac{d}{2} \rceil + 1$
$r = 3$	**???**	**???**	$\lceil \frac{n^2+2n+4}{3} \rceil^*$	**S.A. bound**	n^2		**???**	**???**	$\lceil \frac{d(d+3)}{6} \rceil$

Table 1.1: A summary of known bootstrap percolation results for grids, $r \in \{0, 1, 2, 3\}$.

While it is possible to study bootstrap percolation on any graph G, much of the contemporary research focuses on multidimensional grids [1–5,7–9,19–21]. We therefore introduce the following notation. For all $n \in \mathbb{N}$, let $[n] = \{1, 2, \ldots, n\}$. We denote by $\prod_{i=1}^{d}[a_i]$ the grid graph with vertex set $\prod_{i=1}^{d}[a_i]$ and edges between vertices that differ by 1 in exactly one coordinate. Note that $\prod_{i=1}^{d}[a_i] = P_{a_1} \square \cdots \square P_{a_d}$, where $\square$ denotes the Cartesian product of graphs, and P_k denotes a path on k vertices. Furthermore, define:

$$m(a_1, \ldots, a_d, r) = m\left(\prod_{i}^{d}[a_i], r\right).$$

There are a number of natural generalizations of the problem posed in Question 1. In this thesis, we discuss those obtained by varying the structure of G and the value of r. Below, we outline some of the existing results for graphs that are the Cartesian product of paths and cycles, and $r \in \{0, 1, 2, 3\}$. Some of these results are summarized in Table 1.1.

1.1.1 Results on grids and tori

In this section, we highlight existing extremal bootstrap percolation results on grids and tori. Some of the following bounds are not known to be tight and require supplemental constructions, which are often difficult to obtain. We further sub-divide this discussion into results on the grid (of which there are many), and results on the torus (of which there are few).

Grids

From the puzzle posed in Question 1, we readily obtain variant problems by altering three parameters: the size and shape of the grid G, the grid's dimension d, and the threshold number of neighbors r. We examine each of these problems in turn.

In the prior discussion of the perimeter argument, we showed that, for square grids, it holds that $m([n]^2, 2) \geq n$, and verified this to be tight with a diagonal construction. The following result (attributed to Pete [20]) generalizes this result to all rectangular grids $[a_1] \times [a_2]$. A proof is included for completeness.

Figure 1.3: Tight constructions for lethal sets where $a_1 + a_2 \leq 4$.

Theorem 1.1. *For $a_1, a_2 \geq 1$,*

$$m(a_1, a_2, 2) = \left\lceil \frac{a_1 + a_2}{2} \right\rceil.$$

Proof. We obtain a lower bound on $m(a_1, a_2, 2)$ by applying the perimeter argument. Note that the perimeter of the $a_1 \times a_2$ grid is $2(a_1+a_2)$, and so the $m(a_1, a_2, 2) \geq \lceil \frac{a_1+a_2}{2} \rceil$. (We take the ceiling because the size of infected sets must be integral. See Figure 1.4.) For the upper bound, we proceed by induction on $a_1 + a_2$. For $a_1 + a_2 \leq 4$, the lethal sets in Figure 1.3 match the lower bounds given by the perimeter argument (1, 2, 2, and 2, respectively). For $a_1 + a_2 > 4$, suppose without loss of generality that $a_1 \leq a_2$, and so $a_2 \geq 3$. By hypothesis, $[a_1] \times [a_2 - 2]$ admits a lethal set A_0 at the perimeter bound. We show that A_0, plus the addition of any infection in the final column of $[a_1] \times [a_2]$, is lethal and matches the perimeter bound.

Observe that A_0 infects all vertices of $[a_1] \times [a_2]$, apart from the final two columns. The additional vertex in the final column is then sufficient to infect all remaining healthy vertices. Finally, by incrementing a_2 by two, the perimeter bound is incremented by exactly one. This completes the proof. □

Let us take a moment to examine the issue of integrality in the perimeter bound. When non-integrality occurs, either adjacent vertices are infected in the same generation, or a vertex is infected by more than r neighbors. Note that in both cases, this decreases the perimeter of infection. One way to think about this is to consider each vertex as having "infectious potential": vertices $v \in A_0$ can infect up to $d(v)$ healthy vertices, whereas vertices $v \in A_i$ for $i > 0$ can infect at most $d(v) - r$. An integral perimeter bound mandates that each vertex realize its potential, whereas a non-integral bound leaves a small margin for error. Figure 1.4a illustrates the integral case, where each cell is infected by exactly two neighboring cells; this condition ensures that $P(A_i) = P([A_0])$ for all i. Conversely, in Figure 1.4b, the cell demarcated with an "X" experiences infection on three sides, thereby reducing its infectious potential. The existence of such a cell is guaranteed by the fact the perimeter bound in this case is non-integral.

We can further generalize in the case where $r = 2$. In 2006, Balogh and Bollobás [1] proved the following general form of Theorem 1.1 for all d-dimensional grids $(a_1, \ldots, a_d)$, $a_i \geq 1$:

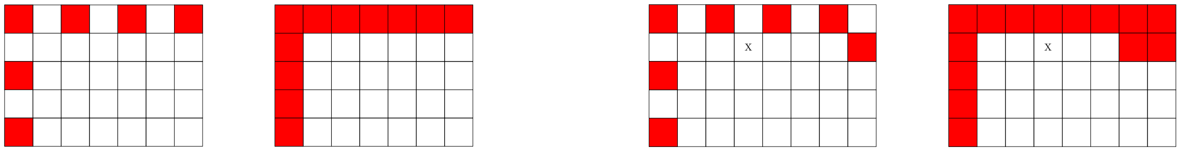

(a) $a+b \equiv 0 \pmod 2$ (b) $a+b \equiv 1 \pmod 2$

Figure 1.4: Tight constructions for lethal sets on the $[a] \times [b]$ grid.

Theorem 1.2 (Balogh and Bollobás). *For $d \geq 1$ and $a_1, \ldots, a_d \geq 1$,*

$$m(a_1, \ldots, a_d, 2) = \left\lceil \frac{\sum_{i=1}^{d}(a_i - 1)}{2} \right\rceil + 1.$$

Theorem 1.2 completes the picture for infections with a threshold of two on grids. We now ask whether similar results exist for larger r. Unfortunately, while generalizing to d-dimensional grids yields nice results for $r = 2$, attempts to obtain a holistic understanding of $m(a_1, \ldots, a_d, r)$ for arbitrary r have been largely fruitless. Even the case of $r = 3$ remains stubbornly inaccessible for nearly all large d. However, certain breakthroughs have been made for $d = 2$, $d = 3$, and $G = [2]^d$.

We first consider 3-neighbor percolation on two-dimensional square grids. In 2021, Benevides, Bermond, Lesfari and Nisse proved that

$$m(n, n, 3) = \left\lceil \frac{n^2 + 2n + 4}{3} \right\rceil$$

for even n, and

$$\left\lceil \frac{n^2 + 2n}{3} \right\rceil \leq m(n, n, 3) \leq \left\lceil \frac{n^2 + 2n}{3} \right\rceil + 1$$

for odd n. Additionally, they showed that these bounds are tight in the following cases: if $n = 5 \pmod 6$, or $n = 2^k - 1$ for some $k \in \mathbb{N}$, then $m(n, n, 3) = \lceil \frac{n^2+2n}{3} \rceil$; and if $n \in \{9, 13\}$, then $m(n, n, 3) = \lceil \frac{n^2+2n}{3} \rceil + 1$. Constructions that achieve this bound are illustrated in Chapter 5. We add to this picture with the following theorem, proven in Chapter 5, and corollary:

Theorem 1.3. *Suppose that $a, b \geq 1$ such that*

$$m(a, b, 3) = \frac{2ab + a + b}{3}.$$

Then there exists $k \geq 1$ such that $a = b = 2^k - 1$.

Corollary 1.4. *For all $n \geq 1$,*

$$m(n,n,3) = \begin{cases} \left\lceil \frac{n^2+2n+4}{3} \right\rceil & n \equiv 0 \pmod 2; \\ \frac{n^2+2n}{3} & n = 2^k - 1,\ k \in \mathbb{N}; \\ \frac{n^2+2n+1}{3} & n \equiv 5 \pmod 6; \\ \frac{n^2+2n+3}{3} & \textit{otherwise.} \end{cases}$$

Proof. The first three cases follow from Theorem 1 of [7] and the observation that if $n \equiv 5 \pmod 6$, then $\lceil \frac{n^2+2n}{3} \rceil = \frac{n^2+2n+1}{3}$. In the final case, n is congruent to either 1 or 3 modulo 6. This implies that $n^2 + 2n$ is divisible by three. From Theorem 1 of [7], we have that $m(n,n,3) \leq \frac{n^2+2n+3}{3}$. Furthermore, since n is not of the form $2^k - 1$, it follows from Theorem 1.3 that $m(n,n,3) > \frac{n^2+2n}{3}$. Therefore, $m(n,n,3) = \frac{n^2+2n+3}{3}$. $\square$

This result resolves the question of the minimum lethal set for two dimensional square grids. For the more general case of rectangular grids, the problem remains unsolved. However, our experimentation suggests that nearly all grids $[a_1] \times [a_2]$ for $a_1, a_2 > 2$ fall within a constant factor of the bound given in Theorem 1.5, below.

One significant and well-known result for d-neighbor percolation on d-dimensional grids is the following lower bound, taken as a d-dimensional analog of the perimeter bound. This result is referenced frequently throughout this document, and referred to interchangeably as the *surface area* or *SA bound*. We shall use the shorthand notation $SA(G)$ to refer to the surface area bound of a grid G. We prove the statement in full generality, while noting that we only make use of the case where $d = 3$. We also note that, like the perimeter bound, the following proof belongs to bootstrap percolation folklore. While it appears to have been first published in 1997 by Balogh and Pete [6], variations also appear in [11, 19, 20].

Theorem 1.5. *For any $d \geq 1$ and $a_1, a_2, \ldots, a_d \geq 1$,*

$$m(a_1, a_2, \ldots, a_d, d) \geq \frac{\sum_{j=1}^{d} \prod_{i \neq j} a_i}{d}.$$

Proof. We apply the same "invariant" strategy presented in the perimeter argument. For simplicity, consider $\prod_{i=1}^{d} [a_i]$ to be embedded within the larger graph $\prod_{i=1}^{d} \{0, \ldots, a_i + 1\}$. Note that in $\prod_{i=1}^{d} \{0, \ldots, a_i + 1\}$, each vertex $v \in \prod_{i=1}^{d} [a_i]$ has degree $2d$. Let A_0 be a lethal set in $\prod_{i=1}^{d} [a_i]$ under the d-neighbor bootstrap process. For $t > 0$, let A_t be the set of infected vertices in $\prod_{i=1}^{d} [a_i]$ at generation t. Denote by m_t the number of edges between vertices $u \in A_t$ and $v \in \prod_{i=1}^{d} \{0, \ldots, a_i + 1\} \setminus A_t$. We show that $m_{t-1} \geq m_t$ for all $t > 0$.

By definition, each vertex $v \in A_t \setminus A_{t-1}$ has at least d neighbors in A_{t-1}. Therefore, since $d(v) = 2d$, v has no more than d neighbors outside of A_t. This implies that the number of edges from $A_{t-1} \cup \{v\}$ to $\prod_{i=1}^{d}\{0, \ldots, a_i + 1\} \setminus A_{t-1} \cup \{v\}$ cannot exceed m_{t-1}. Furthermore, this holds for every vertex $v \in A_{t-1}$, and so $m_{t-1} \geq m_t$.

Since A_0 is lethal, we have that

$$2d|A_0| \geq m_0 \geq m_1 \geq \cdots \geq 2 \sum_{j=1}^{d} \prod_{i \neq j} a_i,$$

where the final expression gives the total number of edges between the fully infected grid and the surrounding larger grid. Dividing through by $2d$ gives the result. $\square$

We note that the prior argument is precisely the same as the so-called perimeter argument outlined in Section 1.0.1. Here, the quantity m_t is a d-dimensional analogue of the perimeter of infection $P(A_t)$ at time-step t, and the lower bound

$$2 \sum_{j=1}^{d} \prod_{i \neq j} a_i$$

is the d-dimensional "perimeter" of the grid. Again, observe that equality can only be obtained when no vertices of A_0 are adjacent, and all vertices $v \in A_t$, for $t > 0$, are infected by exactly d neighbors. Any defect causes a reduction in "perimeter" of two units, corresponding to a $1/d$ increase in the bound.

We note that in the case where $a_1 = \cdots = a_d = n$, the bound given in Theorem 1.5 simplifies to $m(n, \ldots, n, d) \geq n^{d-1}$. Somewhat surprisingly, although it is not too difficult to find sets that meet this bound and appear to be lethal, verifying this claim is non-trivial. To the best of our knowledge, the first published proof of this fact appears in a 2019 paper by Przykucki and Shelton [21].

Theorem 1.6 (Lower bound [6]. Upper bound [21])**.** *For all $n, d \geq 1$,*

$$m(\underbrace{n, \ldots, n}_{d}, d) = n^{d-1}.$$

The primary aim of this thesis is to prove that the surface area bound is tight for sufficiently large grids when $r = 3$. This process employs a number of general constructions (discussed in Chapter 6), as well as a recursive strategy (discussed in Chapter 3). In Chapter 5, we prove the following result:

Theorem 1.7. *For all $a_1, a_2, a_3 \geq 11$,*

$$m(a_1, a_2, a_3, 3) = \left\lceil \frac{a_1a_2 + a_2a_3 + a_1a_3}{3} \right\rceil.$$

Unfortunately, the complete resolution of the $r = 3$ case on grids remains elusive.

Tight constructions exist for cubes $[n]^3$ and hypercubes $[2]^d$, but more general results are difficult to obtain. See Chapter 7 for suggestions on areas of further research.

Tori

In addition to varying the parameters r and d, we might also change the very structure of G. It is natural to shift from grids (the Cartesian product of paths) to tori (the Cartesian product of cycles). In fact, it could be argued that bootstrap percolation on the torus is *more* natural than the grid, since tori are regular and grids are not. This problem has been studied by Benevides, Bermond, Lesfari and Nisse. In 2021, they obtained the following lower bound for the Cartesian product of two cycles [7]. Their proof is included here for completeness.

Theorem 1.8. *For $a, b \geq 1$,*

$$m(C_a \square C_b, 3) \geq \left\lceil \frac{ab+1}{3} \right\rceil.$$

Proof. Let $G = C_a \square C_b$, and let I be a lethal set on G. Let $H = V(G) \setminus I$, and note that $|H| = ab - |I|$. Let m_H be the number of edges in the subgraph of G induced by H, and m_{IH} be the number of edges between vertices in I and vertices in H. Note that m_{IH} is similar to the notion of perimeter on a grid.

Observe that $G[H]$ must be cycle-free: cycles in $G[H]$ constitute immune regions, and contradict the lethality of I. Therefore, $G[H]$ is a forest, and so $m_H = |H| - c$, where c is the number of components in $G[H]$. Additionally, note that $m_{IH} \leq 4|I|$, since G is 4-regular. Finally, observe that the total degree of $G[H]$ is $2m_H = 4|H| - m_{IH}$.

Chaining together these inequalities, we obtain:

$$\begin{aligned} 4|I| \geq m_{IH} &= 4|H| - 2m_H \\ &= 4|H| - 2(|H| - c) = 2|H| + 2c \\ &= 2(ab - |I|) + 2c. \end{aligned}$$

Combining like terms and simplifying, we have

$$|I| \geq \frac{ab+c}{3} \geq \frac{ab+1}{3}.$$

□

Observe that the conditions $c \geq 1$ and $m_{IH} \leq 4|I|$ prevent us from obtaining exact equality. Specifically, if I is lethal, $G[H]$ has one component, and no vertices in I are adjacent, then $|I|$ is minimized. Note that these conditions are quite similar to those on grids; the difference is that equality in the bound on grids mandates that no vertex be infected by more than r neighbors, whereas equality on three-dimensional tori appears more complex.

Theorem 1.8 is generalized to all tori by Hambardzumyan, Hatami and Qian in [13]. Specifically, they provide a recursive formula for the size of minimum lethal sets on tori under r-bond bootstrap percolation, an instance of the graph bootstrap percolation problem introduced by Bollobas in 1968 [10]. One might think of r-bond percolation as an analogue of bootstrap percolation on the edges of a graph, whereby an uninfected edge becomes infected if one of its endpoints is adjacent to at least r infected edges. The minimum lethal edge set under the r-bond process on a graph G is denoted by $m_e(G, r)$.

In [17], Morrison and Noel note that a lethal set of vertices can be converted into a lethal set of edges under the r-bond process by simply infecting an arbitrary set of r edges incident to every infected vertex. This observation provides the following lower bound on $m(G, r)$:

$$\frac{m_e(G, r)}{r} \leq m(G, r).$$

In Theorem 8 of [13], a recursive formula is given for $m_e(G_d, r)$, where G_d is the Cartesian product of d cycles. As $m_e(G_d, r) \leq r \cdot m(G_d, r)$, we are able to leverage this result to obtain a lower bound on $m(C_{a_1} \Box C_{a_2} \Box C_{a_3}, 3)$. In particular, we have the following theorem.

Theorem 1.9. *Let $G_3 = C_{a_1} \Box C_{a_2} \Box C_{a_3}$. Then*

$$m(G_3, 3) \geq \frac{(a_1 - 1)(a_2 - 1) + (a_2 - 1)(a_3 - 1) + (a_3 - 1)(a_1 - 1) + 3}{3}.$$

Note that the above bound is precisely one less than the surface area bound on the grid $[a_1 - 1] \times [a_2 - 1] \times [a_3 - 1]$. The following corollary to Theorem 1.7 provides an upper bound on $m(G_3, 3)$ for all $a_1, a_2, a_3 \geq 12$:

Corollary 1.10. *Let $G_3 = C_{a_1} \Box C_{a_2} \Box C_{a_3}$, where $a_1, a_2, a_3 \geq 12$. Then*

$$m(G_3, 3) \leq \frac{(a_1 - 1)(a_2 - 1) + (a_2 - 1)(a_3 - 1) + (a_3 - 1)(a_1 - 1) + 6}{3}.$$

Proof. Let $G = [a_1 - 1] \times [a_2 - 1] \times [a_3 - 1]$ and observe that, by Theorem 1.7,

$$\frac{(a_1 - 1)(a_2 - 1) + (a_2 - 1)(a_3 - 1) + (a_3 - 1)(a_1 - 1) + 6}{3} = SA(G, 3) + 2.$$

Consider $[a_1 - 1] \times [a_2 - 1] \times [a_3 - 1] \subset V(G_3)$, and let A_0 be a perfect lethal set on the grid induced by these vertices. Let $u = (a_1, a_2, a_3)$ and $v = (a_1, 1, 1)$ be vertices in G_3 (see Figure 1.5). We show that $A_0 \cup \{u, v\}$ is lethal on G_3.

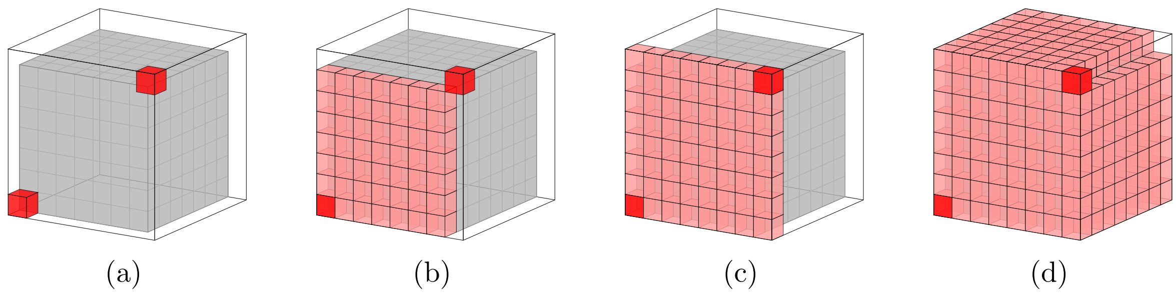

Figure 1.5: Four stages of infection on the grid G (gray) inset in the larger torus, with infected vertices u and v (dark red).

Note that A_0 infects all vertices $[a_1-1]\times[a_2-1]\times[a_3-1]$. Consider $[a_1]\times[a_2-1]\times[a_3-1]$, and observe that the infection spreads outward across this face from v (Figure 1.5b). With all of $a_1\times[a_2-1]\times[a_3-1]$ infected, u spawns infections down $a_1\times a_2\times[a_3-1]$ and $a_1\times[a_2-1]\times a_3$ (Figure 1.5c). This permits infection of faces $[a_1-1]\times[a_2]\times[a_3-1]$ and $[a_1-1]\times[a_2-1]\times[a_3]$ (Figure 1.5d). Finally, $[a_1-1]\times a_2\times a_3$ are infected (not pictured).

This constitutes all vertices of G_3, and so we conclude that $A_0\cup\{u,v\}$ is lethal on G_3. $\square$

1.1.2 Other problems

Thus far, we have focused on the extremal problem of determining the smallest possible lethal set on d-dimensional grids and tori. Unsurprisingly, this is one of many existing areas of research in bootstrap percolation. In this section, we highlight a different, related problem: what is is the maximum time it takes for a lethal set to infect all vertices of a grid?

As before, we shall begin with 2-neighbor percolation on $[n]^2$. We shall say that a lethal set $A_0\subseteq V(G)$ percolates in time T if we obtain $[A_0]$ in T time-steps. For $r\in\mathbb{N}$, let

$$T(G,r)=\max\{T\in\mathbb{N}\mid \exists \text{ a set } A_0\subseteq V(G) \text{ that } r\text{-neighbor percolates in time } T\}.$$

In 2015, Benevides and Przykucki [9] determined the asymptotic value of $T([n]^2,2)$. Their result is reproduced below.

Theorem 1.11 (Benevides, Przykucki)**.** *The maximum percolation time on* $[n]^2$ *is* $T([n]^2,2)=\frac{13}{18}n^2+O(n)$.

Interestingly, this time is not achieved with minimum lethal sets (lethal sets of size n). In fact, the same authors showed in an earlier paper that the maximum percolation time for lethal sets A_0 on $[n]^2$, where $|A_0|=n$, is the nearest integer value to $\frac{5n^2-2n}{8}$ [8].

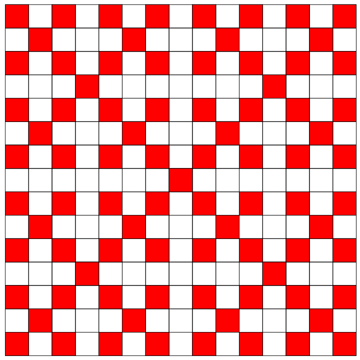

(a) $T([n]^2, 3) = \frac{n-1}{2}$

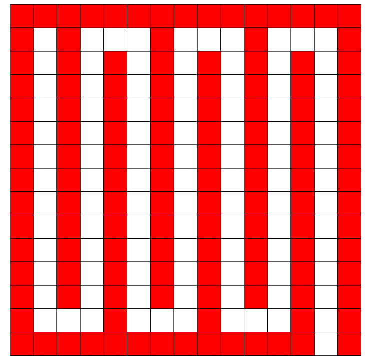

(b) $T([n]^2, 3) \geq \frac{(n-1)(n-1)}{2}$

Figure 1.6: Lethal sets on $[2^k - 1]^2$ with different percolation times.

The fact that minimum lethal sets do not always percolate slowest holds for grids $[n]^2$ under 3-neighbor percolation, where $n = 2^k - 1$. In Chapter 5, we prove that $m([n]^2, 3) = \frac{n^2+2n}{3}$ for $n = 2^k - 1$, and show that this is achieved for exactly one lethal configuration of vertices A_0. It is easy to see that A_0 percolates in time $(n-1)/2$ and so, if $|A_0| = \frac{n^2+2n}{3}$, then $T([n]^2, 3) = \frac{n-1}{2}$ (see Figure 1.6a). By removing the restriction on $|A_0|$, we are able to improve this to $T([n]^2, 3) \geq (n-1)(n-1)/2$ (see Figure 1.6b). It is not clear whether this lower bound is best possible; further discussion can be found in Chapter 7.

In 2018, Hartarsky investigated maximum r-neighbor percolation time on d-dimensional hypercubes, for $r \geq 3$ [14]. In particular, they determined the following value of $T([2]^d, r)$, up to a polylogarithmic factor:

Theorem 1.12 (Hartarsky)**.** *For all $r \geq 3$,*

$$T([2]^d, r) = \frac{2^d}{d}(\log d)^{-O(1)}.$$

Interestingly, the proof of Theorem 1.12 makes use of connections between maximum induced paths in the hypercube (the Snake-in-a-Box problem) and maximum percolation time. The association between bootstrap percolation and induced paths in hypercubes was also laid out in a 2014 paper by Shende [23]. In Chapter 7, we note that the structure of lethal sets in two-dimensional grids $[a_1] \times [a_2]$ bears resemblance to maximum induced paths in $[a_1] \times [a_2]$.

1.2 Structure of this Thesis

As stated by Theorem 1.7, the primary goal of this thesis is to prove a tight bound for 3-neighbor bootstrap percolation on three-dimensional grids of sufficiently large size. This task requires the use of two major lemmas, as well as both original and previously published ideas and constructions. In an effort to present this material in a coherent manner, the thesis is structured as follows.

Chapters 2 and 3 are dedicated to building a conceptual and intuitive framework upon which to prove Theorem 1.7. In Chapter 2, we present lemmas regarding the structure of lethal sets in both two-dimensional and d-dimensional grids. These lemmas will prove useful in our examination of general constructions of lethal sets (see Chapter 6). We also discuss the design and function of a visualization tool developed to assist in the examination of lethal sets. In Chapter 3, we prove a lemma that will allow us to recursively develop large families of lethal sets that match the surface area bound, and summarize all families of lethal sets that we are able to obtain.

Chapter 4 leverages the results of Chapters 2 and 3 to prove Theorem 1.7. We first show that grids $[a_1] \times [a_2] \times [a_3]$, $a_1, a_2, a_3 \geq 5$ with integral surface area bound admit tight lethal sets, and then extend this result to all grids of size 11. Chapter 5 further builds on this, highlighting some new results for 3-neighbor percolation on grids $[a_1] \times [a_2]$.

Chapter 6 and Appendix A examine the structure and lethality of percolating sets discovered in this research. In particular, Chapter 6 proves the lethality of the constructed families of sets presented in Chapter 2, and Appendix A illustrates the phases of infection on individual lethal sets.

Finally, Chapter 7 summarizes our results and provides recommendations for future research in similar and related problems.

Chapter 2
Tools and Techniques

While it is difficult to identify specific patterns across all lethal sets A_0 under the r-neighbor bootstrap process, there are certain structures that appear frequently enough to warrant discussion. In this chapter, we examine such structures. We also introduce the following shorthand notation, which will appear throughout the remainder of this thesis.

Definition 2.1. Let $a_1, \ldots, a_d$ be integers such that $a_1, \ldots, a_d \geq 1$. We define $G(a_1, \ldots, a_d)$ to be the grid graph $\prod_{i=1}^{d}[a_i]$. Furthermore, we refer to the smallest value a_d as the *thickness* of $G(a_1, \ldots, a_d)$.

2.1 The d-Walls Lemma

We begin with the following definition and lemma, which articulate more clearly the notion of a lethal set "spanning" a grid (as we saw in Figure 1.2).

Definition 2.2. Let $G = \prod_{i=1}^{d}[a_i]$ be a d-dimensional grid graph. For some $k \in [a_j]$, let $F_{j,k} = \prod_{i=1}^{j-1}[a_i] \times \{k\} \times \prod_{i=j+1}^{d}[a_i]$ be the kth *plane* of G in the jth dimension.

Definition 2.3. Let $G = \prod_{i=1}^{d}[a_i]$ be a d-dimensional grid graph, and for some $k \in [a_j]$, let $F_{j,k}$ be a plane of G. If $k = 1$ or $k = a_j$, we refer to $F_{j,k}$ as a *face* of G.

Lemma 2.4. *Let A_0 be an infected set on $G = \prod_{i=1}^{d}[a_i]$. Let $\overline{A_0} = V(G) \setminus A_0$, and let $H = G[\overline{A_0}]$ be the subgraph of G induced by $\overline{A_0}$. If H does not contain a path between $F_{j,1}$ and F_{j,a_j}, for all $1 \leq j \leq d$, then A_0 is lethal on G under d-neighbor percolation.*

Proof. We proceed by induction on $|V(H)| = \prod_{i=1}^{d} a_i - |A_0|$. If $|V(H)| = 0$, then all vertices of G are infected and we are done. Suppose $|V(H)| > 0$, and consider a connected component Y of H. By hypothesis, for all $j \in [d]$, either $V(Y) \cap F_{j,1} = \emptyset$ or $V(Y) \cap F_{j,a_j} = \emptyset$ (or both). Suppose, without loss of generality, that $V(Y) \cap F_{j,a_j} = \emptyset$. Let $\mathbf{x} = (x_1, \ldots, x_d)$ by the lexicographically maximum vertex in $V(Y)$, and observe that

$$\left\{\bigcup_{j\in[d]} F_{j,x_j+1}\right\} \cap V(Y) = \emptyset.$$

In particular, note that $(x_1 + 1, x_2, \ldots, x_d), \ldots, (x_1, \ldots, x_d + 1) \in N_S(\mathbf{x})$. Therefore, $\mathbf{x}$ becomes infected. Furthermore, since $|V(H) \setminus \{\mathbf{x}\}| < |V(H)|$, the resulting graph percolates by induction. This completes the proof. □

Definition 2.5. Let G be the grid graph $\prod_{i=1}^{d}[a_i]$. For each $j \in [d]$, let $k_j \in [a_j]$ be some integer between 1 and a_j, inclusive. We define

$$M = \bigcup_{j\in[d]} F_{j,k_j},$$

and refer to M as a *union of mutually orthogonal planes* of G.

Corollary 2.6. *Let G be the grid graph $\prod_{i=1}^{d}[a_i]$ and let M be a union of mutually orthogonal planes of G. If a set A_0 is lethal on M, then it is lethal on G.*

Proof. Since A_0 is lethal on M, there exists a time t where $M \subseteq A_t$. Therefore, for all $j \in [d]$, the graph $G[\overline{A_t}]$ cannot contain a path between $F_{j,1}$ and F_{j,a_j}. By Lemma 2.4, A_0 is lethal on G. □

Corollary 2.6 gives a cleaner characterization of certain lethal sets on d-dimensional grids in terms of their $(d-1)$-dimensional planes, provided these planes are mutually orthogonal. Here, we return to the notion first introduced in Chapter 1 of the capacity of a lethal set to span a grid. In particular, we see that the set in Figure 1.2a is comprised of lethal sets under the 2-neighbor bootstrap process on the two one-dimensional orthogonal planes $F_{1,1}$ and $F_{2,1}$ of $[10]^2$. In this regard, the problem of obtaining perfect d-neighbor lethal sets on d-dimensional grids is reduced to the problem of determining a "good" union M of mutually orthogonal $(d-1)$-dimensional planes. In Chapter 6, we apply this idea to obtain an infinite family of three-dimensional grids from three orthogonal two-dimensional planes. However, we caution that the challenge of determining a "good" union M is non-trivial in general.

The following corollaries will be useful in our discussion of lethal sets on three-dimensional grids $G(a_1, a_2, a_3)$.

Corollary 2.7. *Let G be the grid graph $G(a_1, a_2, a_3)$. If a set A_0 is lethal on mutually orthogonal faces $F_{1,1} \cup F_{2,1} \cup F_{3,1}$ of G, then A_0 is lethal on G.*

Proof. By hypothesis, A_0 is lethal on $F_{1,1} \cup F_{2,1} \cup F_{3,1}$. Therefore, there exists some time t for which $F_{1,1} \cup F_{2,1} \cup F_{3,1} \subseteq A_t$, and so $G[\overline{A_t}]$ satisfies the conditions of Lemma 2.4. We conclude that A_0 is lethal on G. □

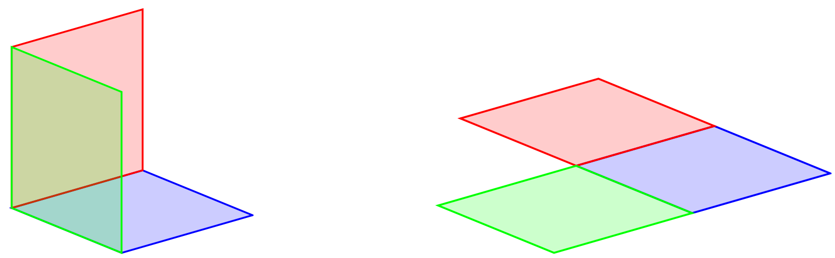

Figure 2.1: Three perpendicular faces of $G(a_1, a_2, a_3)$ (left) and their representation as a flat unfolded surface (right).

Corollary 2.8. *Let G be the grid graph $G(b_1, b_2, b_3)$, where $b_1, \dots, b_d \geq 2$. Let M be a subset of $V(G)$ such that every component of $G[\overline{M}]$ is a grid $G(a_1, \dots, a_d)$ such that $a_j < b_j$, for all $j \in [d]$. Then, if a set A_0 is lethal in $G[M]$, then it is lethal in G.*

Proof. Suppose A_0 is lethal in $G[M]$ and consider some component $C = G(a_1, \dots, a_d)$. Let F_{j,a_j+1} be a plane of G flanking the face of C in the jth dimension. Observe that

$$\left\{ \bigcup_{j \in [d]} F_{j,a_j+1} \right\} \cap M$$

is a union of mutually orthogonal planes in the graph $G(a_1 + 1, \dots, a_d + 1)$. Since A_0 is lethal in $G[M]$, by Corollary 2.6, A_0 is lethal in C. This holds for all components of $G[\overline{M}]$, and so we conclude that A_0 is lethal in G. $\square$

In the case of three-dimensional grids G, it is instructive to think of "unfolding" planes of G into two-dimensional surfaces. An illustration of this for $G(a_1, a_2, a_3)$ is shown in Figure 2.1. We refer to these planes of G as *manifolds*, and to the unfolded surfaces as *unfoldings*. If a manifold M satisfies the conditions of Corollary 2.8, then we say that an unfolding of M is *proper*. In Chapter 6, we examine other manifolds and their proper unfoldings.

Since, by Corollary 2.6, any lethal set on M is also lethal on G, it is often easier to identify lethal sets by examining these flattened unfolded structures. In fact, in the particular case of $M = F_{1,1} \cup F_{2,1} \cup F_{3,1}$, the surface area bound on $G(a_1, a_2, a_3)$ can be written in terms of the surface area bounds on flat, two-dimensional grids.

Lemma 2.9. *For $a_1 \geq a_2 \geq a_3 \geq 1$,*

$$SA(a_1, a_2, a_3) = SA(a_1 + a_3 - 1, a_2 + a_3 - 1, 1) - SA(a_3 - 1, a_3 - 1, 1).$$

Proof. Taking the surface area bound on the righthand side of the above equation, we obtain

$$\mathrm{SA}(a_1 + a_3 - 1, a_2 + a_3 - 1, 1) = \frac{a_1 a_2 + a_1 a_3 + a_2 a_3 + a_3^2 - 1}{3}$$

and

$$\mathrm{SA}(a_3 - 1, a_3 - 1, 1) = \frac{a_3^2 - 1}{3}.$$

Adding these two expressions together gives

$$\frac{a_1 a_2 + a_1 a_3 + a_2 a_3}{3},$$

which is precisely the surface area bound for $G(a_1, a_2, a_3)$. □

In the context of Figure 2.1, this lemma tells us that a percolating set on the $G(a_1, a_2, a_3)$ grid (left of Figure 2.1) is precisely the same size as a percolating set on the complete flattened rectangle minus the size of a percolating set on the missing region (right of Figure 2.1). In practice, this lemma allows us to leverage an understanding of lethal sets on two-dimensional grids to obtain lethal sets in three dimensions. However, care is required in this process, as the region excluded from the two-dimensional unfolding must contain precisely the same number of infected vertices as the surface area bound.

2.2 3-Neighbor Percolation on 2D Grids

The above discussion suggests that an understanding of the behavior of 3-neighbor percolation on two-dimensional grids is of use in our investigation of 3-neighbor percolation on $G(a_1, a_2, a_3)$ grids. In Chapter 5 we examine the problem of 3-neighbor percolation on square two-dimensional grids, and answer a question posed by Benevides, Bermond, Lesfari and Nisse regarding the value of $m([n]^2, 3)$. Here, we describe some of the structural properties of lethal sets on two-dimensional grids that will prove useful in that analysis. The following propositions are due to Benevides et al [7].

Proposition 2.10. *Let A_0 be a lethal set on $[a_1] \times [a_2]$ under 3-neighbor percolation. Then A_0 contains all four corner vertices of $[a_1] \times [a_2]$.*

Proof. Since corner vertices in $[a_1] \times [a_2]$ have degree 2, they cannot become infected. Therefore, since A_0 is lethal, it must contain all corner vertices. □

Proposition 2.11. *Let B be the set of vertices on the border of $[a_1] \times [a_2]$, and let $u, v \in B$ be adjacent vertices. If A_0 is a lethal set under 3-neighbor percolation, then $A_0 \cap \{u, v\} \neq \emptyset$.*

Proof. Assume for contradiction that $A_0 \cap \{u, v\} = \emptyset$. By Proposition 2.10, neither u nor v is a corner vertex. Since u, v are border vertices, $d(u) = d(v) = 3$. Because A_0

mod 3	$a_1 \equiv 0$	$a_1 \equiv 1$	$a_1 \equiv 2$
$a_2 \equiv 0$			
$a_2 \equiv 1$			
$a_2 \equiv 2$			

(a) $a_3 \equiv 1 \pmod 3$

mod 3	$a_1 \equiv 0$	$a_1 \equiv 1$	$a_1 \equiv 2$
$a_2 \equiv 0$			
$a_2 \equiv 1$			
$a_2 \equiv 2$			

(b) $a_3 \equiv 2 \pmod 3$

mod 3	$a_1 \equiv 0$	$a_1 \equiv 1$	$a_1 \equiv 2$
$a_2 \equiv 0$			
$a_2 \equiv 1$			
$a_2 \equiv 2$			

(c) $a_3 \equiv 0 \pmod 3$

Table 2.1: Integrality of grids by congruence class. Green indicates integral surface area bound.

is lethal, u and v must become infected. Suppose, without loss of generality, that u is infected first. This is impossible, since $d(u) = 3$ and v is not infected. □

Proposition 2.12. *Let A_0 be a lethal set on $[a_1] \times [a_2]$ under 3-neighbor percolation. Let $H = V([a_1] \times [a_2]) \setminus A_0$. Then the subgraph induced by H is acyclic and each component of this subgraph contains at most one border vertex.*

Proof. Suppose for contradiction that C is a cycle in the subgraph induced by H. Let $v \in V(C)$ be the first vertex of C to become infected. Note that v has two uninfected neighbors in C. Since $d(v) \leq 4$, v cannot become infected, a contradiction.

Suppose P is a path in the subgraph induced by H with endpoints on the border. No vertex v in $V(P)$ can become infected, since v has at most two neighbors outside of P. □

Proposition 2.12 more clearly articulates the notion of immune regions discussed in Chapter 1. While such immune regions exist in higher-dimensional grids, their structure is substantially harder to characterize.

It will be insightful to consider the surface area bound on two-dimensional grids in the context of Propositions 2.10, 2.11 and 2.12. For simplicity, we introduce the following terms. We refer to grids with integral surface area bounds as *divisibility cases* and grids with non-integral bounds as *non-divisibility cases*. The divisibility and non-divisibility cases for three-dimensional grids where $r = 3$ are illustrated in Table 2.1. Note that (a_1, a_2, a_3) is a divisibility case if and only if at least two of the coordinates are multiples of three or $a_1 \equiv a_2 \equiv a_3 \pmod 3$. We refer to the lethal set $A_0 \subseteq V(G)$ in $G(a_1, a_2, a_3)$ that matches the surface area bound as *optimal*. Furthermore, if $G(a_1, a_2, a_3)$ is a divisibility case, we call A_0 *perfect*. For brevity, if $G(a_1, a_2, a_3)$ admits an optimal lethal set, we refer to the tuple (a_1, a_2, a_3) as *optimal*, and if $G(a_1, a_2, a_3)$ admits a perfect lethal set, we refer to the tuple (a_1, a_2, a_3) as *perfect*. We remark that any tuple (a_1, a_2, a_3) is optimal if and only if all other tuples obtained by permuting the values a_1, a_2, a_3 are optimal.

Recall from Chapter 1 that a lethal initial infection A_0 is perfect if it contains no adjacent vertices, and if all vertices $v \in A_0$, $t > 0$, are infected by precisely d neighbors. Therefore, by Propositions 2.10 and 2.11, if $[a_1] \times [a_2]$ admits a perfect lethal set, then $a_1, a_2 \equiv 1 \pmod 2$. Furthermore, every component of the subgraph H

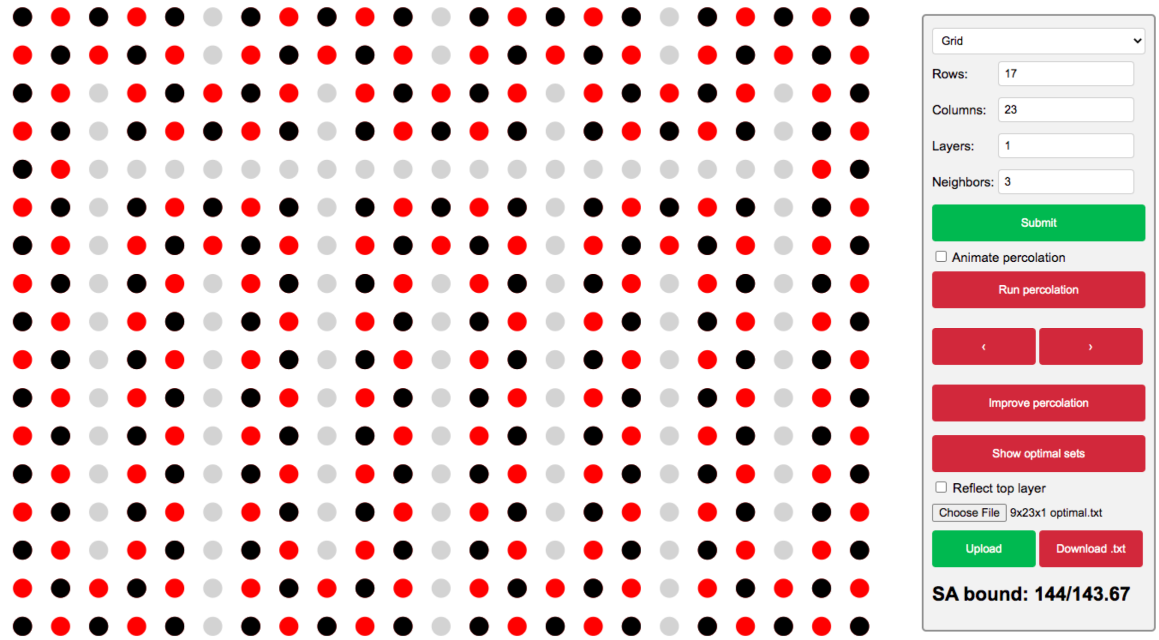

Figure 2.2: The visualization tool with an infected set.

induced by uninfected vertices must contain exactly one border vertex (otherwise the second condition on perfect infections would be violated). In Chapter 6, we use these observations to prove that the only two-dimensional grids that admit perfect lethal sets under 3-neighbor bootstrap percolation are of the form $[2^n - 1]^2$.

2.3 Visualizer

In addition to the conceptual tools presented above, many of the results in this thesis were obtained with the help of a visualization tool. This resource allows a user to experimentally infect vertices in two- and three-dimensional grids, and observe the step-by-step r-neighbor percolation process. As far as we are aware, such a tool did not previously exist for the problem of bootstrap percolation. In this section, we provide an overview of the functionality of this resource (which we refer to as the *visualizer*), and highlight features that could prove useful in further research. The visualizer is located at `https://ahblay.pythonanywhere.com`, and the reader is encouraged to examine the lethal sets presented in later chapters as they appear (although this is not necessary to understand the results).

2.3.1 Control panel

The basic functionality of the visualizer allows a user to enter the parameters of their problem, select a set of initially infected vertices, and step through the percolation process by time step. These options are made available to the user in a control panel, shown on the righthand side of Figure 2.2. The control panel features the following:

- A dropdown menu to choose between percolation on a grid, and percolation on a torus;
- Text boxes to enter the size of the grid (resp. torus);
- A text box to enter the threshold number of neighbors to spawn an infection;
- A submit button, which renders the chosen parameters as a grid of clickable gray circles;
- Buttons to initiate and step through the percolation process, and a checkbox to animate it;
- A button labeled "Improve percolation," which removes unnecessary infections (should they exist);
- An option to select from a list of existing lethal sets;
- A checkbox to reflect infected vertices;
- Buttons to upload/download an infected set as a text file.

We highlight the following: the design and representation of grids as matrices of clickable vertices, the choice between grid and torus, the "Improve percolation" button, the ability to view existing lethal sets as well as upload/download them, and the option to reflect the pattern of infected vertices.

One of the challenges of visualizing the problem of bootstrap percolation arises from the fact that many grids are large and of high dimension. This is perhaps the greatest limitation of the visualizer. The current iteration of the tool renders vertices as clickable regions in an HTML `canvas` element, which does not respond well to re-scaling. As a result, large grids contain very small vertices, which complicates the process of selecting an initial infection. Furthermore, `canvas` does not natively support three-dimensional structures, and so three-dimensional grids are simply rendered as a stack of their two-dimensional layers.

Users are able to select between percolation on a grid, and percolation on a torus. This choice does not impact the representation of the grid (resp. torus). However, when stepping through the phases of infection, vertices at the top of the grid are treated as neighbors of those on the bottom, and similarly for left and right.

In this chapter (and in Chapter 6) we saw (shall see) that certain patterns of infected vertices are always lethal. The fickleness of bootstrap percolation regularly precludes us from simply copying these patterns across all grids to obtain perfect lethal sets.

However, sometimes these patterns can be augmented with additional infections. If a set A_0 is lethal and above the surface area bound, the “Improve percolation” button attempts to remove non-essential infections. It does this by removing a random vertex v from A_0 and checking if the resulting set is lethal. If it is, the new infection $A_0 \setminus \{v\}$ is rendered on the screen.

In pursuit of determining new perfect lethal sets, it is often helpful to examine and alter existing ones. Whenever a user clicks “Run percolation” on a perfect lethal set, a text file containing the lethal configuration of vertices is stored in a database. This file is made accessible to all future users through the “Show optimal sets” window. We hope that ongoing use of this tool will passively allow for the accumulation of a number of lethal sets in two- and three-dimensions. In addition to accessing known lethal sets via the “Show optimal sets” button, users are able to upload sets from a local text file. These files must be configured as a sequence of X’s and O’s, with rows on new lines, and layers separated by a blank line. An example of this format can be obtained by creating an infected grid on the visualizer and selecting “Download .txt”.

The “Reflect top layer” checkbox is another resource designed to increase the efficiency of experimentally generating lethal sets. We have found in our research that certain grids, especially of the form $[a_1] \times [a_2] \times [2]$, have symmetric infections in their top and bottom layers. By choosing “Reflect top layer”, these symmetries are generated automatically.

2.3.2 Improvements

The visualization tool was developed primarily as a means to engage with the structure of lethal sets directly. Initially, it was intended as a private tool to help discern the often complex patterns in these sets. For this reason, it contains a number of quirks and bugs that were either treated as features, or ignored and never resolved. In this section, we discuss some of these issues and suggest possible improvements to make the tool useful to a broader audience.

As we discussed in the prior section, one limitation of HTML `canvas` elements is the inability to conveniently represent three dimensional objects. We circumvented this issue by representing grids as a sequence of two-dimensional layers. While this strategy is effective, it limits a user’s ability to clearly identify patterns that appear between these layers. Through experimentation, we found that toggling between different orientations of the grid allowed us to discover patterns that were otherwise hidden. In the current version of the visualizer, there is no convenient way to obtain different orientations of a grid. We propose an additional button that cycles through the d orientations of a grid. This feature would likely be simple to implement, and yield substantial results.

We also discussed the challenge of clicking on vertices in large grids, due to the inability to effectively zoom in on the `canvas` element. While the best solution to this problem likely requires a complete overhaul of the representation of the grid (using some other front-end library designed to better represent and interact with grid-like structures), an intermediate and simpler possibility is to improve the manner in which vertices are selected. In particular, we propose a change that allows sequences of vertices to be simultaneously selected by clicking and dragging. This should be fairly easy to implement, as one can track the `mouseDown` event in Javascript, and keep a list of the vertices that the cursor touches during this time.

When attempting to construct a lethal set, it is often the case that one begins with a particular configuration of vertices, and makes small changes to accommodate the particular parity or congruence class of the grid. One existing resource to aid in this process is the "Improve percolation" button. In its current state, this button is only able to remove unnecessary vertices from already lethal sets. However, it would we useful if it could also augment existing sets in such a way that they become more infectious. This could take the form of either adding vertices to infectious sets that are below the surface area bound, or changing the position of existing infections to increase the infectiousness of the initial set.

In a similar vein, recall that sets A_0 in non-divisibility cases contain vertices that experience infection from more than r neighbors. If the size of A_0 is well above the surface area bound, the location of such vertices can provide a good indication of where improvements in the structure of A_0 are likely to be found. One possible implementation could be to highlight vertices that do not realize their "infectious potential".

From a cosmetic perspective, the presentation of existing perfect lethal sets is currently difficult to parse and should be improved. We suggest that these files be arranged by the number of layers in the grid. Additionally, there is currently no capacity to represent and store constructions that apply to large families of grids. We currently provide large example files that clearly exhibit a repeating pattern. However, this choice is both less convenient and less convincing.

In the following chapter, we present a useful technique for constructing perfect lethal sets on large grids from known lethal constructions. This idea will prove essential in our proof of Theorem 1.7.

Chapter 3
A Recursive Technique

In the previous chapter, we examined some structures in grids that, if present, immediately guarantee lethality. Most significantly, we proved that lethal sets on mutually orthogonal walls of a grid are lethal on the entire grid. In the following sections, we leverage this result to show that certain configurations of fully infected sub-grids (which we shall call blocks) will cause the larger grid to become infected. Furthermore, we show that, if each of these smaller blocks is infected with a minimum lethal set, then the composite larger brick will also be infected with a minimum lethal set (barring some divisibility considerations).

3.1 The Recursion

The proof of this claim makes use of the so-called *modified bootstrap process* in $[n]^d$, studied by Holroyd in [15] and [16]. This is a strengthened variation of the problem introduced in Chapter 1, whereby vertices in the $[n]^d$ grid become infected if and only if they are adjacent to infected vertices along edges in each of the d directions. For example, in the $[n]^2$ grid, a vertex that sees infection in one of both the North/South and East/West directions will itself become infected, whereas a vertex with infected neighbors only to the East and West will not.

In particular, the following lemma considers composite grids $[n]^d$ where each vertex $\mathbf{x} = (x_1, \ldots, x_d) \in [n]^d$ is itself a smaller block. We prove that lethal sets on these grids can be built from the smaller lethal sets on each component block.

Lemma 3.1. *For $n, d \geq 1$, let $A = (a_{i,j})$ be a $d \times n$ matrix of positive integers, and let $b_i = \sum_{j=1}^{n} a_{i,j}$, for $1 \leq i \leq d$. Let S be a lethal set under the modified process on $[n]^d$, and for each vertex $\mathbf{x} = (x_1, \ldots, x_v) \in S$, let $T_{\mathbf{x}}$ be a lethal set on $\prod_{i=1}^{d} [a_{i,x_i}]$ under d-neighbor percolation. Then*

$$m(b_1, \ldots, b_d, d) \leq \sum_{\mathbf{x} \in S} |T_{\mathbf{x}}|.$$

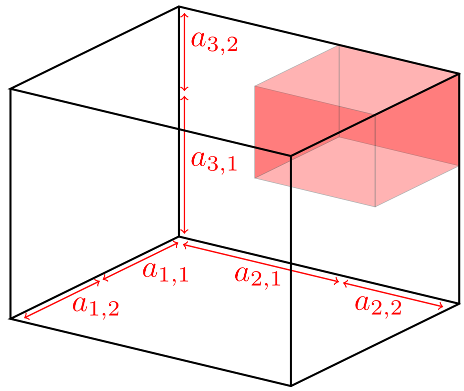

Figure 3.1: A recursively constructed $[b_1] \times [b_2] \times [b_3]$ grid, for $n = 2$, $d = 3$.

Proof. We sub-divide the $\prod_{i=1}^{d}[b_i]$ brick into smaller blocks by partitioning each of the d axes into segments $a_{i,1}, a_{i,2}, \ldots, a_{i,n}$, $1 \le i \le d$. Each block is given by a unique product of these segments, and represented by a vector $\mathbf{x} = (x_1, \ldots, x_d) \in [n]^d$. Formally, for each such $\mathbf{x}$, let $G_{\mathbf{x}}$ be the block with vertex set

$$\prod_{i=1}^{d} \left\{ 1 + \sum_{j=1}^{x_i - 1} a_{i,j}, \ldots, \sum_{j=1}^{x_i} a_{i,j} \right\},$$

and edges between vertices that differ by one in exactly one coordinate. Figure 3.1 illustrates the block $G_{\mathbf{x}}$ for $\mathbf{x} = (1, 2, 2) \in [2]^3$. Observe that $G_{\mathbf{x}}$ is isomorphic to $\prod_{i=1}^{d}[a_{i,x_i}]$.

For each $\mathbf{x} \in S$, let $A_{\mathbf{x}}$ be the vertices of $G_{\mathbf{x}}$ corresponding to the vertices of $T_{\mathbf{x}}$ under isomorphism from $\prod_{i=1}^{d}[a_{i,x_i}]$ to $G_{\mathbf{x}}$, and let $A_0 = \cup A_{\mathbf{x}}$. Observe that $|A_0| = \sum_{\mathbf{x} \in S} |T_{\mathbf{x}}|$. We show that A_0 is lethal on $\prod_{i=1}^{d}[b_i]$.

By the definition of $T_{\mathbf{x}}$, for each $\mathbf{x} \in S$, $A_{\mathbf{x}}$ is lethal on $G_{\mathbf{x}}$. Run the d-neighbor process until all blocks $G_{\mathbf{x}}$ are fully infected. We claim that this is sufficient to infect all remaining vertices of $\prod_{i=1}^{d}[b_i]$. Consider the remaining blocks $G_{\mathbf{x}}$, for $\mathbf{x} \in [n]^d \setminus S$. Since S is lethal under the modified process, at some point in the infection process each $G_{\mathbf{x}}$ is adjacent to fully infected blocks in all d directions. By Corollary 2.8, this is sufficient to infect all the vertices of $G_{\mathbf{x}}$. Repeating this process on each uninfected region of $\prod_{i=1}^{d}[b_i]$ (as they are exposed under the modified process) ultimately results in all vertices becoming infected. This completes the proof. □

We note that although the lemma above is true in full generality, we only apply it in the particular case where $n = 2$ and $d = 3$. The following corollary proves that the bound in Lemma 3.1 is tight for $n = 2$ and $d = 3$, provided that the lethal sets on at least three of the constituent blocks are perfect.

Corollary 3.2. *Let $A = (a_{i,j})$ be a 3×2 matrix of positive integers, and let $b_i = a_{i,1} + a_{i,2}$*

for all $1 \leq i \leq 3$*. Then* $m(b_1, b_2, b_3, 3)$ *is at most*

$$m(a_{1,1}, a_{2,1}, a_{3,1}, 3) + m(a_{1,2}, a_{2,2}, a_{3,1}, 3) + m(a_{1,2}, a_{2,1}, a_{3,2}, 3) + m(a_{1,1}, a_{2,2}, a_{3,2}, 3).$$

Furthermore, this bound is tight if at least three of $\{(a_{1,1}, a_{2,1}, a_{3,1}),\ (a_{1,2}, a_{2,2}, a_{3,1}),\ (a_{1,2}, a_{2,1}, a_{3,2}),\ (a_{1,1}, a_{2,2}, a_{3,2})\}$ *are perfect.*

Proof. The upper bound on $m(b_1, b_2, b_3, 3)$ is a direct consequence of Lemma 3.1, since the set $\{(1,1,1), (2,2,1), (2,1,2), (1,2,2)\}$ of vertices is lethal under the modified process on $[2]^3$.

If all constituent grids are perfect, then:

$$\begin{aligned}
&m(a_{1,1}, a_{2,1}, a_{3,1}, 3) + m(a_{1,2}, a_{2,2}, a_{3,1}, 3) + m(a_{1,2}, a_{2,1}, a_{3,2}, 3) + m(a_{1,1}, a_{2,2}, a_{3,2}, 3) \\
&= \frac{a_{1,1}a_{2,1} + a_{2,1}a_{3,1} + a_{3,1}a_{1,1}}{3} + \frac{a_{1,2}a_{2,2} + a_{2,2}a_{3,1} + a_{3,1}a_{1,2}}{3} \\
&\qquad + \frac{a_{1,2}a_{2,1} + a_{2,1}a_{3,2} + a_{3,2}a_{2,1}}{3} + \frac{a_{1,1}a_{2,2} + a_{2,2}a_{3,2} + a_{3,2}a_{1,1}}{3} \\
&= \frac{(a_{1,1} + a_{1,2})(a_{2,1} + a_{2,2}) + (a_{2,1} + a_{2,2})(a_{3,1} + a_{3,2}) + (a_{3,1} + a_{3,2})(a_{1,1} + a_{1,2})}{3} \\
&= \frac{b_1b_2 + b_2b_3 + b_3b_1}{3}.
\end{aligned}$$

Similarly, suppose, without loss of generality, that $(a_{1,1}, a_{2,1}, a_{3,1})$ is optimal and the remaining grids are perfect. Then:

$$\begin{aligned}
&m(a_{1,1}, a_{2,1}, a_{3,1}, 3) + m(a_{1,2}, a_{2,2}, a_{3,1}, 3) + m(a_{1,2}, a_{2,1}, a_{3,2}, 3) + m(a_{1,1}, a_{2,2}, a_{3,2}, 3) \\
&= \left\lceil \frac{a_{1,1}a_{2,1} + a_{2,1}a_{3,1} + a_{3,1}a_{1,1}}{3} \right\rceil + \frac{a_{1,2}a_{2,2} + a_{2,2}a_{3,1} + a_{3,1}a_{1,2}}{3} \\
&\qquad + \frac{a_{1,2}a_{2,1} + a_{2,1}a_{3,2} + a_{3,2}a_{2,1}}{3} + \frac{a_{1,1}a_{2,2} + a_{2,2}a_{3,2} + a_{3,2}a_{1,1}}{3} \\
&= \left\lceil \frac{(a_{1,1} + a_{1,2})(a_{2,1} + a_{2,2}) + (a_{2,1} + a_{2,2})(a_{3,1} + a_{3,2}) + (a_{3,1} + a_{3,2})(a_{1,1} + a_{1,2})}{3} \right\rceil \\
&= \left\lceil \frac{b_1b_2 + b_2b_3 + b_3b_1}{3} \right\rceil.
\end{aligned}$$

In both cases, we obtain an upper bound on $m(b_1, b_2, b_3, 3)$ matching the lower surface area bound. This completes the proof. □

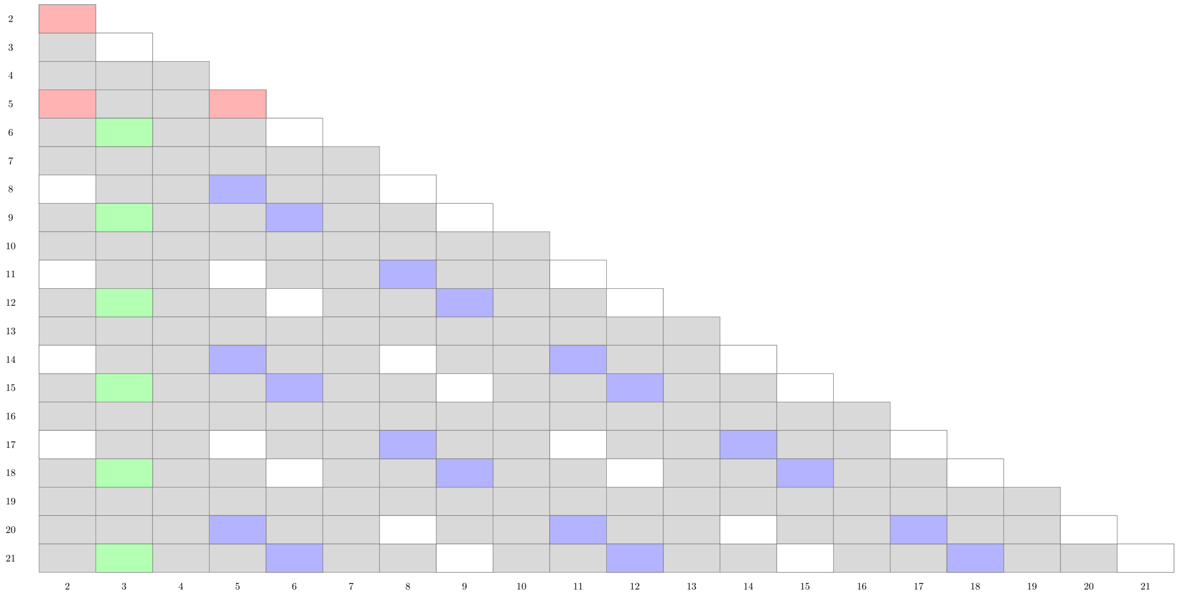

Table 3.1: Thickness 2 constructions used in the proof of Theorem 1.7. Blue and green cells represent infinite families of constructions. Red cells are individual constructions. Divisibility cases are white and non-divisibility cases are gray.

3.2 Building Blocks

Corollary 3.2 provides a prescriptive method for constructing optimal and perfect lethal sets recursively, provided the existence of sufficiently many small building blocks. In the following chapter, we use this technique to obtain perfect lethal sets on all $G(b_1, b_2, b_3)$ grids, for $b_1, b_2, b_3 \geq 5$, and optimal lethal sets on all $G(b_1, b_2, b_3)$ grids, for $b_1, b_2, b_3 \geq 11$. To facilitate this process, we first summarize some useful families of lethal sets, as well as particular applications of Corollary 3.2 that hold for general grids. We note that the existence of these families is predicated on a number of constructions, which are analyzed in greater detail in Chapter 6. A summary of the lethal sets obtained in Propositions 3.3 – 3.10 is illustrated in Tables 3.1, 3.2, and 3.3)

Proposition 3.3. *For all $k \geq 1$ such that $k \neq 2$, $(3, 3, k)$ is perfect.*

Proof. We obtain $(3, 3, k)$ for $k \equiv 0 \pmod 2$ and $k > 2$ from Construction 6.8, and $(3, 3, k)$ for $k \equiv 1 \pmod 2$ and $k > 2$ from Construction 6.9. The case of $(3, 3, 1)$ is given in Benevides et al. [7], and reproduced as Construction 5.7. □

Proposition 3.4. *For all $k \equiv 0 \pmod 6$ such that $k > 3$, $(k, 2, 3)$ is perfect.*

Proof. We obtain $(k, 2, 3)$ for $k \equiv 0 \pmod 6$ and $k > 3$ from Construction 6.5. □

Proposition 3.5. *For all $k \geq 2$, $(3, 6, k)$ is perfect.*

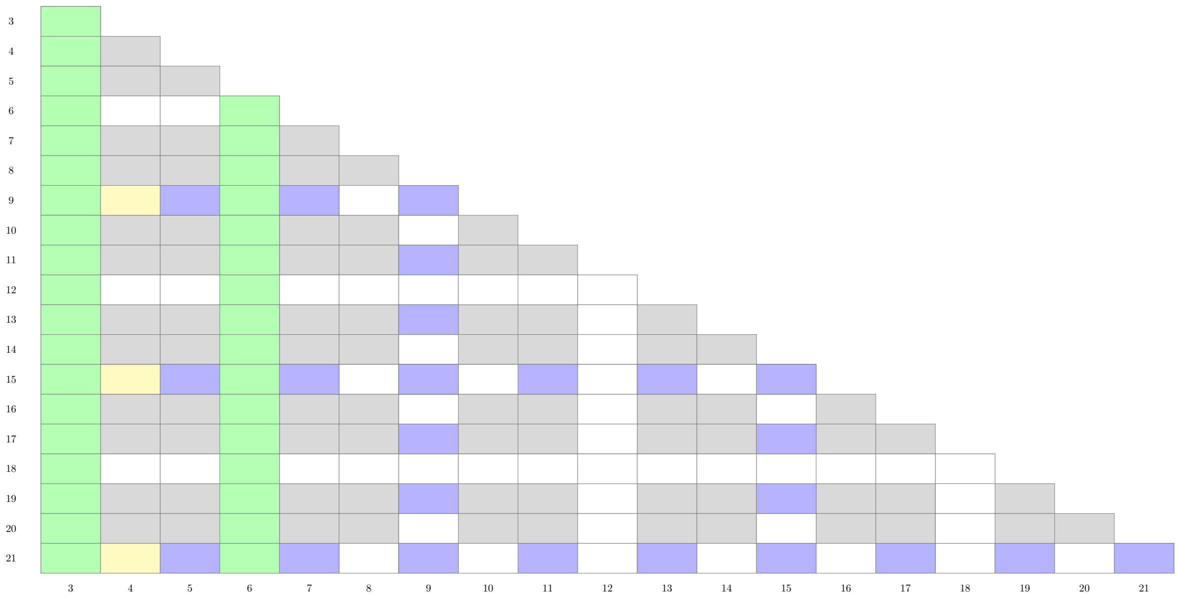

Table 3.2: Thickness 3 constructions used in the proof of Theorem 1.7. Blue, green and yellow cells represent infinite families of constructions. Divisibility cases are white and non-divisibility cases are gray.

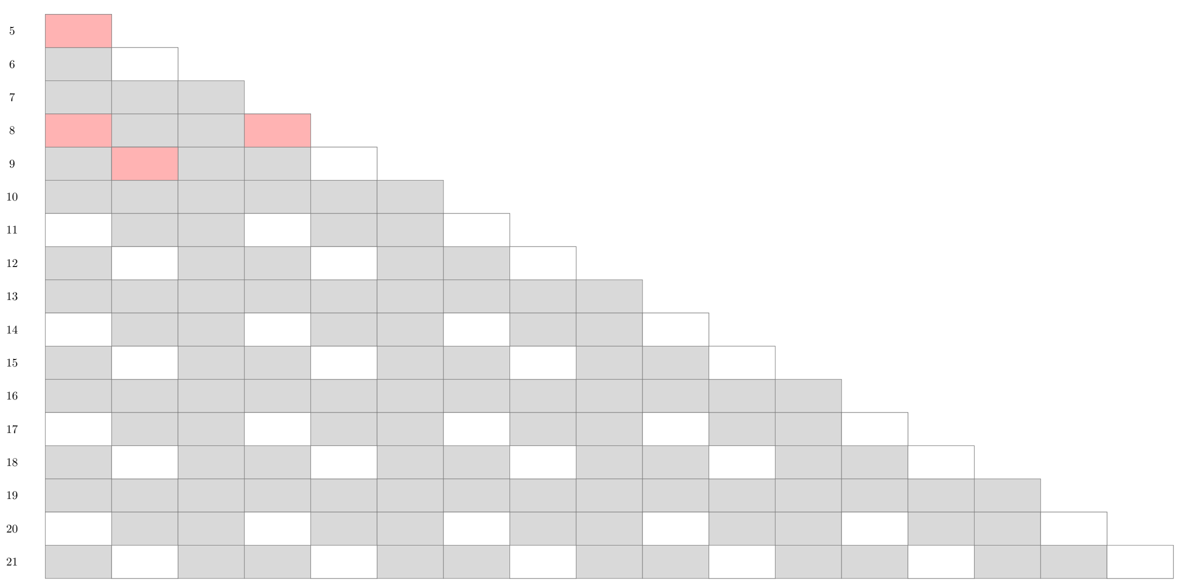

Table 3.3: Thickness 5 constructions used in the proof of Theorem 1.7. Red cells are individual constructions. Divisibility cases are white and non-divisibility cases are gray.

Proof. We obtain $(3,6,k)$ for $k \equiv 0 \pmod 2$ and $k \geq 4$ from Construction 6.11, and $(3,6,k)$ for $k \equiv 1 \pmod 2$ and $k \geq 5$ from Construction 6.9. The remaining tuples $(3,6,2)$ and $(3,6,3)$ are obtained from Propositions 3.4 and 3.3. ☐

Proposition 3.6. *For all $k \equiv 3 \pmod 6$ and $l \equiv 1 \pmod 2$ such that $l > 1$, $(3,k,l)$ is perfect.*

Proof. We obtain such tuples from Construction 6.9. ☐

Proposition 3.7. *For all $k, l \in \{0,2,3,5\} \pmod 6$ such that $k \not\equiv l \pmod 6$, $k \equiv l \pmod 3$, and $k, l > 2$, $(k,l,2)$ is perfect.*

Proof. We obtain $(k,l,2)$ for $k,l \in \{2,5\} \pmod 6$ such that $k \not\equiv l \pmod 6$ and $k,l > 2$ from Construction 6.6. We obtain $(k,l,2)$ for $k,l \in \{0,3\} \pmod 6$ such that $k \not\equiv l \pmod 6$ and $k,l \geq 6$ from Construction 6.7. The remaining tuples are of the form $(k,3,2)$ for $k \equiv 0 \pmod 6$ and these are obtained from Construction 6.5. ☐

Proposition 3.8. *For all $k \equiv 3 \pmod 6$, $(k,4,3)$ is perfect.*

Proof. We obtain $(k,4,3)$ for $k \equiv 3 \pmod 6$ and $k \geq 9$ from Construction 6.10. The case of $(4,3,3)$ is given by Proposition 3.3. ☐

Proposition 3.9. *For all $k \equiv 3 \pmod 6$ such that $k > 3$, $(k,2,3)$ is perfect.*

Proof. We obtain $(k,2,3)$ for $k \equiv 3 \pmod 6$ and $k > 3$ from Construction 6.4. ☐

Proposition 3.10. *For all $k \geq 1$, $(2^k - 1, 2^k - 1, 1)$ is perfect.*

Proof. The construction for such tuples is presented in [7] and reproduced as Construction 5.7. ☐

Combining the above propositions with Corollary 3.2, we are able to obtain the following lemmas.

Lemma 3.11. *Suppose (b_1, b_2, b_3) is optimal and $b_1, b_2, b_3 \neq 2$. Then (b_1+3, b_2+3, b_3+3) is optimal.*

Proof. By Proposition 3.3, each of $(b_1,3,3), (3,b_2,3), (3,3,b_3)$ is perfect. Therefore, by Corollary 3.2, (b_1+3, b_2+3, b_3+3) is optimal. ☐

Lemma 3.12. *Suppose (b_1, b_2, b_3) is optimal, $b_1, b_2 \geq 2$, and $b_3 \neq 2$. Then (b_1+3, b_2+3, b_3+6) is optimal.*

Proof. By assumption, (b_1, b_2, b_3) is optimal. Both of $(b_1,3,6)$ and $(3,b_2,6)$ are perfect by Proposition 3.5. By Proposition 3.3, $(3,3,b_3)$ is perfect. Therefore, by Corollary 3.2, (b_1+3, b_2+3, b_3+6) is optimal. ☐

In the following chapter, we shall see that the existence of the perfect lethal sets on the families of grids presented above, coupled with Corollary 3.2, is enough to prove Theorem 1.7. Speaking analogically, Propositions 3.3 – 3.10 (and the individual constructions in Appendix A) are the atomic pieces required to generate all molecular lethal sets. It should be noted that the atomic constructions used in this thesis are in no way special; there is likely a simpler combination of constructed lethal sets that also generates all grids $G(a_1, a_2, a_3)$, for $a_1, a_2, a_3 \geq 11$. These are simply the constructions that we were able to obtain. It would be interesting to determine, in general, the smallest number of constructed lethal sets required to build all other lethal sets in d-dimensional grids using Corollary 3.2.

Chapter 4
Grids with Side Length at Least Five

Recall from Definition 2.1 that $G(a_1, a_2, a_3)$ represents the $[a_1] \times [a_2] \times [a_3]$ grid G, and that $\min\{a_1, a_2, a_3\}$ is the thickness of G. For example, the tuple $G(5, 3, 3)$ represents the thickness 3 grid $[5] \times [3] \times [3]$. In the following lemmas, we use the notation $(a_1, a_2, a_3)+(x_1, x_2, x_3) = (a_1+x_1, a_2+x_2, a_3+x_3)$ to represent an instance of Corollary 3.2 on the 3×2 matrix A:

$$A = \begin{bmatrix} a_1 & x_1 \\ a_2 & x_2 \\ a_3 & x_3 \end{bmatrix}.$$

For example, the expression $(5, 3, 3) + (3, 3, 3)$ indicates an application of Corollary 3.2, using the matrix $A = \left[\begin{smallmatrix} 5 & 3 & 3 \\ 3 & 3 & 3 \end{smallmatrix}\right]^T$, to obtain the tuple $(8, 6, 6)$.

We shall call a thickness *complete* if it can be shown that all divisibility cases in that thickness admit perfect lethal sets. In this section, we demonstrate that thickness 5, thickness 6 and thickness 7 are all complete. As these belong to the residue classes 2, 0, and 1 modulo 3, respectively, we then use Lemma 3.11 to show that all larger grids are also complete.

4.1 Completeness of Thickness 5

We show that all divisibility cases for grids of thickness 5 admit perfect lethal sets. Observe that divisibility cases for thickness 5 consist of grids $G(x, y, 5)$ where x and y are in residue classes $\{0, 2, 3, 5\}$ modulo 6 (see Table 4.1). We separate these divisibility cases into the following four cases and show that each case is complete:

1. $G(x, 5, 5)$ for $x \in \{2, 5\} \pmod 6$ and $x \geq 5$;
2. $G(x, 6, 5)$ for $x \in \{0, 3\} \pmod 6$ and $x \geq 5$;
3. $G(x, y, 5)$ for $x, y \in \{0, 2, 3, 5\} \pmod 6$, $x \not\equiv y \pmod 6$ and $x \geq 5$;
4. $G(x, y, 5)$ for $x, y \in \{0, 2, 3, 5\} \pmod 6$, $x \equiv y \pmod 6$ and $x \geq 5$;

	5	6	7	8	9	10	11	12	13	14	15	16	17
5	1												
6		2											
7													
8	1			4									
9		2			4								
10													
11	1			3			4						
12		2			3			4					
13													
14	1			4			3			4			
15		2			4			3			4		
16													
17	1			3			4			3			4

Table 4.1: The four thickness 6 cases analyzed in Lemmas 4.1 (blue), 4.2 (green), 4.3 (red), and 4.4 (yellow).

Lemma 4.1. *All grids $G(x, 5, 5)$ for $x \in \{2, 5\} \pmod 6$ and $x \geq 5$ admit perfect lethal sets.*

Proof. Consider $(5, 2, 2) + (a, 3, 3)$, for $a \equiv 0 \pmod 3$ and $a > 3$. Observe that $(5 + a, 5, 5)$ obtains all grids of the form described in Case 1, apart from $G(5, 5, 5)$ and $G(8, 5, 5)$.

By Corollary 3.2, it suffices to show that $(5, 2, 2), (5, 3, 3), (a, 2, 3), (a, 3, 2)$ are all perfect. We have that $(5, 2, 2)$ is perfect by Construction A.2 in Appendix A, and $(5, 3, 3)$ is given by Proposition 3.3. Since $a > 3$, Propositions 3.4 and 3.9 give $(a, 2, 3)$.

By Theorem 1.6 and Construction A.5 in Appendix A, we obtain the remaining grids $(5, 5, 5)$ and $(8, 5, 5)$, respectively. We conclude that all grids in Case 1 admit perfect lethal sets. $\square$

Lemma 4.2. *All grids $G(x, 6, 5)$ for $x \in \{0, 3\} \pmod 6$ and $x \geq 5$ admit perfect lethal sets.*

Proof. Consider $(6, 3, 2) + (a, 3, 3)$, for $a \equiv 0 \pmod 3$ and $a > 3$. Observe that $(6 + a, 6, 5)$ obtains all grids of the form described in Case 2, apart from $G(6, 6, 5)$ and $G(9, 6, 5)$.

By Corollary 3.2, we must show that $(6, 3, 2), (6, 3, 3), (a, 3, 3), (a, 3, 2)$ are all perfect. Since $a > 3$, $(6, 3, 2)$ and $(a, 3, 2)$ are given by Propositions 3.4 and 3.9. Similarly, $(6, 3, 3)$ and $(a, 3, 3)$ are given by Proposition 3.3.

To obtain $(6, 6, 5)$, we consider $(3, 3, 1) + (3, 3, 4)$. By Corollary 3.2, we must show that $(3, 3, 1), (3, 3, 4), (3, 3, 4), (3, 3, 1)$ are all perfect. These are obtained, respectively, by Propositions 3.3 and 3.8. Construction A.6 gives $(9,6,5)$. We conclude that all grids in Case 2 admit perfect lethal sets. $\square$

Lemma 4.3. *All grids $G(x,y,5)$ for $x,y \in \{0,2,3,5\} \pmod 6$, $x \not\equiv y \pmod 6$, and $x,y \geq 5$ admit perfect lethal sets.*

Proof. Consider $(a,b,2)+(6,6,3)$, for $a,b \in \{0,2,3,5\} \pmod 6$, $a \not\equiv b \pmod 6$, and $a,b > 2$. Observe that $(a+6,b+6,5)$ obtains all grids of the form described in Case 3, apart from $G(a,8,5)$ for $a \equiv 5 \pmod 6$ and $a \geq 11$.

By Corollary 3.2, we must show that $(a,b,2),(a,6,3),(6,b,3),(6,6,2)$ are all perfect. By Proposition 3.7, $(a,b,2)$ is perfect. Both $(a,6,3)$ and $(6,b,3)$ follow from Proposition 3.5. We obtain $(6,6,2)$ from $(3,3,1)+(3,3,1)$. By Proposition 3.10, $(3,3,1)$ is perfect, and so by Corollary 3.2, $(6,6,2)$ is perfect.

To obtain $(a,8,5)$, for $a \equiv 5 \pmod 6$ and $a \geq 17$, we consider $(8,5,2)+(a,3,3)$, for $a \equiv 3 \pmod 6$ and $a > 3$. By Corollary 3.2, we must show that $(8,5,2)$, $(8,3,3)$, $(a,5,3)$, $(a,2,3)$ are all perfect. We obtain $(8,5,2)$ from Proposition 3.7 and $(8,3,3)$ from Proposition 3.3. Since $a \equiv 3 \pmod 6$, Proposition 3.6 gives $(a,5,3)$, and Proposition 3.9 gives $(a,2,3)$.

The above argument omits the singular grid $(11,8,5)$. However, we may obtain $(11,8,5)$ from $(2,3,6)+(3,5,5)$. By Corollary 3.2, we must show that $(2,3,6)$, $(2,5,5)$, $(3,3,5)$, $(3,5,6)$ are all perfect. We obtain $(2,5,5)$ from Construction A.3, $(3,3,5)$ from Proposition 3.3, and $(2,3,6)$ and $(3,5,6)$ from Proposition 3.5. We conclude that all grids in Case 3 admit perfect lethal sets. $\square$

Lemma 4.4. *All grids $G(x,y,5)$ for $x,y \in \{0,2,3,5\} \pmod 6$, $x \equiv y \pmod 6$, and $x \geq 5$ admit perfect lethal sets.*

Proof. Consider $(a,b,2)+(6,3,3)$, for $a,b \in \{0,2,3,5\} \pmod 6$, $a \not\equiv b \pmod 6$, and $a,b > 2$. Observe that $(a+6,b+3,5)$ obtains all grids of the form described in (4), apart from $(8,8,5)$.

By Corollary 3.2, we must show that the grids $(a,b,2),(a,3,3),(6,b,3),(6,3,2)$ are all perfect. By Proposition 3.7, $(a,b,2)$ is perfect. Both $(6,3,2)$ and $(6,b,3)$ follow from Proposition 3.5. We obtain $(a,3,3)$ from Proposition 3.3.

To obtain $(8,8,5)$, we consider the construction $(2,2,2)+(6,6,3)$. By Corollary 3.2, we must show that $(2,2,2),(2,6,6),(3,2,6),(3,6,2)$ are all perfect. We obtain $(2,2,2)$ from Theorem 1.6 and $(3,6,2)$ from Proposition 3.5. The construction $(3,3,1)+(3,3,1)$ gives $(6,6,2)$. By Proposition 3.10, $(3,3,1)$ is perfect, and so by Corollary 3.2, $(6,6,2)$ is perfect. We conclude that all grids of the form given in (3) admit perfect lethal sets. $\square$

Lemma 4.5. *Thickness 5 is complete.*

Proof. By Lemmas 4.1, 4.2, 4.3, and 4.4, all divisibility cases for thickness 5 admit perfect lethal sets. $\square$

	6	7	8	9	10	11	12	13	14	15	16	17	18
6	1												
7	4												
8	1												
9		2	3	2									
10	1			3									
11	4			2									
12	1	4	1		1	4	1						
13	4			2			4						
14	1			3			1						
15		2	3	2	3	2		2	3	2			
16	1			3			1			3			
17	4			2			4			2			
18	1	4	1		1	4	1	4	1		1	4	1

Table 4.2: The four thickness 6 cases analyzed in Lemmas 4.6 (blue), 4.7 (green), 4.8 (red), and 4.9 (yellow).

4.2 Completeness of Thickness 6

We show that all divisibility cases for grids of thickness 6 admit perfect lethal sets. Observe that divisibility cases for thickness 6 consist of grids $G(x, y, 6)$ where, without loss of generality, x is in residue classes $\{0, 3\}$ modulo 6, and y is either even or odd (see Table 4.2). We separate these divisibility cases into the following four cases and show that each case is complete:

1. $G(x, y, 6)$ for $x \equiv 0 \pmod 6$, $y \equiv 0 \pmod 2$, and $x, y \geq 6$;

2. $G(x, y, 6)$ for $x \equiv 3 \pmod 6$, $y \equiv 1 \pmod 2$, and $x, y \geq 6$;

3. $G(x, y, 6)$ for $x \equiv 3 \pmod 6$, $y \equiv 0 \pmod 2$, and $x, y \geq 6$;

4. $G(x, y, 6)$ for $x \equiv 0 \pmod 6$, $y \equiv 1 \pmod 2$, and $x, y \geq 6$.

Lemma 4.6. *All grids $G(x, y, 6)$ for $x \equiv 0 \pmod 6$, $y \equiv 0 \pmod 2$, and $x, y \geq 6$ admit perfect lethal sets.*

Proof. Consider $(3n, m, 3) + (3, 3, 3)$, for $n, m \equiv 1 \pmod 2$ and $m > 1$. Observe that $(3n + 3, m + 3, 6)$ obtains all grids of the form described in Case 1.

By Corollary 3.2, we must show that $(3n, m, 3), (3n, 3, 3), (3, m, 3), (3, 3, 3)$ are all perfect. By Proposition 3.6, $(3n, m, 3)$ is perfect for all $m > 1$. Since $n, m \neq 2$, $(3n, 3, 3), (3, m, 3), (3, 3, 3)$ are all perfect by Proposition 3.3. We conclude that all grids in Case 1 admit perfect lethal sets. □

Lemma 4.7. *All grids* $G(x, y, 6)$ *for* $x \equiv 3 \pmod 6$*,* $y \equiv 1 \pmod 2$*, and* $x, y \geq 6$ *admit perfect lethal sets.*

Proof. Consider $(3n, m, 3) + (6, 6, 3)$, for $n, m \equiv 1 \pmod 2$ and $m > 1$. Observe that $(3n+6, m+6, 6)$ obtains all grids of the form described in Case 2, apart from $G(x, 7, 6)$, for $x \equiv 3 \pmod 6$ and $x \geq 9$.

By Corollary 3.2, we must show that $(3n, m, 3), (3n, 6, 3), (6, m, 3), (6, 6, 3)$ are all perfect. By Proposition 3.6, $(3n, m, 3)$ is perfect for all $m > 1$. Since $n, m > 1$, $(3n, 6, 3), (6, m, 3), (6, 6, 3)$ are all perfect by Proposition 3.5.

To obtain $(x, 7, 6)$, for $x \equiv 3 \pmod 6$ and $x \geq 9$, we consider $(6, 3, 3) + (x-6, 4, 3)$. By Corollary 3.2, we must show that $(6, 3, 3), (6, 4, 3), (x-6, 3, 3), (x-6, 4, 3)$ are all perfect. We obtain $(6, 3, 3)$ and $(x-6, 3, 3)$ from Proposition 3.5. Proposition 3.5 gives $(6, 4, 3)$. Proposition 3.8 gives $(x-6, 4, 3)$. We conclude that all grids in Case 2 admit perfect lethal sets. $\square$

Lemma 4.8. *All grids* $G(x, y, 6)$ *for* $x \equiv 3 \pmod 6$*,* $y \equiv 0 \pmod 2$*, and* $x, y \geq 6$ *admit perfect lethal sets.*

Proof. Consider $(3n, m, 3) + (6, 3, 3)$, for $n, m \equiv 1 \pmod 2$ and $m > 1$. Observe that $(3n+6, m+3, 6)$ obtains all grids of the form described in Case 3.

By Corollary 3.2, we must show that $(3n, m, 3), (3n, 3, 3), (6, m, 3), (6, 3, 3)$ are all perfect. By Proposition 3.6, $(3n, m, 3)$ is perfect for all $m > 1$. Since $m \neq 2$, $(6, m, 3), (6, 3, 3)$ are both perfect by Proposition 3.3. We obtain $(3n, 3, 3)$ by Proposition 3.3. We conclude that all grids in Case 3 admit perfect lethal sets. $\square$

Lemma 4.9. *All grids* $G(x, y, 6)$*, where* $x \equiv 0 \pmod 6$*,* $y \equiv 1 \pmod 2$*, and* $x, y \geq 6$ *admit perfect lethal sets.*

Proof. Consider $(3n, m, 3) + (3, 6, 3)$, for $n, m \equiv 1 \pmod 2$ and $m > 1$. Observe that $(3n+3, m+6, 6)$ obtains all grids described in Case 3, apart from $G(x, 7, 6)$, for $x \equiv 0 \pmod 6$ and $x \geq 6$.

By Corollary 3.2, we must show that $(3n, m, 3)$, $(3n, 6, 3)$, $(3, m, 3), (3, 6, 3)$ are all perfect. By Proposition 3.6, $(3n, m, 3)$ is perfect for all $m > 1$. Since $n, m > 1$, $(3n, 6, 3)$ and $(3, 6, 3)$ are both perfect by Proposition 3.5. Similarly, $(3, m, 3)$ is perfect by Proposition 3.3.

To obtain $(x, 7, 6)$, for $x \equiv 0 \pmod 6$ and $x \geq 6$, we consider $(3, 3, 3) + (x-3, 4, 3)$. By Corollary 3.2, we must show that $(3, 3, 3), (3, 4, 3), (x-3, 3, 3), (x-3, 4, 3)$ are all perfect. We obtain $(3, 3, 3), (3, 4, 3)$ and $(x-3, 3, 3)$ from Proposition 3.3. Since $x \equiv 0 \pmod 6$, Proposition 3.8 gives $(x-3, 4, 3)$. We conclude that all grids given in Case 4 admit perfect lethal sets. $\square$

Lemma 4.10. *Thickness 6 is complete.*

	7	8	9	10	11	12	13	14	15	16	17	18	19
7	1												
8													
9			3										
10	2			1									
11													
12			4			3							
13	1			2			1						
14													
15			3			4			3				
16	2			1			2			1			
17													
18			4			3			4			3	
19	1			2			1			2			1

Table 4.3: The four thickness 7 cases analyzed in Lemmas 4.11 (blue), 4.12 (green), 4.13 (red), and 4.14 (yellow).

Proof. All divisibility cases for thickness 6 are grids $G(x, y, 6)$ such that at least one of $\{x, y\}$ is congruent to 0 modulo 3. Lemmas 4.6, 4.7, 4.8, and 4.9 cover all such cases. The result follows. $\square$

4.3 Completeness of Thickness 7

We show that all divisibility cases for grids of thickness 7 admit perfect lethal sets. Observe that divisibility cases for thickness 7 consist of grids $G(x, y, 7)$ for x, y in residue classes $\{0, 1, 3, 4\}$ modulo 6 (see Table 4.3). We separate these divisibility cases into the following four cases and show that each case is complete:

1. $G(x, y, 7)$ for $x, y \in \{1\} \pmod 3$, $x \equiv y \pmod 6$, and $x, y \geq 7$;
2. $G(x, y, 7)$ for $x, y \in \{1\} \pmod 3$, $x \not\equiv y \pmod 6$, and $x, y \geq 7$;
3. $G(x, y, 7)$ for $x, y \in \{0\} \pmod 3$, $x \equiv y \pmod 6$, and $x, y \geq 7$;
4. $G(x, y, 7)$ for $x, y \in \{0\} \pmod 3$, $x \not\equiv y \pmod 6$, and $x, y \geq 7$.

Lemma 4.11. *All grids $G(x, y, 7)$ for $x, y \in \{1, 4\}$, $x \equiv y \pmod 6$, and $x, y \geq 7$ admit perfect lethal sets.*

Proof. Consider $(a, b, 2) + (8, 5, 5)$ for $a, b \in \{2, 5\} \pmod 6$, $a \not\equiv b \pmod 6$, and $a, b > 2$. Observe that $(a + 8, b + 5, 7)$ obtains all grids described in Case 1 above, apart from $G(10, 10, 7)$ and $G(a, 7, 7)$, for $a \equiv 1 \pmod 6$.

By Corollary 3.2, we must show that $(a, b, 2), (a, 5, 5), (8, b, 5), (8, 5, 2)$ are all perfect. By Proposition 3.7, $(a, b, 2)$ and $(8, 5, 2)$ are perfect. By Lemma 4.5, $(a, 5, 5)$ and $(8, b, 5)$ are perfect.

To obtain $(a, 7, 7)$, for $a \equiv 1 \pmod 6$ and $a \geq 7$, we consider $(4, 4, 4) + (a-4, 3, 3)$. By Corollary 3.2, we must show that $(4, 4, 4), (4, 3, 3), (a-4, 4, 3), (a-4, 3, 4)$ are all perfect. By Theorem 1.6, we have that $(2, 2, 2)$ and $(4, 4, 4)$ are perfect. Proposition 3.3 gives $(4, 3, 3)$. Since $a - 4 \equiv 3 \pmod 6$, we obtain $(a-4, 4, 3)$ from Proposition 3.8.

To obtain $(10, 10, 7)$, consider $(5, 5, 5) + (5, 5, 2)$. By Corollary 3.2, we must show that $(5, 5, 5), (5, 5, 2), (5, 5, 2), (5, 5, 5)$ are all perfect. Lemma 4.5 gives us $(5, 5, 5)$, and Construction A.3 gives us $(5, 5, 2)$. We conclude that all grids in Case 1 admit perfect lethal sets. $\square$

Lemma 4.12. *All grids $G(x, y, 7)$ for $x, y \in \{1, 4\}$, $x \not\equiv y \pmod 6$, and $x, y \geq 7$ are complete.*

Proof. Consider $(a, b, 2) + (5, 5, 5)$ for $a, b \in \{2, 5\} \pmod 6$, $a \not\equiv b \pmod 6$, and $a, b > 2$. Observe that $(a+5, b+5, 7)$ obtains all grids described in Case 2 above, apart from $G(a, 7, 7)$, for $a \equiv 4 \pmod 6$.

By Corollary 3.2, we must show that $(a, b, 2), (a, 5, 5), (5, b, 5), (5, 5, 2)$ are all perfect. By Proposition 3.7, $(a, b, 2)$ is perfect. We obtain $(a, 5, 5)$ and $(5, b, 5)$ from Lemma 4.5, and $(5, 5, 2)$ is given by Construction A.3.

To obtain $(a, 7, 7)$, for $a \equiv 4 \pmod 6$, we consider $(7, 4, 4) + (a-7, 3, 3)$. Since $a \equiv 4 \pmod 6$ and $a \geq 7$, we have that $a \geq 10$. By Corollary 3.2, we must show that $(7, 4, 4), (7, 3, 3), (a-7, 4, 3), (a-7, 3, 4)$ are all perfect. We obtain $(7, 4, 4)$ from $(2, 2, 2) + (5, 2, 2)$. Theorem 1.6 and Construction A.2 show that $(2, 2, 2)$, $(2, 2, 2)$, $(5, 2, 2)$, $(5, 2, 2)$ are all perfect. Proposition 3.3 gives us $(7, 3, 3)$. Since $a - 7 \equiv 3 \pmod 6$, we obtain $(a-7, 4, 3)$ from Proposition 3.8. We conclude that all grids in Case 2 admit perfect lethal sets. $\square$

Lemma 4.13. *All grids $G(x, y, 7)$ for $x, y \in \{0, 3\}$, $x \equiv y \pmod 6$, and $x, y \geq 7$ are complete.*

Proof. Consider $(a, b, 2) + (6, 9, 5)$ for $a, b \in \{0, 3\} \pmod 6$, $a \not\equiv b \pmod 6$, and $a, b > 2$. Observe that $(a+6, b+9, 7)$ contains all grids described in Case 3 above, apart from $G(9, 9, 7)$.

By Corollary 3.2, we must show that $(a, b, 2), (a, 9, 5), (6, b, 5), (6, 9, 2)$ are all perfect. By Proposition 3.7, $(a, b, 2)$ and $(6, 9, 2)$ are perfect. By Proposition 3.6, $(a, 9, 5)$ is perfect. We obtain $(6, b, 5)$ from Lemma 4.5, for $b \geq 5$, and $(6, 3, 5)$ from Proposition 3.5.

To obtain $(9, 9, 7)$, consider $(6, 6, 4) + (3, 3, 3)$. By Corollary 3.2, we must show that $(6, 6, 4), (6, 3, 3), (3, 6, 3), (3, 3, 4)$ are all perfect. We obtain $(6, 6, 4)$ from $(3, 3, 1) +$

$(3,3,3)$. Construction A.1 shows that $(3,3,1)$ is perfect. Proposition 3.3 gives us $(6,3,3)$, $(3,3,3)$ and $(4,3,3)$. We conclude that all grids in Case 3 admit perfect lethal sets. $\square$

Lemma 4.14. *All grids $G(x,y,7)$ for $x,y \in \{0,3\}$, $x \not\equiv y \pmod 6$, and $x,y \geq 7$ are complete.*

Proof. Consider $(a,b,2)+(6,6,5)$ for $a,b \in \{0,3\} \pmod 6$, $a \not\equiv b \pmod 6$, and $a,b > 2$. Observe that $(a+6,b+6,7)$ contains all grids described in Case 4 above.

By Corollary 3.2, we must show that $(a,b,2),(a,6,5),(6,b,5),(6,6,2)$ are all perfect. By Proposition 3.7, $(a,b,2)$ is perfect. We obtain $(6,b,5)$ from Lemma 4.5, for $b \geq 5$, and $(6,3,5)$ from Proposition 3.5. We obtain $(6,6,2)$ from $(3,3,1)+(3,3,1)$. By Proposition 3.10, $(3,3,1)$ is perfect, and so by Corollary 3.2, $(6,6,2)$ is perfect. We conclude that all grids in Case 4 admit perfect lethal sets. $\square$

Lemma 4.15. *Thickness 7 is complete.*

Proof. By Lemmas 4.11, 4.12, 4.13, and 4.14, all divisibility cases for thickness 7 admit perfect lethal sets. $\square$

4.4 Proof of the Main Result

We are now in a position to prove Theorem 1.7. We first state the following auxiliary result for divisibility cases.

Corollary 4.16. *Let $G(a_1,a_2,a_3)$ be a divisibility case, for $a_1,a_2,a_3 \geq 5$. Then (a_1,a_2,a_3) is perfect.*

Proof. By Lemmas 4.5, 4.10, and 4.3, all divisibility cases for $G(a_1,a_2,5)$, $G(a_1,a_2,6)$, and $G(a_1,a_2,7)$ admit perfect lethal sets. Observe that $(a_1,a_2,a_3)+(3,3,3)$ gives a one-to-one mapping from divisible grids of thickness a_3 to divisible grids of thickness a_3+3. By Lemma 3.11, if (a_1,a_2,a_3) is perfect, then $(a_1,a_2,a_3)+(3,3,3)$ is perfect. Therefore, since each residue class modulo 3 is complete, all divisibility cases $G(a_1,a_2,a_3)$, for $a_1,a_2,a_3 \geq 5$, admit perfect lethal sets. $\square$

The proof of Theorem 1.7 requires further implementation of the recursive process outlined in Lemma 3.1. In particular, we leverage Corollary 4.16 to prove the following helpful lemma:

Lemma 4.17. *Let $G(a_1,a_2,a_3)$ be any grid such that $a_1,a_2,a_3 \geq 5$. If (a_1,a_2,a_3) is optimal, then $(a_1,a_2,a_3)+(3b_1,3b_2,3b_3)$ is optimal for $b_1,b_2,b_3 \geq 2$.*

mod 3	$\equiv 2$	$\equiv 0$	$\equiv 1$
$\equiv 2$		$(5,6,5)$ $(2,0,2)$	$(5,7,5)$ $(2,1,2)$
$\equiv 0$	$(6,5,5)$ $(0,2,2)$		$(6,7,5)$ $(0,1,2)$
$\equiv 1$	$(7,5,5)$ $(1,2,2)$	$(7,6,5)$ $(1,0,2)$	$(7,7,5)$ $(1,1,2)$

mod 3	$\equiv 0$	$\equiv 1$	$\equiv 2$
$\equiv 0$			
$\equiv 1$		$(7,7,6)$ $(1,1,0)$	$(7,8,6)$ $(1,2,0)$
$\equiv 2$		$(8,7,6)$ $(2,1,0)$	$(8,8,6)$ $(2,2,0)$

mod 3	$\equiv 1$	$\equiv 2$	$\equiv 0$
$\equiv 1$		$(7,8,7)$ $(1,2,1)$	$(7,9,7)$ $(1,0,1)$
$\equiv 2$	$(8,7,7)$ $(2,1,1)$	$(8,8,7)$ $(2,2,1)$	$(8,9,7)$ $(2,0,1)$
$\equiv 0$	$(9,7,7)$ $(0,1,1)$	$(9,8,7)$ $(0,2,1)$	

Table 4.4: Residue tuples for non-divisibility cases in thicknesses 5, 6, and 7. Top tuple is grid dimension, bottom tuple is residues modulo 3.

Proof. By Corollary 3.2, we must show that $(a_1, 3b_2, 3b_3), (3b_1, a_2, 3b_3), (3b_1, 3b_2, a_3)$ are all perfect. Since $3b_1 \equiv 3b_2 \equiv 3b_3 \equiv 0 \pmod 3$, each of these grids is divisible. Furthermore, each grid has minimum thickness 5 and so, by Corollary 4.16, each grid is perfect. $\square$

Let (r_1, r_2, r_3) be the tuple of residues of (a_1, a_2, a_3) modulo 3. Given an optimal grid $G(a_1, a_2, a_3)$ such that $a_1, a_2, a_3 \geq 5$, Lemma 4.17 says that all other grids of size at least $G(a_1 + 6, a_2 + 6, a_3 + 6)$ with the same (r_1, r_2, r_3) are optimal. Therefore, by obtaining optimal lethal sets on the smallest grids for each residue tuple (r_1, r_2, r_3), we are able to obtain a lower bound on the size of all optimal grids under 3-neighbor percolation (see Table 4.4).

Proof of Theorem 1.7. Let (a_1, a_2, a_3) be such that $a_1, a_2, a_3 \geq 11$. Observe that each a_i can be written as $3b_i + r_i$, for $b_i \geq 2$ and some $r_i \in \{5, 6, 7\}$. We therefore have that $(a_1, a_2, a_3) = (r_1, r_2, r_3) + (3b_1, 3b_2, 3b_3)$, for $r_1, r_2, r_3 \in \{5, 6, 7\}$. By Lemma 4.17, (a_1, a_2, a_3) is optimal if (r_1, r_2, r_3) is optimal.

Corollary 4.16 gives us the optimality of divisibility cases. Therefore, we need only consider non-divisible grids $G(r_1, r_2, r_3)$. In particular, we must show that $(6, 5, 5)$, $(7, 5, 5)$, $(7, 6, 5)$, $(7, 7, 5)$ and $(7, 7, 6)$ are all optimal. We obtain $(7, 7, 6)$ from $(4, 4, 3) + (3, 3, 3)$. The construction for $(4, 4, 3)$ is given in Construction A.7. By Lemma 3.11, $(7, 7, 6)$ is optimal. Constructions for $(6, 5, 5)$, $(7, 5, 5)$, $(7, 6, 5)$, $(7, 7, 5)$ are given in Appendix A.

Since each of the non-divisibility grids $G(r_1, r_2, r_3)$ admits an optimal lethal set, we conclude that all grids $G(a_1, a_2, a_3)$ where $a_1, a_2, a_3 \geq 11$ are optimal. $\square$

Chapter 5
Thickness One

While results from the previous chapters resolve the question of $m(a_1, a_2, a_3, 3)$ for $a_1, a_2, a_3 \geq 11$, our constructions for smaller grids remain incomplete. Nevertheless, computer examples seem to suggest that most grids of minimum size at least 2 are optimal. Grids of thickness 1 tell a different story. In this chapter, we prove that the only perfect grids in thickness 1 are those of the form $[2^n - 1]^2$. This answers a question posed by Benevides, Bermond, Lesfari and Nisse in [7].

The broad structure of the proof is as follows: Let A_0 be a perfect lethal set on the grid $G(a_1, a_2, 1)$. We show that the structure of A_0 guarantees both that a_1, a_2 are odd, and that there exists a perfect lethal set on the smaller grid $G(\frac{a_1-1}{2}, \frac{a_2-1}{2}, 1)$. Repeated applications of this process of reduction guarantee the existence of a perfect lethal set on the grid $G(a_0, 1, 1)$, for some $a_0 \geq 1$. Since the only such grid that admits a perfect lethal set is $G(1, 1, 1)$, we are forced to conclude that $a_1 = a_2 = 2^k - 1$ for some $k > 0$.

5.1 Preliminaries

For the remainder of the chapter, let $G = [a_1] \times [a_2]$. Recall that every perfect lethal set matches the surface area bound. In particular,

$$|A_0| = \frac{a_1 a_2 + a_1 + a_2}{3}.$$

We begin with the following observations regarding the structure of A_0:

Proposition 5.1. *If A_0 is a perfect lethal set on G, then A_0 contains alternating vertices along the border of G.*

Proof. Since A_0 is perfect, it must form an independent set in G. By Proposition 2.11, no two adjacent border vertices are both uninfected. Together, these conditions ensure that A_0 intersects the border of G in an alternating pattern (see Figure 5.2). □

Proposition 5.2. *If A_0 is a perfect lethal set on G, then $a_1, a_2 \equiv 1 \pmod 2$.*

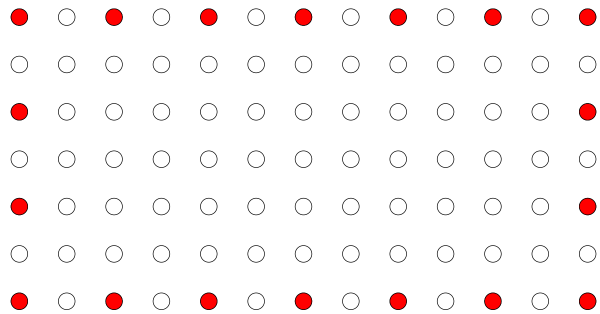

Figure 5.1: Alternating infection along the border of $[7] \times [13]$.

Proof. By Propositions 5.1 and 2.10, $a_1, a_2 \equiv 1 \pmod 2$. □

Proposition 5.3. *Let A_0 be a perfect lethal set on G under 3-neighbor percolation. Let H be the subgraph of G induced by $V(G) \setminus A_0$. Then H is acyclic and each component of H contains exactly one border vertex.*

Proof. By Proposition 2.12, we have that each component of H contains at most one border vertex. We show that each component of H contains exactly one border vertex.

By assumption, H is a forest. Therefore, the number of components of H is given by $|V(H)| - |E(H)|$. Note that $|V(H)| = |V(G)| - |A_0|$. Since A_0 is perfect and lethal,

$$\begin{aligned} |V(H)| &= a_1a_2 - \frac{1}{3}(a_1a_2 + a_1 + a_2) \\ &= \frac{1}{3}(2a_1a_2 - a_1 - a_2). \end{aligned}$$

To determine $|E(H)|$, we calculate the number of edges removed from G to obtain H. Recall that A_0 is an independent set. Therefore, no two vertices of A_0 remove the same edge. Since all interior vertices of G have degree 4, we have that the number of edges removed from G to obtain H is

$$\frac{4}{3}(a_1a_2 + a_1 + a_2) - (a_1 + a_2 - 2) - 4,$$

where the terms $(a_1 + a_2 - 2)$ and 4 account for the border vertices of degree 3 and degree 2, respectively. Therefore, the number of edges in H is

$$\begin{aligned} |E(H)| &= |E(G)| - \frac{4}{3}(a_1a_2 + a_1 + a_2) - (a_1 + a_2 - 2) - 4 \\ &= 2a_1a_2 - a_1 - a_2 - \frac{1}{3}(4a_1a_2 + a_1 + a_2 - 6) \\ &= \frac{1}{3}(2a_1a_2 - 4a_1 - 4a_2 + 6). \end{aligned}$$

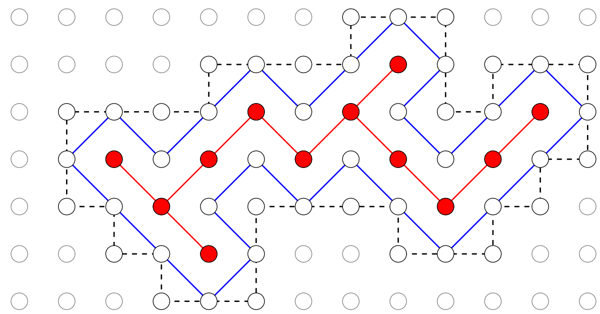

Figure 5.2: $[7] \times [13]$ grid with component K (red), C_H (blue), and C_G (dashed).

The number of components of H is given by

$$\begin{aligned} |V(H)| - |E(H)| &= \frac{1}{3}(2a_1a_2 - a_1 - a_2) - \frac{1}{3}(2a_1a_2 - 4a_1 - 4a_2 + 6) \\ &= a_1 + a_2 - 2. \end{aligned}$$

As there are exactly $a_1 + a_2 - 2$ border vertices in H, each component must contain exactly one border vertex. □

Consider the coordinates of the vertices of G, starting at $(1,1)$ in the lower left and ranging to (a_1, a_2) in the upper right. Refer to a vertex (x, y) as "even" or "odd" depending on the parity of $x + y$. If a set $S \subseteq V(G)$ contains all vertices of the same parity, call S monochromatic. The following lemma leverages the prior propositions to prove that any perfect lethal set on G must be monochromatic.

Lemma 5.4. *Let A_0 be a perfect lethal set on G. Then A_0 is monochromatic.*

Proof. From Proposition 5.1, observe that A_0 contains all even vertices along the border of G. Suppose for contradiction that A_0 also contains odd vertices. We show that this implies the existence of a cycle in the subgraph induced by $V(G) \setminus A_0$, contradicting Proposition 5.3.

Let H be a graph with vertices $V(H) = V(G)$ and edges uv if and only if u and v are diagonally adjacent in G. Consider the subgraph of H induced by the odd vertices of A_0 and let K be a connected component. Observe that K is acyclic: any cycle in K encloses a component of $G[\overline{A_0}]$, contradicting Proposition 5.3. Furthermore, by Proposition 5.1, all vertices of K are in the interior of G. Let C_H be the cycle induced in H by $N_G(K)$. Note that since A_0 is an independent set, $N_G(K) \cap A_0 = \emptyset$ and $C_H \cap A_0 = \emptyset$. Consider the closed walk induced in G by the vertices $V(C_H) \cup N_H(K) \setminus A_0$. This walk describes a cycle C_G in $G[\overline{A_0}]$, which contradicts Proposition 5.3. □

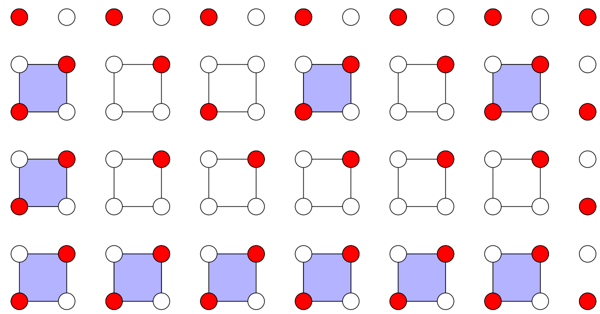

Figure 5.3: $[7] \times [13]$ grid with $T_{x,y}$ colored blue if $|T_{x,y} \cap A_0| = 2$. Note that A_0 is *not* perfect.

5.2 Reduction

Using propositions from the prior section, we show that it is possible to obtain a perfect lethal set on the smaller grid $G' = G(\frac{a_1-1}{2}, \frac{a_2-1}{2}, 1)$ obtained from G. Let the vertices of G' be 2×2 tiles of G given by

$$T_{x,y} = \{2x-1, 2x\} \times \{2y-1, 2y\},$$

for $(x, y) \in [1, \frac{a_1-1}{2}] \times [1, \frac{a_2-1}{2}]$, and with adjacencies between tiles that differ by one in each of the cardinal directions. Note that Proposition 5.2 ensures that $|V(G')|$ is an integer. Furthermore, observe that for any tile $T_{x,y} \in V(G')$, $|A_0 \cap T_{x,y}| \in \{1, 2\}$. This follows from the fact that A_0 is an independent set, and $G[\overline{A_0}]$ is acyclic. For all $T_{x,y} \in V(G')$, color $T_{x,y}$ blue if $|A_0 \cap T_{x,y}| = 2$, and white otherwise. Let b and w be the number of blue and white tiles in $V(G')$, respectively. We determine b by solving the following system of equations:

$$\begin{aligned} b + w &= \frac{(a_1-1)(a_2-1)}{4} \\ 2b + w &= \frac{a_1a_2 + a_1 + a_2}{3} - \frac{a_1 + a_2}{2}. \end{aligned}$$

This gives the following expression for b:

$$\begin{aligned} \frac{a_1a_2 + a_1 + a_2}{3} - \frac{a_1 + a_2}{2} - \frac{(a_1-1)(a_2-1)}{4} &= \frac{a_1a_2 + a_1 + a_2 - 3}{12} && (5.1) \\ &= \frac{(\frac{a_1-1}{2})(\frac{a_2-1}{2}) + \frac{a_1-1}{2} + \frac{a_2-1}{2}}{3}. && (5.2) \end{aligned}$$

Note that this is precisely the surface area bound for the $(\frac{a_1-1}{2}, \frac{a_2-1}{2}, 1)$ grid.

We prove that the blue tiles form a lethal set in G'. We begin with the following observation:

Proposition 5.5. *All white tiles have their A_0-vertex in the bottom left corner.*

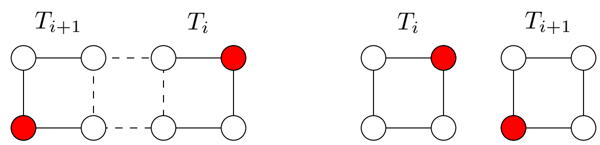

Figure 5.4: Possible configurations of adjacent white tiles.

Proof. For contradiction, suppose that there exists a white tile T_0 with one infected vertex in the upper right. By Proposition 5.3, there exists a path $w_1 \dots w_k$ in $G[\overline{A_0}]$ from $T_0 \setminus A_0$ to the border. We consider the sequence of tiles $T_0, \dots, T_n$ containing this path. Note that if w_k is in the top or right face of G, then it is not contained in any tile in this sequence.

We claim that T_n contains an infected vertex in the bottom-left corner. Recall that w_k must be odd. Therefore, if w_k is in the bottom or left face of G, then it must lie in either the top-left or bottom-right corner of T_n. This implies T_n must have an infected vertex in the bottom-left; otherwise, T_n would contain adjacent uninfected vertices on the border of G. Now suppose that w_k is in the top or right face of G. In this case, T_n contains w_{k-1}. However, since w_{k-1} is adjacent to w_k by definition, w_{k-1} must be even and so must be the top-right vertex of T_n. Since $w_{k-1} \notin A_0$, this implies that T_n cannot have an infected vertex in the top-right. Furthermore, since every tile must contain at least one infected vertex, T_n must contain an infected vertex in the bottom-left corner.

Therefore, since T_0 contains an infection in the top right by assumption, there exist consecutive tiles T_i, T_{i+1} such that T_i has an infection in the top right, and T_{i+1} has an infection in the bottom left. Observe that T_{i+1} cannot be to the right (or above) T_i, as shown in Figure 5.4. We therefore assume that T_{i+1} is to the left of (or below) T_i (note that these cases are symmetric). Figure 5.4 shows that if T_{i+1} is white, then this configuration creates a 4-cycle. Therefore, T_{i+1} must be blue. Note that the bottom-right vertex of T_{i+1} is in $w_1 \dots w_k$. Denote this vertex as w_v.

We have two possibilities: either w_v is on the bottom face of G, or there exists a vertex $w_{v+1} \in w_1 \dots w_k$ that is adjacent to w_v. Note that the first case is not possible, as it implies that w_{v-1} is also on the bottom face of G, violating Proposition 5.1. Therefore, there must exist a vertex $w_{v+1} \in w_1 \dots w_k$ that is adjacent to w_v. However, this implies the configuration of tiles shown in Figure 5.5, which gives a 4-cycle. This final contradiction completes the proof that all white tiles must have their A_0-vertex in the bottom left corner.

□

We are now prepared to prove that the blue tiles form a lethal set in G'.

Lemma 5.6. *The set of blue tiles is lethal and perfect in* $[\frac{a_1-1}{2}] \times [\frac{a_2-1}{2}]$ *under 3-neighbor percolation.*

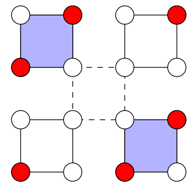

Figure 5.5: A 4-cycle resulting from the only possible configuration of T_i and T_{i+1}.

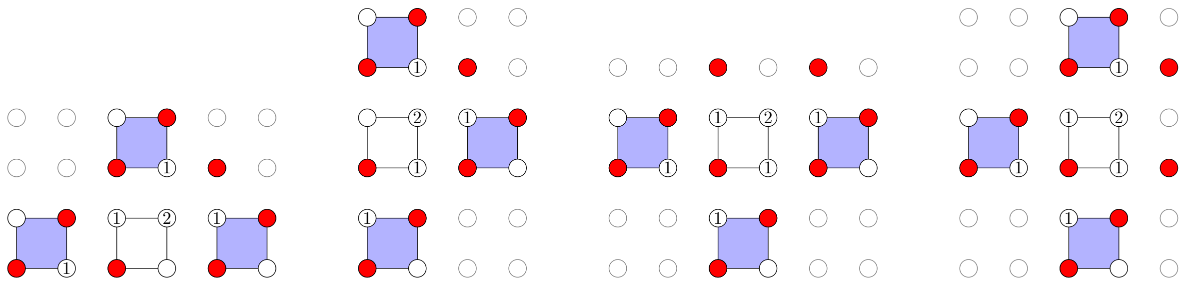

Figure 5.6: The four configurations of blue tiles leading to infection.

Proof. In Equation 5.2, we saw that the number of blue tiles matches the lower bound for 3-neighbor percolation in $[(a_1-1)/2] \times [(a_2-1)/2]$. We now show that the 3-neighbor process infects white tiles if and only if they are adjacent to at least 3 blue tiles.

For sufficiency, consider the four cases illustrated in Figure 5.6. In each of these configurations, the upper right vertex of the white tile (labeled with a "2") becomes infected after two iterations. Each case requires the assistance of one to two extra infections outside of the three blue tiles. However, these infections constitute the bottom left vertex in adjoining tiles, which is always infected.

For necessity, we show that any cycle or border-to-border path in the white tiles of G' implies a cycle or border-to-border path in $G[\overline{A_0}]$. Observe that, by Proposition 5.5, the vertices $(T_i \cup T_j) \setminus A_0$ of any adjacent white tiles T_i, T_j induce a connected component in G. Therefore, any cycle or border-to-border path in G' implies the existence of a cycle or border-to-border path in $G[\overline{A_0}]$. We conclude that the blue tiles form a perfect lethal set in $[(a_1-1)/2] \times [(a_2-1)/2]$ under 3-neighbor percolation. $\square$

We have shown that the existence of a perfect lethal set on $[a_1] \times [a_2]$ implies the existence of a perfect lethal set on $[(a_1-1)/2] \times [(a_2-1)/2)]$. Suppose, without loss of generality, that $a_1 \geq a_2$. Then, by Proposition 5.2, it must be the case that $a_2 = 2^k - 1$ for some $k > 0$. By repeated applications of Lemma 5.6, we ultimately obtain a grid $[a_0] \times [1]$, for some $a_0 \geq 1$, that admits a perfect lethal set. Clearly, the only such grid is the single vertex. Therefore, it must follow that $a_1 = a_2 = 2^k - 1$. We conclude that the only two-dimensional grids that admit perfect lethal sets under 3-neighbor percolation are square grids of the form $[2^n - 1]^2$. Furthermore, this process fixes the location of infected vertices in a particular configuration. This configuration is published in

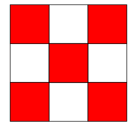

Figure 5.7: A perfect percolating set for $G(3,3,1)$.

Benevides et al [7], and reproduced below.

5.3 Purina

We refer to this construction colloquially as the Purina construction, due to the similarly between its instance $G(3,3,1)$ and the logo of the pet food brand. No funding has been offered, but we are open to the possibility. A more extensive discussion on this pattern can be found in [7].

Construction 5.7 (Benevides, Bermond, Lesfari, Nisse)**.** *All grids of the form $G(2^n - 1, 2^n - 1, 1)$ are perfect.*

Proof. This is a recursive construction built from the base component piece shown in Figure 5.7. Note that this $G(3,3,1)$ construction is lethal under the 3-neighbor bootstrap process, and that it meets the surface area bound:

$$\frac{1}{3}(ab + bc + ca) = \frac{1}{3}(9 + 3 + 3) = 5.$$

For larger grids of size $G(2^n - 1, 2^n - 1, 1)$, join four copies of $G(2^{n-1} - 1, 2^{n-1}, 1)$ about two perpendicular corridors, and infect the vertex at their intersection (Figure 5.8). Observe that the resulting set is lethal: each of the four smaller grids is lethal by hypothesis, and the remaining vertices induce a forest with disconnected boundary points, which percolates by Proposition 2.12. Furthermore, note that

$$\begin{aligned} SA(2^n - 1, 2^n - 1, 1) &= \frac{1}{3}(2^{2n} - 1) \\ &= 4 \cdot \frac{1}{3}(2^{2n-2} - 1) + 1 = 4 \cdot SA(2^{n-1} - 1, 2^{n-1}, 1) + 1, \end{aligned}$$

and therefore this construction is perfect. □

Although the only two-dimensional grids that admit perfect lethal sets under 3-neighbor percolation are square grids of the form $[2^n - 1]^2$, there is at least one family of two-dimensional grids that admits optimal lethal sets (i.e. meets the rounded surface area bound). These sets are qualitatively different from the Purina construction: while Purina exhibits an almost recursive structure, the sets presented in Construction 6.3

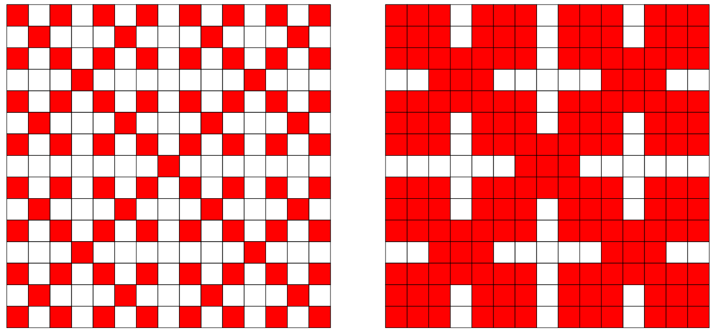

Figure 5.8: A perfect percolating set for $G(15, 15, 1)$.

rely on "corridors," down which the infection spreads. The notion of "corridors" is not new; constructions with much of the same character as these are given for non-Purina grids in [7]. We examine such grids in the following chapter, making particular note of their use in our analysis of other infinite families of grids that admit perfect lethal sets.

Chapter 6
Constructions

In this chapter, we present diagram-supported constructions for grids that admit optimal and perfect lethal sets under the 3-neighbor process. The proofs are organized by the thickness of the grid. All constructions in this chapter belong to infinite families of grids. We use two strategies in our analysis of these constructions, outlined below.

We examine Constructions 6.4, 6.7, 6.8, 6.11, and 6.12 by region, and observe that certain pieces of the grid can be expanded to arbitrarily large sizes without adversely affecting the spread of infection. In particular, we split these grids into components A, B, X, where A and B bookend a central, periodic segment X. Our discussion will make use of the following definition and lemma:

Definition 6.1. For a grid $G = [a_1] \times [a_2] \times [a_3]$, define the kth *level* of G as the subgraph $L_k = [a_1] \times [a_2] \times \{k\}$, for $k \in [a_3]$.

Lemma 6.2. *Let $G = [a_1] \times [a_2] \times [a_3]$ and let L_k be the kth level of G. Suppose all vertices in L_k are infected. Then any lethal set in L_{k+1} (resp. L_{k-1}) under the 2-neighbor process is lethal in the union of L_k and L_{k+1} (resp. L_{k-1}) under the 3-neighbor process.*

Proof. Each vertex $v \in L_{k+1} \cup L_{k-1}$ has an infected neighbor in L_k. Therefore, if v has two infected neighbors in its own level, it has at least 3 infected neighbors in G. $\square$

Proofs of the lethality of the remaining families all leverage Lemma 2.4. As a consequence, their structure remains broadly the same, even as the constructions themselves appear quite different. We shall outline this structure here, before examining the specific proofs.

We begin by demonstrating that the grid $G = G(a_1, a_2, a_3)$ admits a manifold M. Recall from Corollary 2.8 that a manifold on G is the union of shared perpendicular faces of sub-grids $G_{i,j,\ell}$ of G. To show that a particular subset M of $V(G)$ is a manifold, we identify the regions $R_1, \ldots, R_n$ that partition $V(G) \setminus M$ and are flanked by three perpendicular walls. In our diagrams, these regions are represented by the volumes bordered by three perpendicular blue, green, and red walls. We then identify a proper

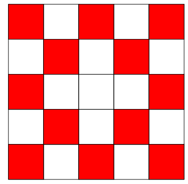

Figure 6.1: An optimal percolating set for $G(5, 5, 1)$.

unfolding H of M and show that H admits a lethal set A, where $|A| = SA(G)$. Finally, we apply Corollary 2.8 to prove that G is perfect.

6.1 Thickness 1

We present a construction that is optimal on all grids $G(a, b, 1)$, where $a \equiv 5 \pmod 6$, $b \equiv 1 \pmod 2$, and $a, b \geq 5$. As such grids constitute non-divisibility cases, this construction is not perfect. However, by leveraging Lemma 2.9, we shall see that it can be used to obtain perfect lethal sets on certain grids of thickness 3.

As indicated by Proposition 2.12, a fundamental characteristic of lethal constructions is the existence of an initially uninfected corridor, bounded by walls of infection. This structure is apparent in the second diagrams of Figures 5.8 and 6.3 in the previous chapter. These corridors correspond to forests in the complement $G[\overline{A_0}]$ of the infected set A_0. In this section, we provide a general method for constructing such corridors in $(a, b, 1)$ grids where $a \equiv 5 \pmod 6$ and $b \equiv 1 \pmod 2$.

Construction 6.3. *All tuples* $(a, b, 1)$*,* $a \equiv 5 \pmod 6$*,* $b \equiv 1 \pmod 2$*, and* $a, b \geq 5$ *are optimal.*

Proof. For $G(a, b, 1)$, $a \equiv 5 \pmod 6$, $b \equiv 1 \pmod 2$, we construct an optimal infected set and show that it is lethal by Proposition 2.12. For the base case, consider the $[5] \times [5] \times [1]$ grid G illustrated in Figure 6.1. Observe that this construction is optimal. Now consider the grid G' resulting from the insertion of a $[5] \times [2k] \times [1]$ block X, as shown in Figure 6.2. Note that the subgraph induced by the uninfected vertices of G' satisfies the conditions of Proposition 2.12. Furthermore, note that if any grid $G(5, n, 1)$ is optimal, the grid $G(5, n + 2, 1)$ resulting from such a construction has surface area bound $SA(5, n, 1) + 4$, which agrees with the number of infected vertices.

To extend this construction in the vertical direction, we introduce a "kink" in the snaking infection. This "kink" requires six rows to produce a repeating pattern. The structure of this design is shown in Figure 6.3, with the "kinked" region labeled "Y". For grids of smaller width, the same construction gives optimal percolating sets; however, the snaking pattern is increasingly difficult to recognize in thin grids. $\square$

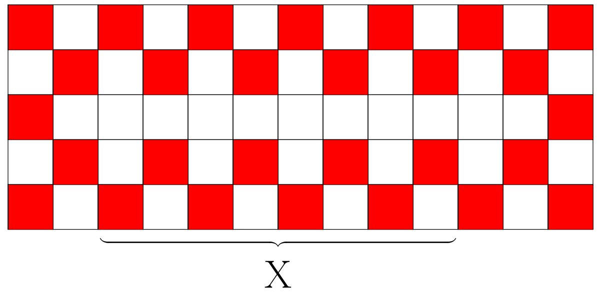

Figure 6.2: An optimal percolating set for $G(5, 13, 1)$.

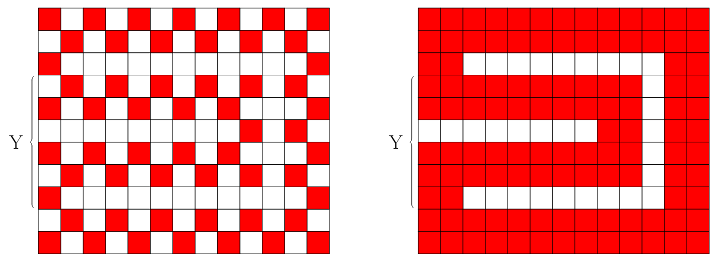

Figure 6.3: An optimal percolating set for $G(11, 13, 1)$.

6.2 Thickness 2

We examine four infinite families of grids and show that each admits a lethal set of perfect size. We note that such lethal sets are likely to exist for nearly all divisibility cases in thickness two; however, constructions are elusive and those presented here are sufficient to prove the main result of this thesis.

Construction 6.4. *All tuples $(a, 3, 2)$ with $a \equiv 3 \pmod 6$ and $a > 3$ are perfect.*

Proof. Let $G = G(6k+3, 3, 2)$ be a grid such that $k > 0$. Let $A = \{1\} \times [3] \times [2]$, $B = \{6k+2, 6k+3\} \times [3] \times [2]$, and $X_i = \{6(i-1)+2, 6(i-1)+3, \dots, 6(i-1)+7\} \times [3] \times [2]$ for $i \in [k]$, be regions of G. Denote by AX^kB the union of regions $A \cup X_1 \cup \cdots \cup X_k \cup B$, and note that $G = AX^kB$. Let $A_t^k \subseteq V(G)$ be the set of infected vertices in G at time t, and suppose that each X_i contains the same pattern of infected vertices (see Figure 6.4). We show that the initial infection A_0^k is lethal and perfect.

Consider the union of regions $AX^k = A \cup X_1 \cup \cdots \cup X_k$ (see Figure 6.5). Note that this omits the region B. Let L_1 and L_2 be the top and bottom levels of AX^k, respectively. Observe that after one time step, the subgraph $L_1[\overline{A_1^k}]$ satisfies the conditions of Proposition 2.12, and so A_0^k is lethal on L_1.

Now consider AX^kB and observe that the top level becomes fully infected (see Figure 6.6). Therefore, by Lemma 6.2, it is sufficient to prove that A_0^k is lethal on the bottom level under the 2-neighbor bootstrap process. Figure 6.7 illustrates the key steps of this process on the smaller grid AXB, starting at $t = 1$. Infection spreads

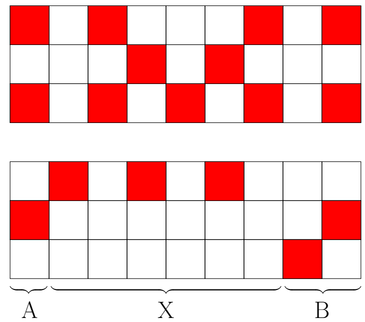

Figure 6.4: The regions A, X, B on $G = AXB$ with infectious set A_0.

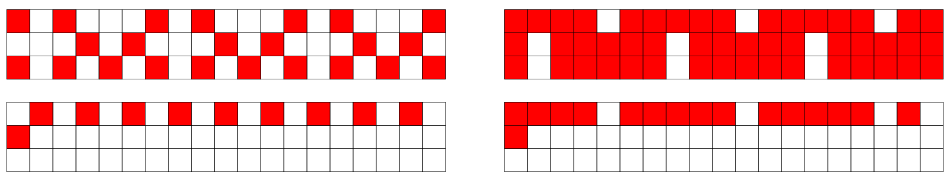

Figure 6.5: An infection on AX^3, $t = 0$ and $t = 1$.

down rows delineated by red arrows, ultimately infecting all vertices in the bottom level. We conclude that A_0^k is lethal on G under the 3-neighbor process.

To prove that A_0^k is perfect, observe that $|A_0^k| = 3 + 10k + 4$. The surface area bound for $G(6k+3, 3, 2)$ is given by

$$\frac{(3)(6k+3) + (3)(2) + (2)(6k+3)}{3} = \frac{30k+21}{3} = 10k + 7.$$

Since these two values are equal, A_0^k is tight and lethal, and therefore perfect. $\square$

Construction 6.5. *All tuples* $(a, 3, 2)$ *with* $a \equiv 0 \pmod 6$ *and* $a \geq 6$ *are perfect.*

Proof. Let $G = G(a, 3, 2)$ where $a \equiv 0 \pmod 6$ and $a \geq 6$, and let M be the manifold of G illustrated in Figure 6.8a and H be its proper unfolding (see Figure 6.8b). Observe that M is indeed a manifold: it partitions $V(G) \setminus M$ into two sets R_1 and R_2, both bounded by mutually orthogonal red, green, and blue faces (see Figure 6.8a). Furthermore, note that H is obtained from M by cutting along seams between red and green faces, and flattening the figure. It follows that H is a proper unfolding of G.

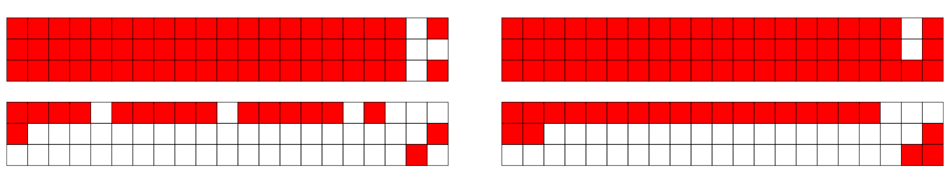

Figure 6.6: An infection on G.

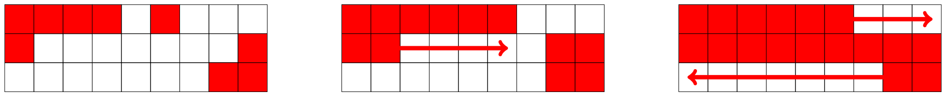

Figure 6.7: The 2-neighbor process on $G(9,3,1)$ for $t=1$, $2 \leq t \leq 6$, and $7 \leq t \leq 14$.

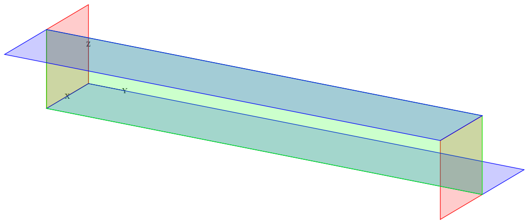

(a) A manifold of $G(3,12,2)$.

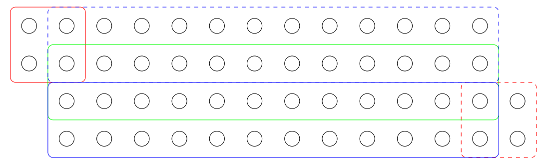

(b) A proper unfolding of G.

Figure 6.8: A proper unfolding of $G(3,12,2)$. Colored rectangles indicate faces of G. Dashed lines indicate that cells appear on different layers.

Let $X_1, \ldots, X_k$ be the periodic regions of H of width 6 (see Figure 6.9). Denote by X^k the union of these regions. Let A_0 be a set of initially infected vertices in H and $A_t \subseteq V(H)$ be the set of infected vertices in H at time t. Note that each X_i, for $i \in [k]$, contains the same pattern of infected vertices (see Figure 6.9). We show that A_0 is lethal and perfect.

Figure 6.9 shows A_0 in H. Observe that A_0 infects all vertices of X^k by Proposition 2.12. We show that the remaining healthy vertices of H become infected. Consider re-folding H, and note that both pairs of cells marked with an "X" in H represent the same cell in G. This is enough to infect the remaining regions of H, and by Corollary 2.8, A_0 is lethal on G.

To prove that A_0 is perfect, observe that $|A_0| = 4+10k+8 = 10k+12$. The surface area bound for $G(6k+6,3,2)$, where k is the number of repeated regions X, is given by

$$\frac{(3)(6k+6)+(3)(2)+(2)(6k+6)}{3} = \frac{30k+36}{3} = 10k+12.$$

Since these two values are equal, A_0 is tight and lethal, and therefore perfect. $\square$

Construction 6.6. *All tuples* $(a,b,2)$ *with* $a,b \in \{2,5\} \pmod 6$*,* $a \not\equiv b \pmod 6$*, and* $a,b > 2$ *are perfect.*

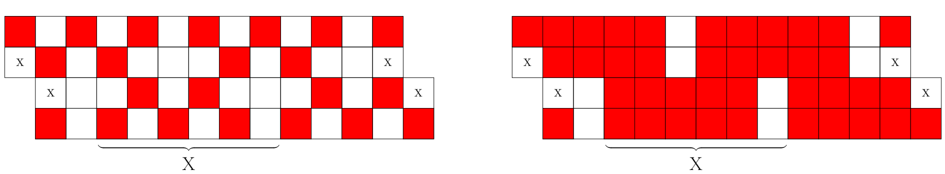

Figure 6.9: A lethal set on H showing the repeated region X ($t=1$ and $t=2$).

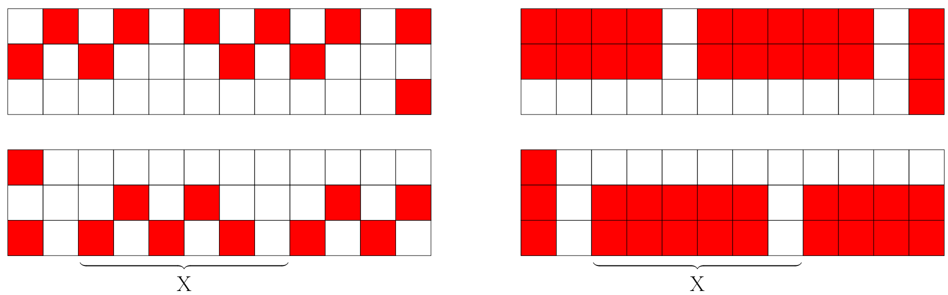

Figure 6.10: A perfect lethal set for $G(3, 12, 2)$ with region X.

Proof. Let $G = G(a, b, 2)$ be a grid with $a, b \in \{2, 5\} \pmod 6$, $a \not\equiv b \pmod 6$, and $a, b > 2$, and let M be a manifold of G and H be its proper unfolding (Figure 6.11). Note that M partitions the vertices of $V(G) \setminus M$ into two disjoint sets R_1 and R_2, both bounded by mutually orthogonal red, green, and blue faces. Note, also, that H is obtained from M by cutting along seams between red and green faces, and flattening the figure. Therefore, H is a proper unfolding of G.

Let $X_1, \ldots, X_{k_1}$ be the repeated regions of H in the x-direction, and $Y_1, \ldots, Y_{k_2}$ be the repeated regions of H in the y-direction (see Figure 6.12). Denote by X_iY_j the region obtained from $X_i \cap Y_j$, and let $X^{k_1}Y^{k_2}$ be the union of all X_iY_j. Let $A_t \subseteq V(H)$ be the set of infectious vertices in H at time t, and suppose that for $i \in [k_1] \setminus \{1, k_1\}$ and $j \in [k_2]$, each X_iY_j contains the same pattern of infected vertices (see Figure 6.14). We show that A_0 is lethal and perfect.

Consider the initial infection A_0 of H as shown in Figure 6.12. Observe that A_0 infects all vertices of $X \times Y$ by Proposition 2.12. We show that the remaining healthy vertices of H become infected. The individual vertices in the rightmost column of H are infected by Proposition 2.12. Consider re-folding H, and note that the pairs of cells marked with an "X" in H represent the same cell in G. This is enough to infect the remaining regions of H, and by Corollary 2.8, A_0 is lethal on G.

To prove that A_0 is perfect, observe that for $i \in [k_1] \setminus \{1\}$ and $j \in [k_2]$, each X_iY_j block contains exactly 12 infected vertices. For $j \in [k_2 - 1]$, X_1Y_j contains 11 infected vertices, and $X_1Y_{k_2}$ contains 12 infected vertices. In total, the region XY contains exactly

$$12(k_1 - 1)(k_2) + 11(k_2 - 1) + 12$$

initially infected vertices. Of the remaining vertices in H, $14k_1 - 1 + 9k_2 + 8$ are infected. Therefore,

$$\begin{aligned} |A_0| &= 12(k_1 - 1)k_2 + 11(k_2 - 1) + 12 + 14(k_1) - 1 + 9(k_2) + 8 \\ &= 12k_1k_2 + 14k_1 + 8k_2 + 8. \end{aligned}$$

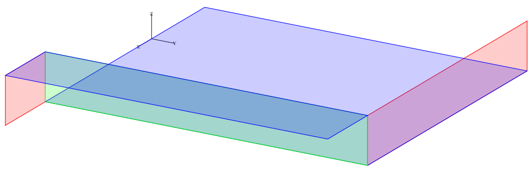

(a) A manifold of $G(11, 20, 2)$.

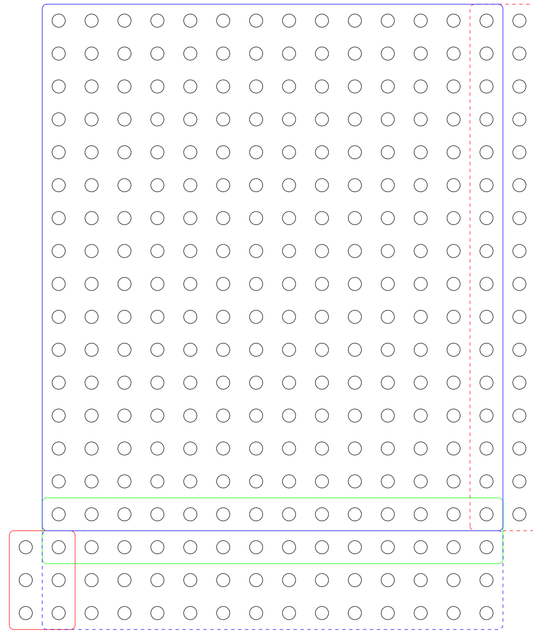

(b) A proper unfolding of G.

Figure 6.11: A proper unfolding of $G(11, 20, 2)$. Colored rectangles indicate faces of G. Dashed lines indicate that cells appear on different layers.

The surface area bound for $G(6k_1 + 2, 6k_2 + 5, 2)$ is given by

$$\begin{aligned} SA(6k_1 + 2, 6k_2 + 5, 2) &= \frac{(6k_1 + 2)(6k_2 + 5) + (6k_2 + 5)(2) + (2)(6k_1 + 2)}{3} \\ &= \frac{36(k_1)(k_2) + 42k_1 + 24k_2 + 24}{3} \\ &= 12k_1k_2 + 14k_1 + 8k_2 + 8. \end{aligned}$$

Since these two values are equal, A_0 is tight and lethal, and therefore perfect. □

Construction 6.7. *All tuples* $(a, b, 2)$ *with* $a, b \in \{0, 3\} \pmod 6$, $a \not\equiv b \pmod 6$ *and* $a, b, \geq 6$ *are perfect.*

Proof. Let $G = G(a, b, 2)$ be a grid with $a, b \in \{0, 3\} \pmod 6$, $a \not\equiv b \pmod 6$, and $a, b \geq 6$, and let $X_1, \ldots, X_{k_1}$ be the repeated regions of G in the x-direction, and $Y_1, \ldots, Y_{k_2}$ be the repeated regions of G in the y-direction (see Figure 6.15). Denote by X_iY_j the region obtained from $X_i \cap Y_j$, and let $X^{k_1}Y^{k_2}$ be the union of all X_iY_j. Let $A_t \subseteq V(H)$ be the set of infected vertices in G at time t, and suppose that for $i \in [k_1]$ and $j \in [k_2]$, each X_iY_j contains the same pattern of infected vertices (see Figure 6.15). We show that A_0 is lethal and perfect.

Let L_1 and L_2 be the top and bottom layers of G, respectively. Observe that after one time step, the subgraph of L_1 induced by the uninfected vertices of $\cup Y_i$ is both

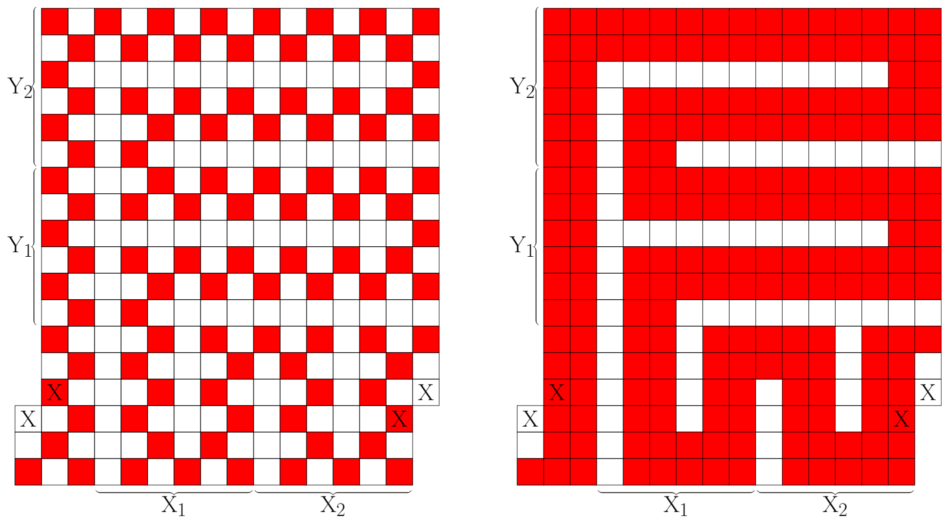

Figure 6.12: A percolating set on the proper unfolding of $G(17, 14, 2)$.

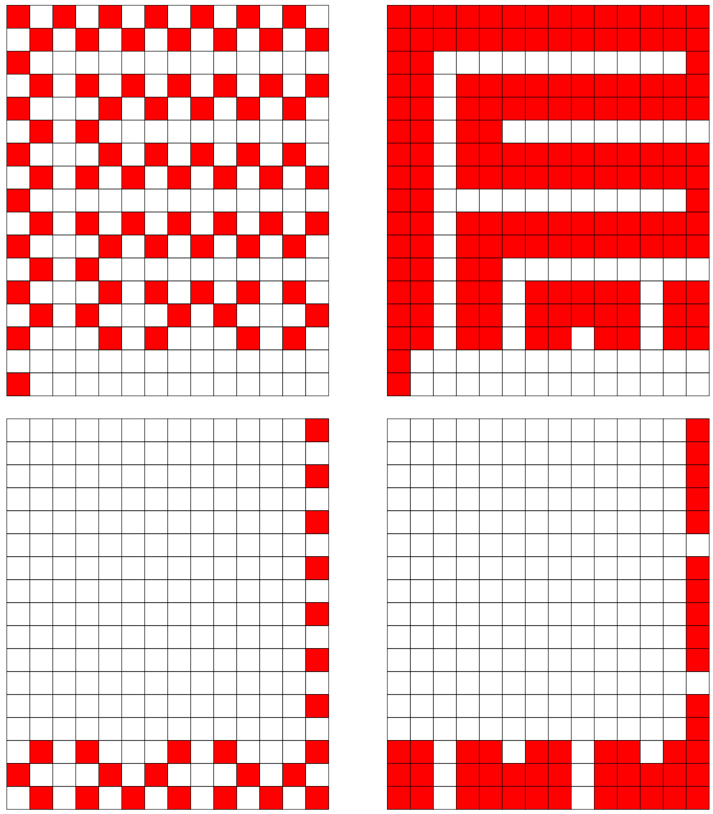

Figure 6.13: A perfect percolating set for $G(17, 20, 2)$.

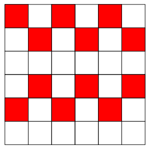

Figure 6.14: A block X_iY_j.

acyclic and contains no border-to-border paths. Therefore, by Proposition 2.12, A_0 is lethal in $(\cup Y_i) \cap L_1$.

Consider these observations in the context of G. Figure 6.16 shows that after 5 additional time-steps, the remaining healthy vertices in L_1 form two paths, marked by red arrows. The vertices in the upper path are infected by Proposition 2.12, and those in the lower path are infected by Lemma 6.2. Therefore, all vertices of L_1 become infected. Furthermore, the infected vertices in L_2 form a lethal set under the 2-neighbor process, and so, by Lemma 6.2, we conclude that A_0 is lethal on G under the 3-neighbor process.

To prove that A_0 is perfect, observe that for $i \in [k_1]$ and $j \in [k_2]$, each X_iY_j block contains exactly 12 infected vertices, and so the total number of infected vertices in XY is $12k_1k_2$.

Of the remaining vertices in G, $16k_1 + 22k_2 + 28$ are infected. Therefore,

$$|A_0| = 12k_1k_2 + 16k_1 + 22k_2 + 28.$$

The surface area bound for $G(6k_1 + 9, 6k_2 + 6, 2)$ is given by

$$\begin{aligned}
SA(6k_1 + 9, 6k_2 + 6, 2) &= \frac{(6k_1 + 9)(6k_2 + 6) + (6k_2 + 6)(2) + (2)(6k_1 + 9)}{3} \\
&= \frac{36k_1k_2 + 48k_1 + 66k_2 + 84}{3} \\
&= 12k_1k_2 + 16k_1 + 22k_2 + 28.
\end{aligned}$$

Since these two values are equal, A_0 is tight and lethal, and therefore perfect. $\square$

We note that it is possible to examine grids of the form described above using a folding argument, *if* they are at least as large as $G(12, 21, 2)$. However, such a process omits an infinite number of smaller grids. Nevertheless, the construction contributes to the set of possible shapes of manifold, and the grid and corresponding unfolded net are given in Figures A.7, A.8 and A.9 in the Appendix.

6.3 Thickness 3

Construction 6.8. *All tuples* $(a, 3, 3)$ *with* $a \equiv 0 \pmod 2$ *and* $a > 2$ *are perfect.*

Proof. Let $G = G(2k, 3, 3)$ be a grid such that $k > 1$. Let $A = \{1, 2, 3\} \times [3] \times [3]$, $B = \{2k\} \times [3] \times [3]$, and $X_i = \{2i + 2, 2i + 3\} \times [3] \times [3]$ for $i \in [k - 2]$, be regions of G. Denote by AX^kB the union of regions $A \cup X_1 \cup \cdots \cup X_k \cup B$, and note that $G = AX^kB$. Let $A_t^k \subseteq V(G)$ be the set of infected vertices in G at time t, and suppose that each X_i contains the same pattern of infected vertices (see Figure 6.17). We show that A_0^k is lethal and perfect.

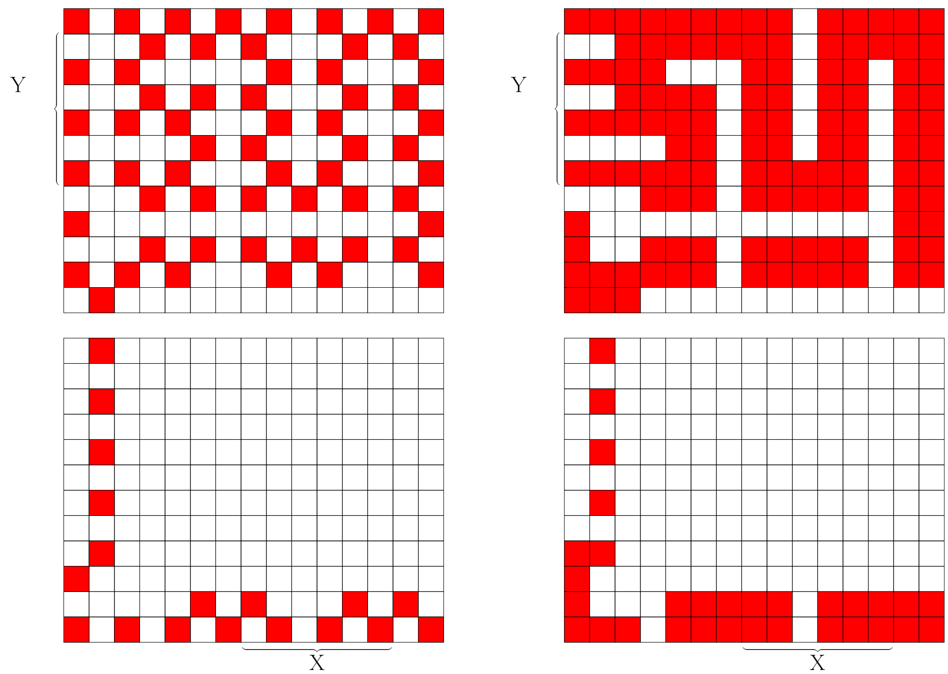

Figure 6.15: A perfect percolating set for $G(12, 21, 2)$.

Consider the union of regions $AX^k = A \cup X_1 \cup \cdots \cup X_k$ (see Figure 6.18). Let L_1, L_2 and L_3 be the top, middle and bottom levels of AX^k, respectively. Observe that after one time-step, the subgraph of $L_2 \setminus \{2k-1\} \times [3] \times \{2\}$ induced by $\overline{A_1^k}$ is acyclic with no border-to-border vertices, and so by Proposition 2.12, A_0^k infects all vertices of L_2 apart from those in the rightmost column (labeled "X"; see Figure 6.18). Therefore, by Lemma 6.2, all vertices in L_1 apart from the rightmost column (labeled "Y") become infected by the 2-neighbor process. Similarly, the red arrow in Figure 6.18) shows the path of infection in L_3.

Consider these observations in the context of G. Figure 6.19 shows that it takes 7 additional time steps to fully infect L_1 and L_2. By Lemma 6.2, the remaining healthy vertices in L_3 become infected. We therefore conclude that A_0^k is lethal on G under the 3-neighbor process.

To prove that A_0^k is perfect, observe that $|A_0^k| = 8 + 4(k-2) + 3 = 4k + 3$. The surface area bound for $G(2k, 3, 3)$ is given by

$$\frac{(2k)(3) + (3)(3) + (3)(2k)}{3} = \frac{12k + 9}{3} = 4k + 3.$$

Since these two values are equal, A_0^k is tight and lethal, and therefore perfect. $\square$

Construction 6.9. *All tuples* $(a, b, 3)$ *with* $a \equiv 3 \pmod 6$, $b \equiv 1 \pmod 2$ *and* $a, b \geq 3$ *are perfect.*

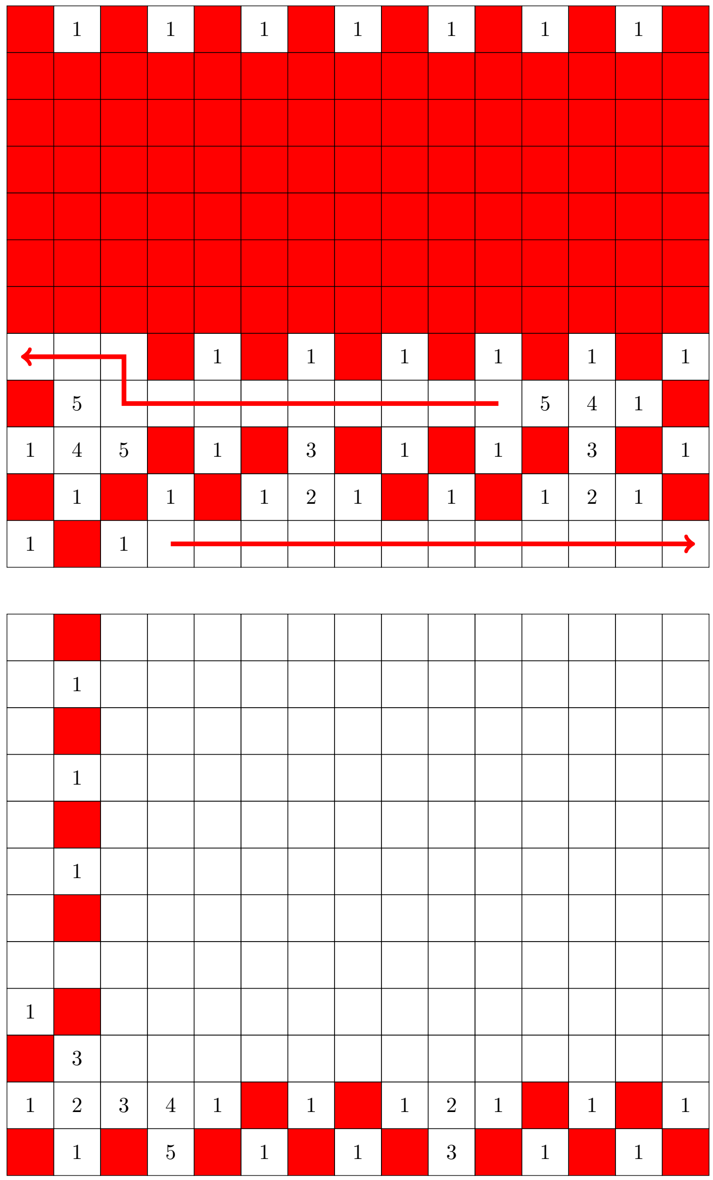

Figure 6.16: Time steps of infection from a perfect lethal set on $G(12, 21, 2)$.

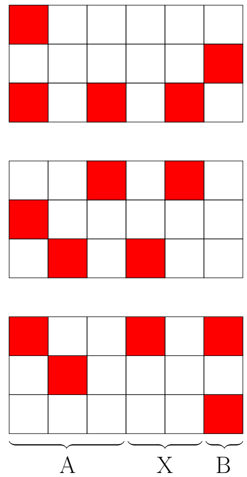

Figure 6.17: The regions A, X, B on $G = AXB$ with infected set A_0.

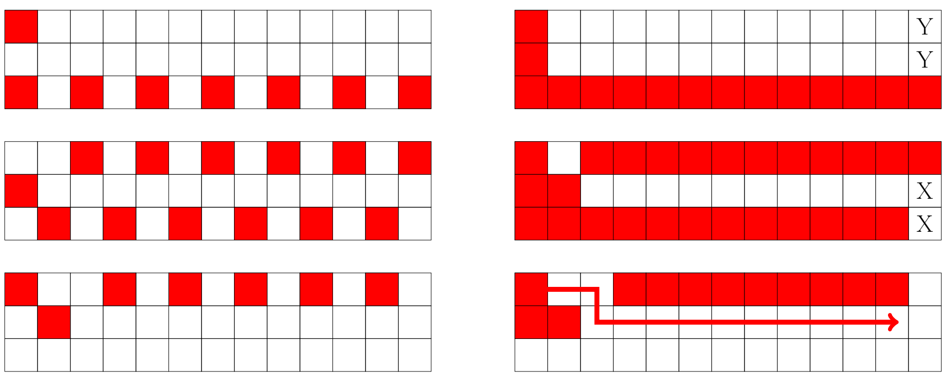

Figure 6.18: An infection on AX^5, $t = 0$ and $t = 1$.

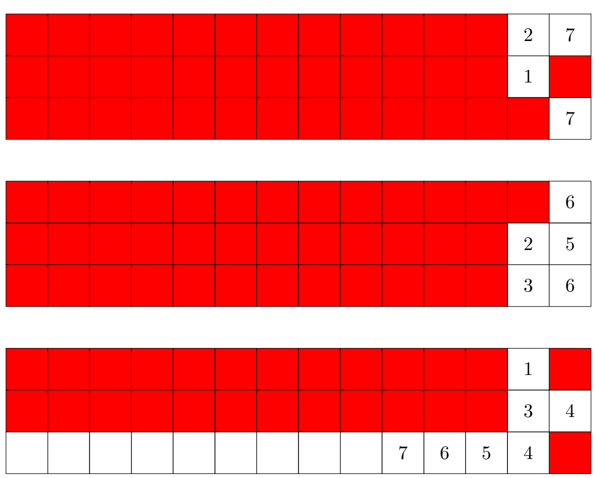

Figure 6.19: Time steps of a perfect lethal infection on $G(3, 14, 3)$.

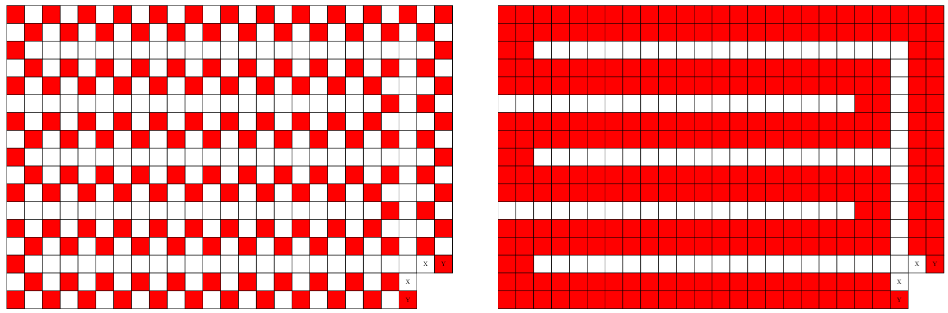

Figure 6.20: A percolating set on the proper unfolding H' of $G(15, 23, 3)$.

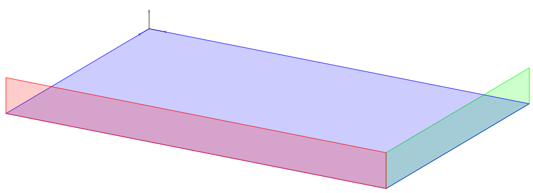

(a) A manifold of $G(15, 23, 3)$.

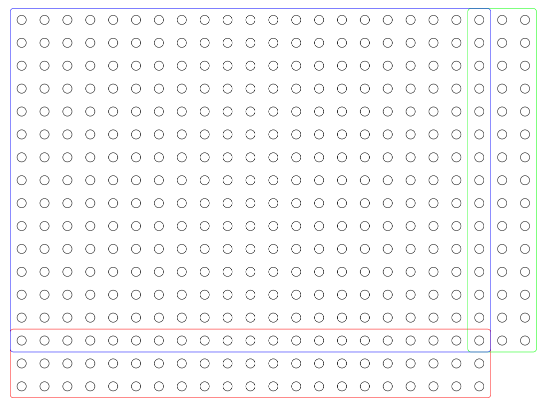

(b) A proper unfolding of G.

Figure 6.21: A proper unfolding of $G(15, 23, 3)$. Colored rectangles indicate faces of G.

Proof. Consider the grid $H = G(a + 2, b + 2, 1)$, where $a \equiv 3 \pmod 6$ and $b \equiv 1 \pmod 2$. Observe that H admits an optimal percolating set by Construction 6.3, and that

$$\mathrm{SA}(a, b, 3) = \lceil \mathrm{SA}(a + 2, b + 2, 1)\rceil - 3.$$

We show that a proper unfolding of G can be obtained from a simple augmentation of H. Let H' be the grid obtained by deleting the four vertices in the bottom, right-most corner of H (see Figure 6.20). Consider the folding pattern illustrated in Figure 6.21, and observe that the pairs of vertices adjacent to the deleted region are duplicates of each other. (In other words, consider folding up the red and green regions in Figure 6.21, and notice that this operation causes vertices to overlap.) Taking this into account, H' percolates by Proposition 2.12. Since H admits an optimal percolating set of size $\lceil \mathrm{SA}(a+2, b+2, 1)\rceil$, and precisely 3 of the vertices deleted from H to obtain H' were infected, it follows that H' admits a perfect lethal set. Finally, by Lemma 2.8, G is perfect. $\square$

Construction 6.10. *All tuples* $(a, 4, 3)$ *with* $a \equiv 3 \pmod 6$ *and* $a \geq 9$ *are perfect.*

Proof. Let $G = G(6k + 3, 4, 3)$ be a grid such that $k \geq 1$, and let $X_1, \ldots, X_k$ be the

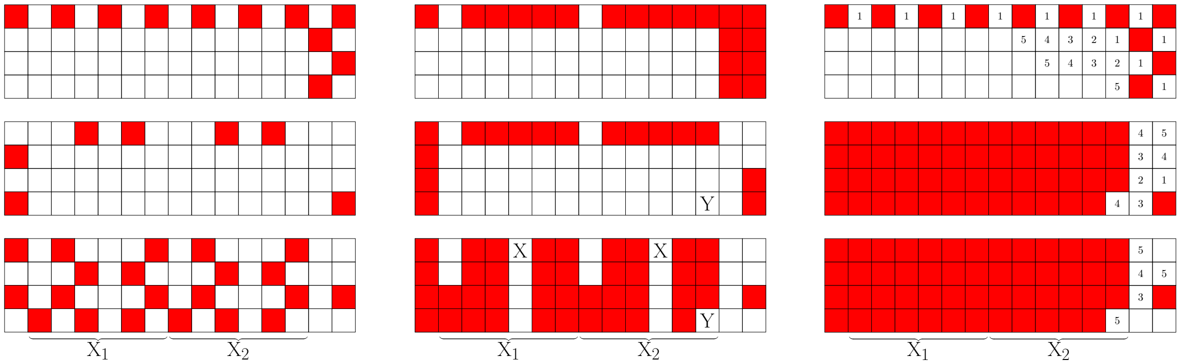

(a) A lethal set on $(4, 15, 3)$, $t = 0$ and $t = 1$. (b) Time steps to infect L_2.

Figure 6.22: Time steps of infection on $G(4, 15, 3)$.

repeated regions of G in the x-direction. Denote the union of these components by X^k. Let $A_t^k \subseteq V(G)$ be the set of infected vertices in G at time t, and suppose that each X_i contains the same pattern of infected vertices (see Figure 6.22a). We show that A_0^k is lethal and perfect.

Let L_1, L_2 and L_3 be the top, middle and bottom levels of G, respectively. Consider L_3 at $t = 1$ (see Figure 6.22a). Observe that the vertices labeled "X" are infected at $t = 2$, and subsequently all vertices in $X^k \cap L_3$ (with the exception of the vertex labeled "Y") are infected by Proposition 2.12. Additionally, the infected vertices in L_2 at $t = 1$ are lethal in $X^k \cap L_2$ under the 2-neighbor process, and so by Lemma 6.2, all vertices of $X^k \cap L_2$ (apart from the one labeled "Y") are infected.

Consider these observations in the context of G. Figure 6.22b shows that it takes 5 additional time steps to fully infect L_2. By Lemma 6.2, the remaining healthy vertices in L_1 and L_3 become infected. We therefore conclude that A_0^k is lethal on G under the 3-neighbor process.

To prove that A_0^k is perfect, observe that for $i \in [k]$, each X_i contains 14 infected vertices. Of the remaining vertices in G, 11 are infected. Therefore, $|A_0| = 14k + 11$. The surface area bound for $G(6k + 3, 4, 3)$ is given by

$$\frac{(6k+3)(4) + (4)(3) + (3)(6k+3)}{3} = \frac{42k+33}{3} = 14k + 11.$$

Since these two values are equal, A_0^k is tight and lethal, and therefore perfect. $\square$

Construction 6.11. *All tuples* $(a, 6, 3)$ *with* $a \equiv 0 \pmod 2$ *and* $a \geq 4$ *are perfect.*

Proof. Let $G = G(2k + 2, 6, 3)$ be a grid such that $k \geq 1$, and let $X_1, \ldots, X_k$ be the repeated regions of G in the x-direction. Denote the union of these regions by X^k. Let $A_t^k \subseteq V(G)$ be the set of infected vertices in G at time t, and suppose that each X_i

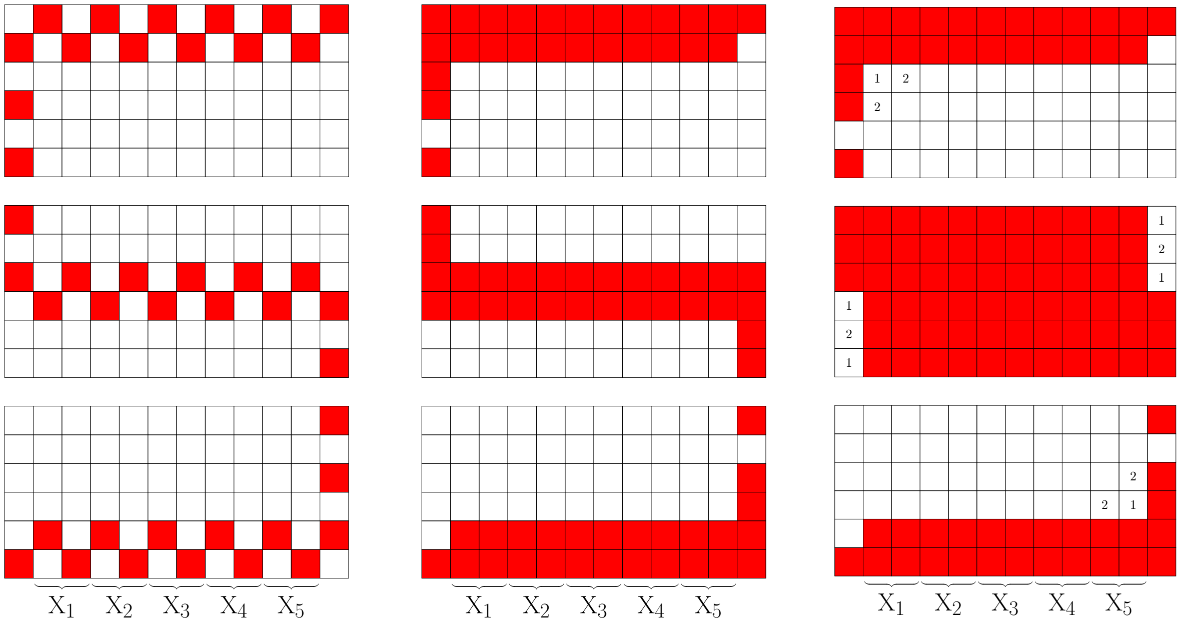

(a) A lethal set on $(6, 12, 3)$, $t = 0$ and $t = 1$.

(b) Time steps to infect L_2.

Figure 6.23: Time steps of infection on $G(6, 12, 3)$.

contains the same pattern of infected vertices (see Figure 6.23a). We show that A_0^k is lethal and perfect.

Let L_1, L_2 and L_3 be the top, middle and bottom levels of G, respectively. Consider L_2 at $t = 1$ (see Figure 6.23a). Observe that all vertices in $X^k \cap L_2$ are infected by Lemma 6.2, due to adjacent infected vertices in L_1 and L_3.

Consider these observations in the context of G. Figure 6.23b shows that it takes 2 additional time steps to fully infect L_2. Since L_1 and L_3 contain lethal sets under the 2-neighbor process, by Lemma 6.2, the remaining healthy vertices in these levels become infected. We therefore conclude that A_0^k is lethal on G under the 3-neighbor process.

To prove that A_0^k is perfect, observe that for $i \in [k]$, each X_i contains 6 infected vertices. Of the remaining vertices in G, 12 are infected. Therefore, $|A_0| = 6k + 12$. The surface area bound for $G(2k + 2, 6, 3)$ is given by

$$\frac{(2k+2)(6) + (6)(3) + (3)(2k+2)}{3} = \frac{18k+36}{3} = 6k + 12.$$

Since these two values are equal, A_0^k is tight and lethal, and therefore perfect. $\square$

Construction 6.12. *All tuples $(a, 6, 3)$ with $a \equiv 1 \pmod 2$ and $a \geq 5$ are perfect.*

Proof. Let $G = G(2k + 3, 6, 3)$ be a grid such that $k \geq 1$, and let $X_1, \ldots, X_k$ be the repeated regions of G in the x-direction. Denote the union of these components by X^k.

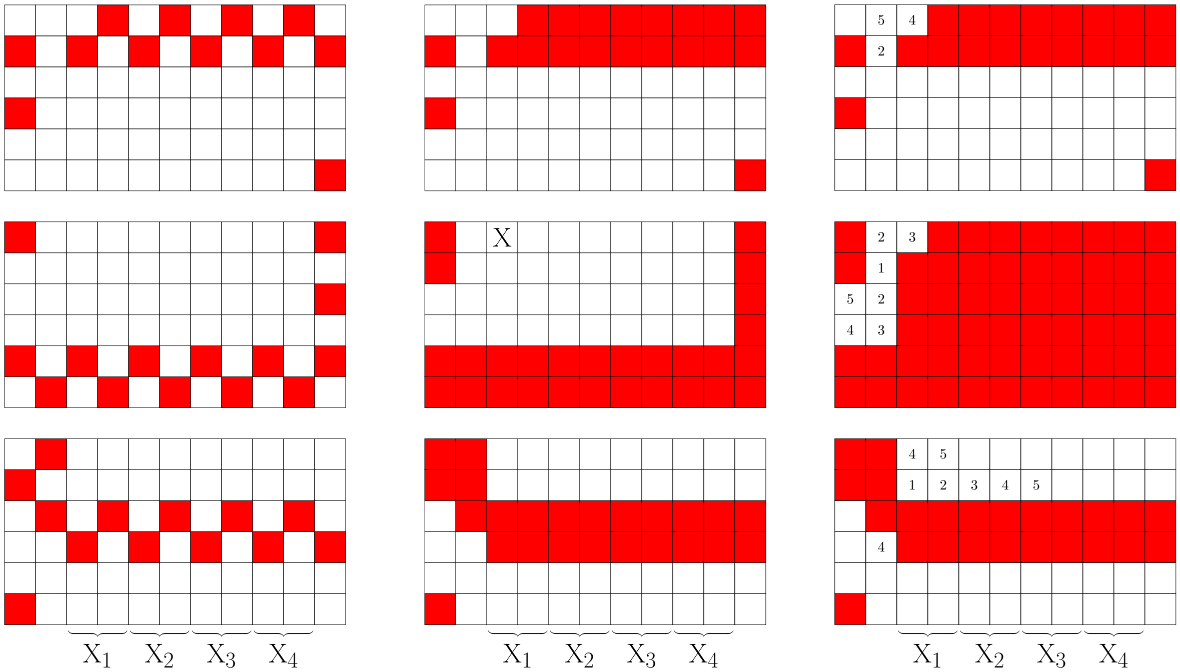

(a) A lethal set on $G(6, 11, 3)$, $t = 0$ and $t = 1$. (b) Time steps to infect L_2.

Figure 6.24: Time steps of infection on $G(6, 11, 3)$.

Let $A_t^k \subseteq V(G)$ be the set of infected vertices in G at time t, and suppose that each X_i contains the same pattern of infected vertices (see Figure 6.24a). We show that A_0^k is lethal and perfect.

Let L_1, L_2 and L_3 be the top, middle and bottom levels of G, respectively. Consider L_2 at $t = 1$ (see Figure 6.24a). Observe that all vertices in $X^k \cap L_2$ (with the exception of the one labeled "X") are infected by Lemma 6.2, due to adjacent infected vertices in L_1 and L_3.

Consider these observations in the context of G. Figure 6.24b shows that it takes 5 additional time steps to fully infect L_2. Since L_1 and L_3 contain lethal sets under the 2-neighbor process, by Lemma 6.2, the remaining healthy vertices in these levels become infected. We therefore conclude that A_0^k is lethal on G under the 3-neighbor process.

To prove that A_0^k is perfect, observe that for $i \in [k]$, each X_i contains 6 infected vertices. Of the remaining vertices in G, 15 are infected. Therefore, $|A_0| = 6k + 15$. The surface area bound for $G(2k + 3, 6, 3)$ is given by

$$\frac{(2k+3)(6) + (6)(3) + (3)(2k+3)}{3} = \frac{18k+45}{3} = 6k + 15.$$

Since these two values are equal, A_0^k is tight and lethal, and therefore perfect. $\square$

Chapter 7
Concluding Remarks

In Chapters 2 and 3, we presented two lemmas regarding the behavior and structure of lethal sets, and used these lemmas (in conjunction with a number of human and computer-generated constructions) to obtain families of perfect sets. In Chapter 4, we used our recursive construction to prove the existence of *perfect* lethal sets on all $[a_1] \times [a_2] \times [a_3]$ grids, for $a_1, a_2, a_3 \geq 5$. We further extended this result to prove the existence of *optimal* lethal sets on all $[a_1] \times [a_2] \times [a_3]$ grids, for $a_1, a_2, a_3 \geq 11$. In Chapter 5, we tackled the case of 3-neighbor percolation on two-dimensional grids, and proved that the only such grids to admit perfect lethal sets are of the form $[2^k - 1]^2$. Finally, in Chapter 6 and Appendix A we presented a number of lethal constructions, many of which extend in one or two dimensions. We discussed the strategy of representing lethal sets on unfolded, two-dimensional surfaces, and noted the nearly ubiquitous presence of corridor-like structures in lethal sets. In the following section, we conclude this thesis with open problems and recommendations for future research.

7.1 Future Work

We conjecture that the bounds of $a_1, a_2, a_3 \geq 5$ and $a_1, a_2, a_3 \geq 11$ for perfect and optimal sets, respectively, can be improved. Experimentally, it appears that tight constructions exist for all $a_1, a_2, a_3 \geq 3$.

Conjecture 7.1. *For all $a_1, a_2, a_3 \geq 3$,*

$$m(a_1, a_2, a_3, 3) = \left\lceil \frac{a_1a_2 + a_2a_3 + a_3a_1}{3} \right\rceil.$$

We anticipate that the process of lowering these bounds will require obtaining additional constructions, either through computational work or the generalization of those presented in this thesis. In particular, a proof of the existence of perfect sets for all grids of thickness 3 would have the immediate effect of reducing the bound on optimal sets to $a_1, a_2, a_3 \geq 8$.

We note that a similar result for $a_1, a_2, a_3 \geq 2$ is impossible. Lethal sets on grids of the form $[a_1] \times [2] \times [2]$ must contain $3a_1/2 + O(1)$ vertices, as consecutive $[2]^2$ layers cannot harbor fewer than 3 infections. This differs significantly from the surface area bound of $\lceil 4a_1/3 \rceil$. It is not clear whether similar restrictions exist for other grids of thickness 2, and we do not claim to know which tuples (a_1, a_2, a_3) admit perfect infections. At present, the smallest divisibility case in which we were unable to determine a perfect lethal set is $[5] \times [17] \times [2]$.

The theorems of this thesis are restricted to the case of $d = 2, d = 3$, and $r = 3$; however, we speculate that similar results exist for all $d = r$.

Conjecture 7.2. *For all $d \geq 4$, there exists some N_d such that if $a_1, \ldots, a_d \geq N_d$, then*

$$m(a_1, a_2, \ldots, a_d, d) = \frac{\sum_{j=1}^{d} \prod_{i \neq j} a_i}{d}.$$

In particular, it would be interesting to apply the techniques of recursion and unfolding to higher dimensions. Unfortunately, just as the 3-dimensional folding strategy relies on lethal 3-neighbor constructions in 2-dimensional grids, so an application of folding to d dimensions relies on the existence of d-neighbor lethal sets in $(d-1)$-dimensional grids. For this reason, we propose the following problem:

Problem 7.3. *Determine $m(a_1, \ldots, a_{d-1}, d)$ for all $d > 3$.*

We note that although Corollary 1.4 resolves the question of $m(n, n, 3)$ for square grids, the case of rectangular grids remains open. Therefore, as a particular case of Problem 7.3, we propose the following:

Problem 7.4. *Determine $m(a_1, a_2, 3)$ for all $a_1, a_2 \geq 3$.*

In the introduction, we showed that for the torus $G_3 = C_{a_1} \square C_{a_2} \square C_{a_3}$ and the grid $G = [a_1 - 1] \times [a_2 - 1] \times [a_3 - 1]$,

$$SA(G, 3) + 1 \leq m(G_3, 3) \leq SA(G, 3) + 2.$$

A natural problem is to determine if the smallest lethal set G_3 is always exactly one above the surface area bound on G.

Problem 7.5. *Determine $m(G_3, 3)$.*

Our computer examples suggest that $m(G_3, 3) = SA(G) + 1$. However, unlike the construction given in Figure 1.5, these examples do not appear to result from any simple augmentation of the smaller grid G. We therefore anticipate that an entirely different proof strategy may be necessary.

A further extension of Problem 7.5 is to consider the Cartesian product of paths and cycles. Denote by $T_{n,i,j}$ the graph resulting from the Cartesian product of i cycles

C_n and j paths P_n. Note that $T_{n,0,d} = [n]^d$ and $T_{n,d,0} = \square_{i=1}^{d} C_n$. Recall that Przykucki and Shelton give $m(T_{n,0,d}, d) = n^{d-1}$ [21]. It would be interesting to determine the following:

Problem 7.6. *For all integers i, j such that $i + j = d$, determine $m(T_{n,i,j}, d)$.*

We proposed in the introduction that the slowest 3-neighbor percolating time on square two-dimensional grids is at least $T([n]^2, 3) \geq \frac{(n-1)^2}{2}$. It would be interesting to determine if this bound is tight, and extend the result to all rectangular grids.

Problem 7.7. *For $G = [a_1] \times [a_2]$, determine $T(G, 3)$.*

With regard to Problem 7.7, we make the following observation. Note that the subgraph H induced by the complement of any lethal set A_0 on $[a_1] \times [a_2]$ must be acyclic (by Proposition 2.12). Therefore, a natural upper bound on $T([a_1] \times [a_2], 3)$ is given by

$$\max\{\mathrm{diam}(C) \mid C \text{ is a component of } H\}.$$

Since the diameter of a graph G is equivalent to the length of the longest induced path in G, $T([a_1] \times [a_2], 3)$ is bounded from above by the length of the longest induced path in $[a_1] \times [a_2]$. We note that this bound is not necessarily tight, as the complement of the longest induced path in $[a_1] \times [a_2]$ may not constitute a lethal set. With this is mind, we propose the following problem:

Problem 7.8. *For $G = [a_1] \times [a_2]$, determine the length of the longest induced path in G.*

Finally, in an 1991 paper by Shapiro and Stephens [22], it was shown that the number of optimal lethal sets in the $[n]^2$ grid under the modified bootstrap process is precisely equal to the nth Schröder number [18]. It would be interesting to determine whether a similar pattern exists in higher dimensions.

Problem 7.9. *Determine the number of lethal sets of size n^2 under the modified bootstrap process in $[n]^3$.*

Appendix A
Individual Constructions

We diagram lethal set constructions for single grids. The initial infection A is colored red, and all other cells are labeled with the time t that they are first infected.

A.1 Perfect Constructions

Construction A.1. *The grid $G(3, 3, 1)$ is perfect.*

Proof. See Figure A.1. □

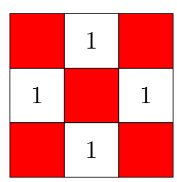

Figure A.1: Time steps of infection from a perfect lethal set on $G(3, 3, 1)$.

Construction A.2. *The grid $G(5, 2, 2)$ is perfect.*

Proof. See Figure A.2. □

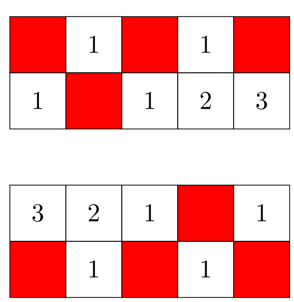

Figure A.2: Time steps of infection from a perfect lethal set on $G(5, 2, 2)$.

Construction A.3. *The grid $G(5,5,2)$ is perfect.*

Proof. See Figure A.3. $\square$

	1		1	
1		1	2	1
	1		3	
1	2	1	4	5
	3		1	

11	10	9		1
10	9	8	3	
9	8	7	6	7
	3		5	8
5	4	1		9

Figure A.3: Time steps of infection from a perfect lethal set on $G(5,5,2)$.

Construction A.4. *The grid $G(6,4,3)$ is perfect.*

Proof. See Figure A.4. $\square$

8	1		11	14	15
7		1		13	
	1	6	7	14	15
1		9	10	17	18

7		1	10	11	
6	3	4	5	12	1
1	2	5		13	
	1	8	9	16	17

	1		9		17
5	4	5	8	13	16
	3	6	7	14	15
1		7		15	

Figure A.4: Time steps of infection from a perfect lethal set on $G(6,4,3)$.

Construction A.5. *The grid $G(8, 5, 5)$ is perfect.*

Proof. See Figure A.5. □

	1		33	34	35	36	37
37	30	23	22	21	20	19	
38	31	10	9		9	16	17
39	32	9	8	7	8	15	18
40	33		1		1		19

1		25	32	33	34	35	
36	29	24	21	20	19	18	17
37	30	9	8	7		15	16
38	31	8	7	6	5	14	15
39	32	7		1		1	

	29	30	31	32	33	36	37
35	28	25		13	14	15	18
36	9		1	8	9	14	15
37	8	5		3	4	13	
	7	6	1	2	3	14	15

33	32	31		13		37	38
34	27	26	1	12	11		19
35		3	2	9	10	11	
38	5	4	1		1	12	1
39		1		1		15	16

	33	34	35	36	37	38	39
1		27		33	34	35	36
	1	28	29	32	33	34	35
39	30	29	30	31		13	
40	31		31	32	33	34	35

Figure A.5: Time steps of infection from a perfect lethal set on $G(8, 5, 5)$.

Construction A.6. *The grid $G(9,6,5)$ is perfect.*

Proof. See Figure A.6. $\square$

38	37		31	32	33	34	35	
11	10	7		11	24	25	28	29
	7	6	1		23	24	27	28
9	8	3		1	22	23	26	27
26	9		19	20	21	22	23	
39	38	37	36	35		1		1

37	36	29	30	31	32	33	36	37
	9	8	5	10	15	20	27	30
1	6	5	4	1		19	26	27
	1	2	3		1		25	26
25		1	18	17	16	1	24	25
34	33		33	34	17		1	

36	35	28	27		15	20	37	38
11	10	9		9	14	19	20	31
8	7		5	8	13	18	19	
1		1	6	7	14	15	20	21
24	21	20	19		15		25	26
33	32	31	32	35	36	37	38	39

35	34	27	26	1		19	38	39
22	21	20	19	10	11	18	19	32
21	20	19	18	11	12	17	18	1
	1		17	16	15	16	19	
23	22	21	20	19	18	17	26	27
	23	30	31	36	37	38	39	40

	33		25		1		39	40
33	32	25	24	3	2	1		33
34	31	26	23		1		1	
35	30	27	22	17		1	20	21
36	29	28	21	20	19		27	28
37		29		37	38	39	40	41

Figure A.6: Time steps of infection from a perfect lethal set on $G(9,6,5)$.

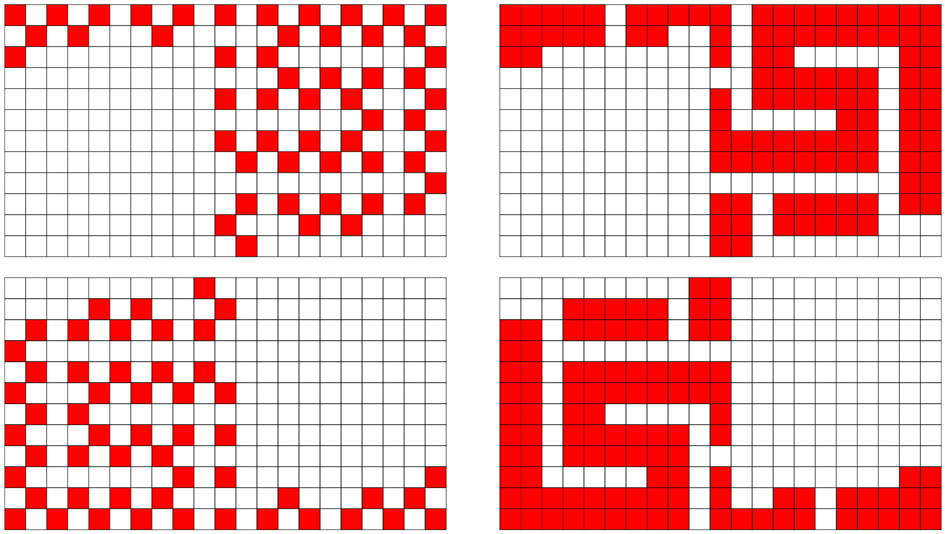

Figure A.7: A perfect percolating set for $G(12, 21, 2)$.

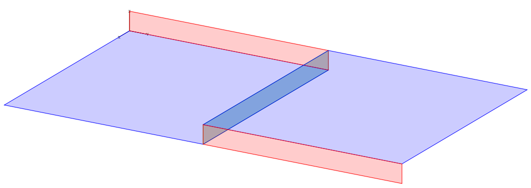

(a) A manifold of $G = (12, 21, 2)$.

(b) A proper unfolding of G.

Figure A.8: A proper unfolding of $G = G(12, 21, 2)$. Colored rectangles indicate planes of G. Dashed lines indicate that cells appear on different layers.

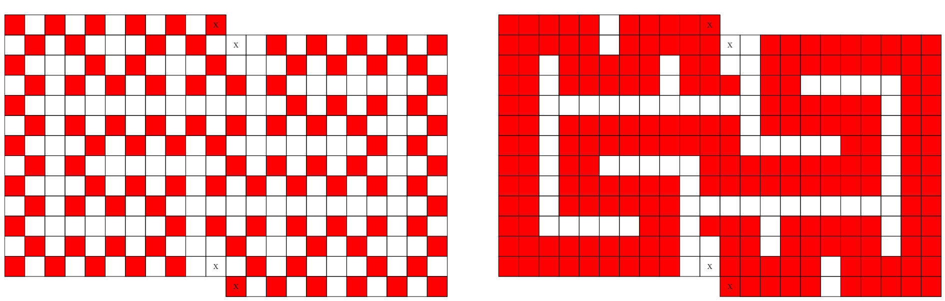

Figure A.9: A percolating set on the proper unfolding of $G(12, 21, 2)$.

A.2 Optimal Constructions

Construction A.7. *The grid $G(4,4,3)$ is optimal.*

Proof. See Figure A.10. $\square$

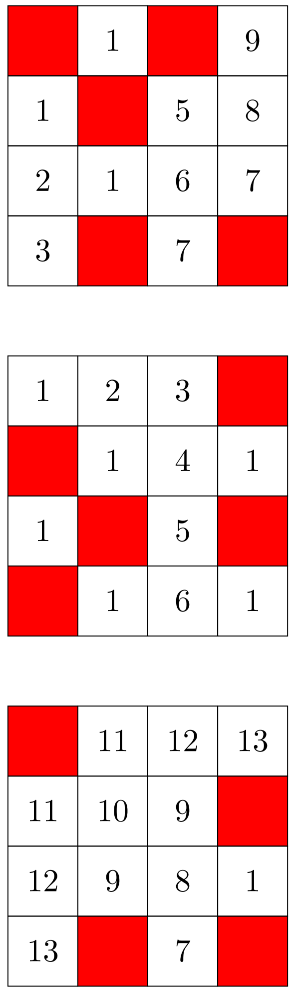

Figure A.10: Time steps of infection from an optimal lethal set on $G(4,4,3)$.

Construction A.8. *The grid $G(6,5,5)$ is optimal.*

Proof. See Figure A.11. □

	29	26	25		1
31	30	11	8	1	
32	31		1		1
33	32	1		1	
34	33		1		1

29	28	25	24	3	
30	27	10	7	2	1
31	10	7	6	1	
32	7	6	5	2	1
33		1	4	3	

	27	24	23	16	15
27	26	9		3	14
	9	8	7		13
29		7	8	9	12
30	1		9	10	11

29	28	23	22	17	
28	25		19	18	15
25	24	21	20	19	16
28	25	22	21	20	13
29	26	23	22	21	

30	29		21		1
29		1	20	19	
	23	22	21	20	17
27	26	23	22	21	
	27	28	29	30	31

Figure A.11: Time steps of infection from an optimal lethal set on $G(6,5,5)$.

Construction A.9. *The grid $G(7,5,5)$ is optimal.*

Proof. See Figure A.12. □

28	27	12	1		1	
27	26	11		1	2	1
26	25		1		3	
25	24	23	24	25	26	27
	1		25	26	27	28

19	16	11		1		1
18	15	10	5	4	3	
17	14	7	6	5	6	7
	1	22	23	24	25	26
1		23	24	25	26	27

	15		1	10	11	
15	14	9	8	9	12	13
16	13		7		13	14
17		21	20	19	16	15
26	25	24	21	20	17	

17	16	1		19	20	21
	11	10	11	18	19	20
13	12	11	12	17	16	15
24	23	22	19	18	1	
27	26	25		1		1

18	17		23	24	25	26
1		1	22	23	24	25
	1		21	20	17	
25	24	23	22	19		1
28	27	26	23		1	2

Figure A.12: Time-steps of infection from an optimal lethal set on $G(3,3,1)$.

Construction A.10. *The grid $G(7,6,5)$ is optimal.*

Proof. See Figure A.13. $\square$

34	33	32	1		3	
33	32	25		1	2	1
32	31	24	21		1	
25	24	23	22	23	24	25
	1		7	24	25	26
1		1		25	26	27

33	32	31		21	22	23
32	31	24	21	20	3	
31	30	21	20	19		1
	3		7	20	21	22
1	2	1	6	21	22	23
	3	4	5	22	23	24

	29	30	31	32	33	34
1		23	22	21	20	19
30	29		19	18	17	18
31	30	1	2	1		19
32	31		1		11	20
33	32	5		9	12	21

1	28	29	32	33	34	35
	25	24	23	22	21	
29	28	21	20	17	16	15
32	31	6	3		11	14
33	32	5	4	5	10	11
34	33	6	5	8	9	

	27		33	34	35	36
1	26	25	26	27	28	29
	27	22	21		13	
33	32	7		1	12	13
34	33		1	6	7	
35	34	7		7		1

Figure A.13: Time steps of infection from an optimal lethal set on $G(7,6,5)$.

Construction A.11. *The grid $G(7,7,5)$ is optimal.*

Proof. See Figure A.14. □

24	23	22	1		1	
21	20	17		1	2	1
20	19	10	9		3	
1		7	10	11	18	19
	1		11	12	19	20
1	2	3	18	19	20	21
	1		19	20	21	22

23	22	21		1		1
20	19	16	5	4	3	
19	18	9	8	5	6	7
	5	6	7		17	18
1	4	5	8	9	18	19
	3	6	17	18	19	20
1		7	18	19	20	21

	19	20	21	22	23	24
19	18	15	12	11	18	19
	17		9	10	17	18
19	18	1		1	16	17
20	19		1		15	
21	20	17	16	15	16	17
22	21	18	17		17	18

21		15	22	23	24	25
20	15	14	13		19	20
17	16	13	12	11	18	19
20	19	14	13	12	15	
21	20	15	14	13	14	1
22	21	18	15	14	15	16
23	22	19		1	16	17

22	1		23	24	25	26
21		1	14	15	20	21
	1		1		19	20
21	20	15		1	16	17
22	21	16	15		1	
23	22	19	16	1		1
24	23	20	17		1	

Figure A.14: Time steps of infection from an optimal lethal set on $G(7,7,5)$.

Bibliography

[1] J. Balogh and B. Bollobás. Bootstrap percolation on the hypercube. *Probability Theory and Related Fields*, 134(4):624–648, 2006.

[2] J. Balogh, B. Bollobás, H. Duminil-Copin, and R. Morris. The sharp threshold for bootstrap percolation in all dimensions. *Transactions of the American Mathematical Society*, 364(5):2667–2701, 2012.

[3] J. Balogh, B. Bollobás, and R. Morris. Bootstrap percolation in three dimensions. *The Annals of Probability*, 37(4):1329–1380, 2009.

[4] J. Balogh, B. Bollobás, and R. Morris. Majority bootstrap percolation on the hypercube. *Combinatorics, Probability and Computing*, 18(1-2):17–51, 2009.

[5] J. Balogh, B. Bollobás, and R. Morris. Bootstrap percolation in high dimensions. *Combinatorics, Probability and Computing*, 19(5-6):643–692, 2010.

[6] J. Balogh and G. Pete. Random disease on the square grid. *Random Structures & Algorithms*, 13(3-4):409–422, 1998.

[7] F. Benevides, J.-C. Bermond, H. Lesfari, and N. Nisse. *Minimum lethal sets in grids and tori under 3-neighbour bootstrap percolation.* PhD thesis, Université Côte d'Azur, 2021.

[8] F. Benevides and M. Przykucki. On slowly percolating sets of minimal size in bootstrap percolation. *the electronic journal of combinatorics*, pages P46–P46, 2013.

[9] F. Benevides and M. Przykucki. Maximum percolation time in two-dimensional bootstrap percolation. *SIAM Journal on Discrete Mathematics*, 29(1):224–251, 2015.

[10] B. Bollobás. Weakly k-saturated graphs. In *Beiträge zur Graphentheorie (Kolloquium, Manebach, 1967)*, volume 25, page 31, 1968.

[11] B. Bollobás. *The Art of Mathematics: Coffee Time in Memphis.* Cambridge University Press, 2006.

[12] J. Chalupa, P. L. Leath, and G. R. Reich. Bootstrap percolation on a bethe lattice. *Journal of Physics C: Solid State Physics*, 12(1):L31, 1979.

[13] L. Hambardzumyan, H. Hatami, and Y. Qian. Lower bounds for graph bootstrap percolation via properties of polynomials. *Journal of Combinatorial Theory, Series A*, 174:105253, 2020.

[14] I. Hartarsky. Maximal bootstrap percolation time on the hypercube via generalised snake-in-the-box. *arXiv preprint arXiv:1707.09214*, 2017.

[15] A. Holroyd. The metastability threshold for modified bootstrap percolation in d dimensions. *Electronic Journal of Probability*, 11:418–433, 2006.

[16] A. E. Holroyd. Sharp metastability threshold for two-dimensional bootstrap percolation. *Probability Theory and Related Fields*, 125(2):195–224, 2003.

[17] N. Morrison and J. A. Noel. Extremal bounds for bootstrap percolation in the hypercube. *Journal of Combinatorial Theory, Series A*, 156:61–84, 2018.

[18] OEIS Foundation Inc. The On-Line Encyclopedia of Integer Sequences, 2022. Published electronically at `http://oeis.org`.

[19] G. Pete. *Disease processes and bootstrap percolation*. PhD thesis, Thesis for diploma at the Bolyai Institute, Jzsef Attila University, Szeged, 1997.

[20] G. Pete. How to make the cube weedy. *Polygon*, 7(1):69–80, 1997.

[21] M. Przykucki and T. Shelton. Smallest percolating sets in bootstrap percolation on grids. *arXiv preprint arXiv:1907.01940*, 2019.

[22] L. Shapiro and A. B. Stephens. Bootstrap percolation, the schröder numbers, and the n-kings problem. *SIAM Journal on Discrete Mathematics*, 4(2):275–280, 1991.

[23] A. M. Shende. Maximal induced paths and minimal percolating sets in hypercubes. *Journal of Algebra Combinatorics Discrete Structures and Applications*, 2(1):17–24.